

*The role of the neural cell adhesion molecule-associated  
polysialic acid in synaptic plasticity in the medial  
prefrontal cortex of the mouse (Mus musculus)*

**Dissertation**

zur Erlangung des akademischen Grades

**doctor rerum naturalium**

**(Dr. rer. nat.)**

genehmigt durch die Fakultät für Naturwissenschaften  
der Otto-von-Guericke-Universität Magdeburg

von Hristo Varbanov, M.Sc.

geb. am 17.07.1983 in Pleven, Bulgarien

Gutachter: Prof. Dr. Alexander Dityatev

Associate Prof. Dr. Juan Nacher

eingereicht am: 27.03.2017

verteidigt am: 28.08.2017

*„Wenn ein Tier oder Mensch seine ganze  
Aufmerksamkeit und seinen ganzen Willen auf  
eine bestimmte Sache richtet, dann erreicht er  
sie auch. Das ist alles.“*

—Hermann Hesse, Demian

## SUMMARY

Hristo Varbanov, MSc:

### ***“The role of the neural cell adhesion molecule-associated polysialic acid in synaptic plasticity in the medial prefrontal cortex of the mouse (*Mus musculus*)”***

In mammals, polysialic acid (polySia) is a linear homopolymer of  $\alpha$ 2,8-glycosidically linked units of the monosaccharide sialic acid. The main carrier of polySia in the human and mouse brain is the neural cell adhesion molecule (NCAM). In the adult brain, polySia is predominantly synthesized and added to the extracellular domain of NCAM by the polysialyltransferase ST8SIA4. PolySia-NCAM is known to play an important role in hippocampal synaptic plasticity as well as in hippocampus-dependent learning. Clinical studies have shown that the expression levels of polySia and NCAM are altered in the hippocampus and prefrontal cortex of schizophrenic patients. However, the impact of polySia on *N*-methyl-D-aspartate receptors (NMDARs) and synaptic plasticity in the prefrontal cortex remains unclear. To this aim, I performed immunohistochemical stainings, electrophysiological whole-cell patch-clamp recordings, and field excitatory postsynaptic potential recordings in medial prefrontal cortex (mPFC) slices from C57BL/6 mice after polySia removal using endosialidase NF (endoNF) and in mPFC slices from ST8SIA4-deficient and NCAM-deficient mice. In the present study, I showed that endoNF treatment of mPFC slices resulted in increased evoked GluN1/GluN2B-NMDAR-mediated currents, which we assessed using relatively low (0.3  $\mu$ M), GluN1/GluN2B-specific concentrations of the GluN2B-selective antagonist Ro 25-6981. Similarly, endoNF caused a pronounced increase in tonic NMDAR-mediated currents, which reflect the activation of extrasynaptic GluN2B-containing NMDARs. Importantly, we reveal that the short-chain polySia containing 12 residues, NANA12, inhibited GluN1/GluN2B-NMDAR-mediated evoked currents in endoNF-treated mPFC slices but not in sham-treated control slices. Moreover, acute polySia removal led to reduced levels of long-term potentiation (LTP) in the mPFC. In mPFC slices from ST8SIA4-deficient mice, I found similar increase in 0.3- $\mu$ M-Ro 25-6981-sensitive NMDAR-mediated evoked currents, which were accompanied by impaired LTP in the mPFC. Notably, blockade of GluN1/GluN2B-NMDARs by application of 0.3- $\mu$ M-Ro 25-6981 or NANA12 fully restored impaired LTP levels in endoNF-treated slices and ST8SIA4-deficient mice. Abnormal LTP levels in endoNF-treated slices and ST8SIA4-deficient mice could be also fully rescued by sarcosine, an inhibitor of the glial glycine transporter type-1 and an agonist of the NMDAR glycine-site. Similarly, sarcosine fully rescued LTP levels in mPFC slices from NCAM-deficient mice. Furthermore, Ro 25-6981, NANA12, or sarcosine had no effects on LTP in sham-treated mPFC slices. Altogether, these findings suggest that polySia-NCAM regulates the balance of synaptic and extrasynaptic NMDARs in the mPFC, thus mediating synaptic plasticity in the mPFC. Moreover, these data indicate that NANA12 might represent a potential therapy for restoration of overactivated extrasynaptic NMDARs observed in models of schizophrenia and Alzheimer’s disease.

## ZUSAMMENFASSUNG

Hristo Varbanov, MSc:

***“Die Rolle der Polysialinsäure assoziiert mit der neuronalen Zelladhäsionsmolekül in synaptischer Plastizität im medialen präfrontalen Kortex der Maus (Mus musculus)“***

Polysialinsäure (polySia) ist ein lineares Homopolymer aus Sialinsäure-Resten, die durch  $\alpha$ 2,8-glykosidische Bindungen miteinander verbunden sind. PolySia in dem Gehirn ist hauptsächlich mit dem neuronalen Zelladhäsionsmolekül NCAM assoziiert. In dem adulten Gehirn wird polySia von der Polysialyltransferase ST8SIA4 produziert. Anschließend fügt ST8SIA4 die entstandenen polySia-Ketten zu der extrazellulären Domäne von NCAM hinzu. Außerdem spielt polySia eine wichtige Rolle in synaptischer Plastizität in Hippokampus so wie auch in Formen des Lernens, die von der Hippokampus-Funktion abhängig sind. Klinische Studien haben gezeigt, dass die Expressionsraten von polySia und NCAM im Hippokampus und präfrontalen Kortex von Schizophrenie-Patienten pathologisch verändert sind. Jedoch bleibt es immer noch unklar, ob diese polySia-NCAM-Veränderungen direkte Einfüsse auf die *N*-Methyl-D-Aspartat-Rezeptoren (NMDAR) und damit zusammenhängende synaptische Plastizität im präfrontalen Kortex haben. Um das zu untersuchen, habe ich zuerst PolySia in Hirnschnitten aus dem medialen präfrontalen Kortex (MPFK) von C57BL/6-Mäusen enzymatisch mittels der Endosialidase NF (EndoNF) abgebaut. Darauf habe ich immunohistologische Färbungen, elektrophysiologische Ganzzelleableitungen mittels der Patch-Clamp-Technik so wie auch extrazelluläre Ableitungen von Feldpotenzialen in EndoNF-MPFK-Hirnschnitten und auch in MPFK-Hirnschnitten aus ST8SIA4- und NCAM-Knockout-Mäusen durchgeführt. In der vorgelegten Studie konnte ich zeigen, dass EndoNF-Behandlung zu Erhöhung von evozierten Strömen führt, die hauptsächlich durch GluN1/GluN2B-NMDAR-Rezeptoren fließen. Um die Fraktion der GluN1/GluN2B-NMDAR-Rezeptoren zu bestimmen, habe ich eine relativ geringe Konzentration (0.3  $\mu$ M) des GluN2B-NMDA-Rezeptor-Kanalblockers Ro 25-6981 benutzt, die hauptsächlich Ströme durch GluN1/GluN2B-NMDA-Rezeptoren blockiert. EndoNF führte zu einer Erhöhung der tonischen Ströme, die wiederum die Aktivierung von extrasynaptischen NMDA-Rezeptoren widerspiegeln. Außerdem blockierte auch Kurzketten-PolySia (NANA12) Ströme durch GluN1/GluN2B-Rezeptoren in MPFK-Schnitten, die mit EndoNF behandelt wurden, aber nicht in Kontrollschnitten. Somit beobachtete ich ähnliche Effekte von NANA12 und Ro 25-6981 (0.3  $\mu$ M). Ich konnte auch demonstrieren, dass endoNF-Behandlung die Langzeitpotenzierung (LTP) in MPFK-Schnitten beeinträchtigt. In Schnitten aus ST8SIA4-Knockout-Mäusen fand ich eine ähnliche Erhöhung von evozierten Strömen, die sensitiv für Ro 25-6981 (0.3  $\mu$ M) waren. In Übereinstimmung mit unseren EndoNF-Schnitten war die Stärke von LTP in ST8SIA4- und NCAM-Knockout-Mäusen ebenso erheblich vermindert. Außerdem führte die Blockade von GluN1/GluN2B-NMDA-Rezeptoren durch NANA12 und Ro 25-6981 (0.3  $\mu$ M) zu einer

kompletten Wiederherstellung von LTP in EndoNF-Schnitten und in ST8SIA4-Knockout-Mäusen. Eine ähnlich erfolgreiche Wiederherstellung von LTP zeigte auch Sarkosin (Sarcosine), ein Inhibitor des Typ-1-Glycin-Transporters und zugleich ein Agonist der NMDA-Rezeptor-Glycin-Bindungsstelle. Hingegen hatten Ro 25-6981, NANA12 und Sarkosin keine Effekte auf LTP in MPFC-Kontrollschnitten. Zusammenfassend zeigen diese Ergebnisse, dass polySia-NCAM die Balance zwischen synaptischen und extrasynaptischen NMDA-Rezeptoren reguliert und dadurch synaptische Plastizität in dem präfrontalen Kortex fördert. Darüber hinaus weisen diese Daten darauf hin, dass die kurzkettige Polysialinsäure NANA12 als eine potenzielle therapeutische Strategie weiterentwickelt werden kann, um die Überaktivierung von extrasynaptischen NMDA-Rezeptoren in Schizophrenie- und Alzheimer-Modellen zu normalisieren.

## CONTENTS

SUMMARY .....	3
ZUSAMMENFASSUNG .....	4
LIST OF ABBREVIATIONS .....	8
1. INTRODUCTION.....	11
1.1. The neural cell adhesion molecule (NCAM).....	11
1.2. Polysialic acid associated with NCAM: structure and biosynthesis.....	14
1.3. Homophilic and heterophilic interactions of NCAM and polySia .....	16
1.3.1. Interaction partners of NCAM.....	16
1.3.2. Interaction partners of polySia .....	20
1.4. PolySia expression in the developing brain.....	22
1.5. Expression of NCAM and polySia in the adult brain .....	24
1.6. PolySia-NCAM in synaptic plasticity during adulthood.....	27
1.7. Role of polySia-NCAM in rodent models of learning and memory .....	31
1.8. <i>N</i> -methyl-D-aspartate receptors: structure and functions .....	34
1.9. The NMDAR glycine-site as a therapeutic target in the treatment of schizophrenia .....	36
1.9.1. Glycine transporter 1 inhibitors in synaptic plasticity and learning .....	38
1.10. Involvement of NCAM and polySia in psychiatric and neurodegenerative diseases.....	40
1.11. Objectives of the thesis.....	41
2. MATERIALS AND METHODS .....	44
2.1. Animals .....	44
2.2. Electrophysiological recordings in mPFC brain slices.....	44
2.2.1. Preparation of acute brain slices.....	44
2.2.2. Extracellular LTP recordings .....	47
2.2.3. Whole-cell patch-clamp recordings.....	49
2.2.4. Chemicals used in electrophysiological experiments.....	52
2.3. Data analysis and statistical comparisons for <i>in vitro</i> electrophysiology.....	54
2.4. Immunohistochemistry in brain slices.....	55
3. RESULTS.....	57
3. 1. Loss of polySia in mPFC slices after endoNF treatment.....	57
3.2. Acute enzymatic removal of polySia increases GluN2B-NMDAR-mediated currents and extrasynaptic, tonic NMDAR-mediated currents in the mPFC .....	59
3.3. PolySia fragments inhibit evoked NMDAR-mediated currents in the mPFC.....	66

3.4. The polySia mimetic tegaserod inhibits NMDAR-mediated currents in mPFC slices .....	72
3.5. Pharmacological restoration of abnormal long-term potentiation in mPFC slices by Ro 25-6981, sarcosine, or NANA12 .....	74
3.6. EndoNF treatment does not alter theta-burst stimulation-evoked inhibitory postsynaptic currents.	80
3.7. Increased GluN2B-mediated currents in ST8SIA4-deficient mice .....	83
3.8. Impaired long-term potentiation in the mPFC of ST8SIA4-deficient mice and its pharmacological rescue.....	87
3.9. Decreased mPFC LTP levels in NCAM-deficient mice can be restored by sarcosine.....	91
4. DISCUSSION .....	94
4.1. Effects of polySia removal on NMDARs and synaptic plasticity in the mPFC .....	95
4.2. Contribution of GluN2A and GluN2B subunits of NMDAR to synaptic plasticity .....	101
4.3. The impact of GABAergic inhibition.....	102
4.4. Pharmacological restoration of synaptic plasticity after polySia removal .....	104
4.5. Downstream mechanisms of GluN2B overactivation .....	106
5. REFERENCES .....	108
AKNOWLEDGEMENTS .....	129
SELBSTSTÄNDIGKEITSERKLÄRUNG – STATEMENT OF INTEREST.....	131
CURRICULUM VITAE .....	132
LIST OF PUBLICATIONS.....	134

## LIST OF ABBREVIATIONS

aCSF, Artificial cerebrospinal fluid

AMPA,  $\alpha$ -amino-3-hydroxy-5-methyl-4-isoxazolepropionic acid

AMPA, AMPA receptor

ANOVA, analysis of Variances

AP5, 2-D,L-aminophosphonovaleric acid

BDNF, brain-derived neurotrophic factor

CREB, cAMP-response-element-binding protein

FGF, fibroblast growth factor

CamKII,  $\text{Ca}^{2+}$ /calmodulin kinase II

CAMs, cell adhesion molecules

CSPG, chondroitin sulfate proteoglycans

DCS, D-cycloserine

ECM, extracellular matrix

EDTA, ethylenediaminetetraacetic acid

EndoN, endosialidase N

EndoNF, endosialidase NF

EPSC, excitatory postsynaptic current

EPSP, excitatory postsynaptic potential

ERK, extracellular signal-related protein kinase

FAK, focal adhesion kinase

fEPSP, field excitatory post synaptic potential

FGF, fibroblast growth factor

FGFR, fibroblast growth factor receptor

Fluo4, fluorescent calcium indicator



GABA, gamma amino butyric acid

GlyT1, glycine transporter type 1

GluR, glutamate receptor

GPT, glutamic-pyruvic transaminase

HEPES, 4-(2-hydroxyethyl)-1-piperazineethanesulfonic acid

HFS, high frequency stimulation

Ig, immunoglobulin

LFS, low frequency stimulation

LTD, long-term depression

LTP, long-term potentiation

MAPK, Mitogen activated protein kinase

mGluR, metabotropic glutamate receptor

mPFC, medial prefrontal cortex

NCAM, neural cell adhesion molecule

PolySia-NCAM, neural cell adhesion molecule associated with polysialic acid

NBQX, 2,3-dioxo-6-nitro-1,2,3,4-tetrahydrobenzo[f]quinoxaline-7-sulfonamide disodium salt

NMDAR, *N*-methyl-D-aspartate receptor

GluN, NMDAR subtype

PBS, phosphate-buffered saline

PKA, protein kinase A

PKC, protein kinase C

PPF, paired pulse facilitation

PolySia, polysialic acid

PrL, prelimbic cortex

PSD, postsynaptic density

PST, polysialyltransferase ST8SIA4

p38, isoform of mitogen-activated protein kinase

Ras-GRF, Ras-guanin nucleotide-releasing factor

Ro 25-6981, (R-(R\*,S\*)-a-(4-hydroxyphenyl)-b-methyl-4-(phenylmethyl)-1-piperidine  
propanol

SEM, standard error of mean

STP, short term potentiation

STX, sialyltransferase X

ST8SIA2, polysialyltransferase (STX)

ST8SIA4, polysialyltransferase (PST)

TBS, theta-burst stimulation

TM, transmembrane domain

# 1. INTRODUCTION

## 1.1. The neural cell adhesion molecule (NCAM)

Cell adhesion molecules (CAMs) are cell-surface molecules that play a major role in the developing central nervous system (CNS). In particular, CAMs promote cell-to-cell adhesion, thereby regulating neuronal interactions required for several key processes, such as axonal guidance, neuronal proliferation, and synaptic targeting (reviewed by (Crossin and Krushel, 2000; Maness and Schachner, 2007)). CAMs are expressed at pre- and postsynaptic sites, where they interact with components of the extracellular matrix (ECM). Thus, they are involved in activity-dependent synaptic plasticity and learning in the adult CNS via modulation of postsynaptic glutamate receptors and ion channels (reviewed by (Schachner, 1997; Ronn et al., 2000; Bukalo and Dityatev, 2012)). In turn, neuronal activity is known to alter the expression of CAMs at the synapse (reviewed by (Fields and Itoh, 1996)). Cell adhesion molecules have been classified into several groups, such as the cadherin, integrin, semaphorin, and immunoglobulin superfamily (Ig CAM) (reviewed by (Walsh and Doherty, 1997; Hirano et al., 2003; Kruger et al., 2005)).

The first Ig CAM superfamily member that was identified and extensively studied in the CNS was the neural cell adhesion molecule (NCAM) (Jorgensen and Bock, 1974; Cunningham et al., 1987). It represents a transmembrane glycoprotein that is expressed in almost all cells types in the brain and mediates  $\text{Ca}^{2+}$ -independent adhesion between neighboring neurons as well as adhesion between neurons and the surrounding ECM (Maness and Schachner, 2007). In the developing CNS, NCAM plays an important role in axon guidance, neuronal proliferation and migration, neurite outgrowth, and synaptic formation ((Dityatev et al., 2000); reviewed by (Maness and Schachner, 2007)). During adulthood, NCAM is involved in synaptic plasticity as well as learning and memory in rodents (reviewed by (Schachner, 1997; Ronn et al., 2000; Dityatev et al., 2008; Bukalo and Dityatev, 2012; Senkov et al., 2012)). In the human brain, altered expression of NCAM has been linked to several neuropsychiatric and neurodegenerative disorders, including schizophrenia, bipolar disorder, depression, and Alzheimer's disease (reviewed by (Brenneman and Maness, 2010; Hildebrandt and Dityatev, 2015)).

NCAM exists in three major membrane isoforms that are termed according to their molecular mass, namely, NCAM180 (**Fig. 1.1**), NCAM140, and NCAM120. They are generated by alternative splicing of a single gene and show a distinct temporal and cell type-specific pattern of expression. All three main isoforms exhibit an extracellular domain consisting of five immunoglobulin-like (Ig) domains and two fibronectin type III homologous repeats. NCAM180 and NCAM140 express a transmembrane domain (TMD), whereas the NCAM120 isoform is attached to the cell membrane by a glycosylphosphatidylinositol (GPI) anchor and is predominantly expressed in glial cells. Both NCAM180 and NCAM140 isoforms express a cytoplasmic domain, but NCAM180, the largest of the three main isoforms, shows an additional 40 kD cytoplasmic domain insert (Cunningham et al., 1987; Maness and Schachner, 2007). NCAM180 has been identified mainly in mature neurons, where it is enriched in postsynaptic densities (PSDs) of postsynaptic membranes (Persohn et al., 1989) and plays an important role in synaptic plasticity (Schuster et al., 1998). In contrast to NCAM180, the NCAM140 isoform is expressed on both pre- and postsynaptic membranes of neurons but also in glial cells; further, NCAM140 has been identified in axon growth cones of neurons during development. Notably, NCAM140 is involved in several signal transduction pathways mediating outgrowth and branching of axons and dendrites (reviewed by (Maness and Schachner, 2007)).

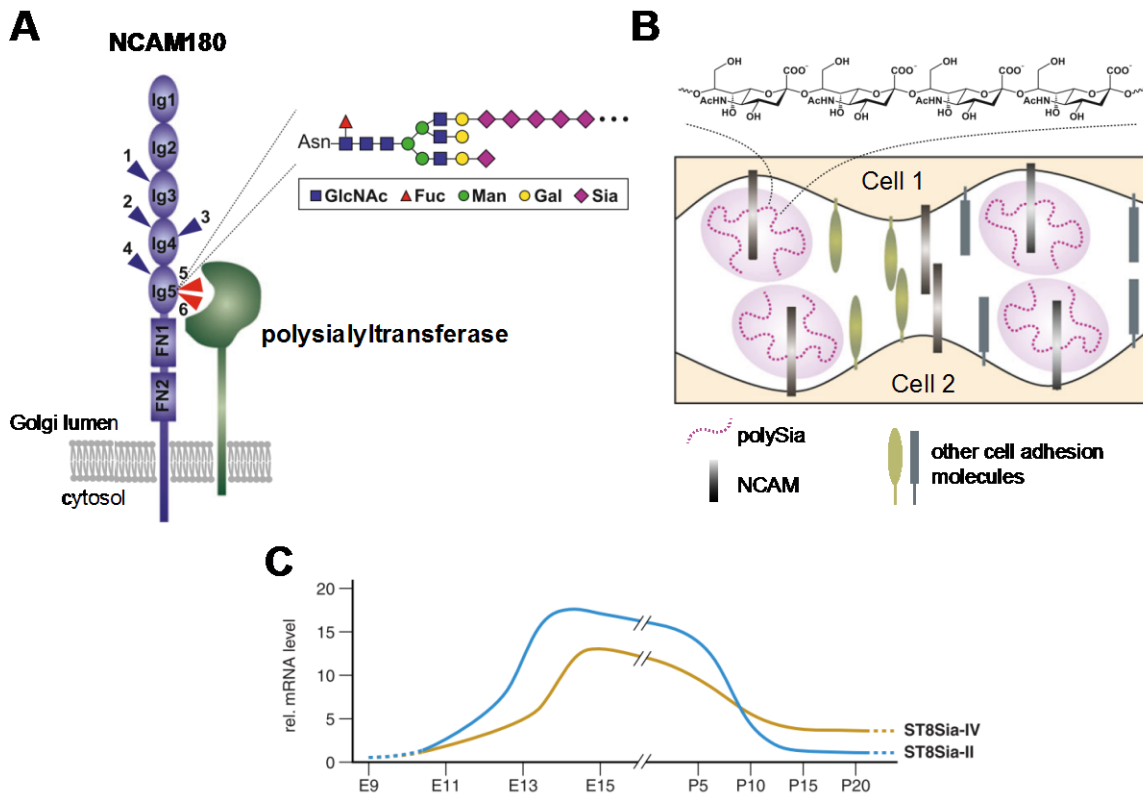


**Fig. 1.1. Structure of the transmembrane protein neural cell adhesion molecule (NCAM) and its associated glycan polysialic acid (polySia).** (A) The extracellular domain of NCAM180 shows six N-glycosylation sites (arrow heads). Please note that polySia, a homopolymer of  $\alpha$ 2–8-linked sialic acid (Sia) residues, is added to the two glycosylation sites located on the 5th immunoglobulin-like module (Ig) by a Golgi-resident polysialyltransferase (ST8SIA2 or ST8SIA4). FN, fibronectin type III repeats; GlcNAc, N-acetylglucosamin; Fuc, fucose, Man, mannose; Gal, galactose; Asn, asparagine. (B) Schematic drawing showing the anti-adhesive action of polySia. Importantly, polySia increases the intercellular space and decreases the interactions of its carrier protein and other cell adhesion molecules. (C) Time course of ST8SIA2 and ST8SIA4 expression during the development of the mouse brain. The graph is based on quantitative real-time RT-PCR analysis from whole brain mRNA extracts (Oltmann-Norden et al., 2008; Schiff et al., 2009). Adapted with modifications from (Schnaar et al., 2014; Hildebrandt and Dityatev, 2015).

## 1.2. Polysialic acid associated with NCAM: structure and biosynthesis

NCAM undergoes several post-translational modifications that have a strong impact on its functional properties. One of these modifications is the polysialylation of NCAM, that is, the synthesis and subsequent addition of the glycan polysialic acid (polySia) to the extracellular region of NCAM by the two Golgi-associated polysialyltransferases ST8SIA2 (also known as STX) and ST8SIA4 (also known as PST) (Livingston and Paulson, 1993; Eckhardt et al., 1995) (reviewed by (Rutishauser, 2008; Schnaar et al., 2014; Hildebrandt and Dityatev, 2015)) (**Fig. 1.1**). In mammals, polySia is a linear homopolymer of  $\alpha$ 2,8-glycosidically linked units of the nine-carbon monosaccharide sialic acid (Sia, also known as *N*-acetylneuraminic acid; **Fig. 1.1A** and **B**). The number of residues in polySia chains can vary from 8 to more than 100 (Rutishauser and Landmesser, 1996; Kleene and Schachner, 2004; Weinhold et al., 2005; Hildebrandt et al., 2007; Rutishauser, 2008; Schnaar et al., 2014; Hildebrandt and Dityatev, 2015). The histochemical labeling of polySia in cell cultures and brain slices can be achieved using monoclonal antibodies recognizing 8–14 residues (Frosch et al., 1985; Rougon et al., 1986; Sato et al., 1995). Because the carboxyl groups of sialic acid are negatively charged, polySia represents a polyanion with a hydration shell that increases the hydrodynamic radius of its carrier protein NCAM (**Fig. 1.1B**). Thus, polySia enlarges the intercellular space between adjacent cells, thereby attenuating homophilic interactions of the carrier protein (Yang et al., 1992; Johnson et al., 2005). It has been shown that polySia can reduce homophilic NCAM-NCAM adhesion (Sadoul et al., 1983; Rutishauser et al., 1985; Johnson et al., 2005) and NCAM-mediated signaling induced by homophilic and heterophilic interactions of NCAM (Seidenfaden et al., 2003; Seidenfaden et al., 2006; Eggers et al., 2011). These findings suggest that a typical adhesive molecule such as NCAM has the ability to convert into a repelling one upon modification with polySia.

It is important to note that the polysialyltransferase ST8SIA2 is responsible for polySia biosynthesis during embryonic development, whereas ST8SIA4 generates polySia predominantly in the adult brain (Ong et al., 1998; Oltmann-Norden et al., 2008). ST8SIA2 and ST8SIA4 belong to the family of mammalian sialyltransferases and display a high level of sequence homology (~60%) (Hildebrandt and Dityatev, 2015). They are composed of a short N-terminal cytosolic domain, a type II transmembrane domain, a stem region, and a large terminal catalytic domain

facing the Golgi lumen (Harduin-Lepers et al., 2005; Schnaar et al., 2014). NCAM carries six N-glycosylation sites, but the attachment of polySia is restricted specifically to the fifth and sixth sites that are located in the fifth Ig-like domain of NCAM (Liedtke et al., 2001). Mutational studies have revealed that polysialylation of NCAM critically depends on its first fibronectin type III domain (FN1) (Nelson et al., 1995; Mendiratta et al., 2005). Moreover, the polysialyltransferases ST8SIA2 and ST8SIA4 are able to synthesize polySia on themselves in a process termed autopolsialylation (Muhlenhoff et al., 1996; Close and Colley, 1998).

In the vertebrate brain, polySia is predominantly associated with NCAM because polySia is almost completely absent in brain slices from mice with genetic ablation of NCAM180, NCAM140, and NCAM120 (Tomasiewicz et al., 1993; Cremer et al., 1994). There is strong evidence that the two transmembrane isoforms NCAM140 and NCAM180 can be polysialylated in the embryonic and adult mouse brain, in contrast to the GPI-anchored NCAM120 isoform, which is not polysialylated (Probstmeier et al., 1994; Oltmann-Norden et al., 2008). The synaptic cell adhesion molecule (SynCAM 1) is a novel carrier of polySia in the early postnatal brain (Galuska et al., 2010). PolySia-SynCAM 1 has been detected exclusively on a subset of NG2 cells, multifunctional glia cells serving as precursor cells for myelinating oligodendrocytes in brain development and myelin repair but also for astrocytes and neurons (reviewed by (Nishiyama et al., 2009; Trotter et al., 2010)). A recent study revealed that polySia-SynCAM 1 is localized in the Golgi compartment of NG2 cells and can be transported to the cell surface upon depolarization (Werneburg et al., 2015). Similarly, polysia-NCAM has been reported to translocate to the cell surface of cultured neurons and endocrine cells in response to  $K^+$  depolarization (Kiss et al., 1994). Outside of the nervous system, the scavenger receptor and glycoprotein CD36 in human milk (Yabe et al., 2003) and neuropilin-2 in human dendritic cells (Curreli et al., 2007) might also serve as acceptors of polySia.

Under physiological conditions, the amount of polySia on the cell surface depends on its biosynthesis and internalization by clathrin-dependent endocytosis and subsequent lysosomal degradation (Minana et al., 2001; Diestel et al., 2007). In general, sialic acids are degraded by the vertebrate sialidases NEU1–NEU4. In humans, mutations in the NEU1 gene have been associated with sialidosis, an autosomal recessive metabolic disease, which leads to increased lysosomal accumulation of sialylated glycopeptides and oligosaccharides (Seyrantepe et al., 2003). In cultured hippocampal slices of P14 rats, NEU1 is able to degrade polySia expressed on immature

hippocampal granule cells, thereby inhibiting their migration in the innermost granule cell layer (Sajo et al., 2016). NEU4 is predominantly expressed in the mouse brain (Shiozaki et al., 2009) and is known to inhibit outgrowth of neurites in hippocampal neuronal cultures (Takahashi et al., 2012). However, conjugation of therapeutic proteins with polySia has been reported to increase their half-life, when applied *in vivo* (Lindhout et al., 2011; Vorobiev et al., 2013). Thus, these studies suggest that sialidases might have only limited action on polySia.

Under experimental conditions, polySia can be specifically degraded using enzymes known as endosialidases. They have been isolated from bacteriophages that take advantage of their endosialidases to degrade and penetrate the polySia-rich capsule of the human pathogen *Escherichia coli* K1. In 2005, Stummeyer and colleagues revealed the crystal structure of the endosialidase-NF (endoNF), the enzyme used in the present study (Stummeyer et al., 2005).

### **1.3. Homophilic and heterophilic interactions of NCAM and polySia**

#### **1.3.1. Interaction partners of NCAM**

Homophilic NCAM-NCAM interactions might occur either in a parallel manner between two NCAM molecules localized on the same cell membrane (*cis* interaction) or in an antiparallel manner between NCAM molecules on opposing cells (*trans* interaction). A crystallographic study has proposed that a binding between NCAM modules Ig1 and Ig2 might lead to a dimerization of NCAM molecules in parallel NCAM-NCAM interactions, while Ig1–Ig3, Ig2–Ig2, and Ig2–Ig3 binding is essential for antiparallel NCAM interactions (Soroka et al., 2003). NCAM-mediated homophilic adhesion has also been described between recombinant modules Ig1 and Ig5 and between modules Ig2 and Ig4 (Ranheim et al., 1996). Moreover, several studies have reported an interaction between modules Ig1 and Ig2 (Kiselyov et al., 1997; Jensen et al., 1999).

In addition to homophilic interactions, NCAM is involved in numerous heterophilic interactions with extra- and intracellular proteins (reviewed by (Buttner and Horstkorte, 2010; Nielsen et al., 2010)). The first fibronectin type III domain of NCAM carries the docking site for polysialyltransferases, the enzymes responsible for the addition of polysialic acid to the fifth Ig-like domain of NCAM (Mendiratta et al., 2005). Both polysialylated and non-polysialylated forms of NCAM140 and NCAM180 are proteolytically cleaved by ADAM10 and



ADAM17/tumor necrosis factor- $\alpha$ -converting enzyme (TACE), metalloproteases of the ADAM (a disintegrin and a metalloprotease) family. These enzymes mediate the generation of soluble 110–115-kD NCAM fragments, which predominantly contain the extracellular domain of NCAM (NCAM-EC) (Hinkle et al., 2006; Kalus et al., 2006). Activation of receptor tyrosine kinase EphA3 by ephrinA5 triggers shedding of polysialylated NCAM by ADAM10, leading to the release of a 250-kD soluble fragment consisting of polySia-NCAM's extracellular region (Brenneman et al., 2014). The ADAM10 cleavage site within polySia-NCAM has been identified in the second fibronectin type III domain. In cultured cortical neurons, ADAM10, EphA3, and NCAM have been found to co-localize in the cell soma and processes, and ADAM10 is involved in ephrinA5-induced growth cone collapse (Brenneman et al., 2014). In the developing medial prefrontal cortex, polySia-NCAM interacts directly with ephrinA5/EphA3 at inhibitory synapses to cooperatively constrain inhibitory perisomatic innervation of pyramidal neurons and arborization of GABAergic basket interneurons (Brenneman et al., 2013).

NCAM can directly bind the fibroblast growth factor receptor (FGFR) via the first and second fibronectin type III domains of NCAM (Kiselyov et al., 2003). It is important to note that NCAM induces axonal outgrowth through activation of the fibroblast growth factor (FGF) receptor pathway (reviewed by (Maness and Schachner, 2007)). In brief, NCAM140 and NCAM180 can both activate the FGF receptor, leading to hydrolysis of phosphoinositol 4,5-bisphosphate to diacylglycerol (DAG) by the enzyme phospholipase C $\gamma$  (PLC $\gamma$ ). Subsequently, DAG is converted to arachidonic acid by the enzyme DAG lipase, which increases calcium influx through N-type and L-type voltage-gated calcium channels and stimulates neurite outgrowth (Saffell et al., 1997; Doherty et al., 2000).

Further interaction partners of the extracellular domain of NCAM include other cell adhesion molecules such as the neural cell adhesion molecule L1 via the Ig4 module of NCAM (Horstkorte et al., 1993) and TAG-1 (also known as axonin-1 or contactin-2) (Milev et al., 1996). In the embryonic brain, NCAM has been shown to interact with several extracellular matrix (ECM) molecules, such as the heparan sulfate proteoglycans (HSPGs) agrin and collagen XVII (Storms et al., 1996a; Storms et al., 1996b), and the chondroitin sulfate proteoglycans (CSPGs) neurocan and phosphacan (Friedlander et al., 1994; Milev et al., 1994; Retzler et al., 1996). The binding sites for heparin and CSPGs are located within the Ig2 module of NCAM (Cole and Akeson, 1989; Kulahin et al., 2005). In hippocampal neurons, polySia-NCAM stimulates the formation of

synapses via interaction with HSPGs, FGF receptor, and *N*-Methyl-D-aspartate receptors (NMDARs) (Dityatev et al., 2004). Moreover, the interaction between polySia-NCAM and HSPGs is involved in the morphological changes in synapses that occur during the first hour after induction of NMDAR-dependent LTP in the CA1 subregion of hippocampal organotypic slice cultures (Dityatev et al., 2004). Interestingly, interactions with CSPG might increase the adhesion between NCAM and HSPGs (Storms et al., 1996a). Thus, these studies suggest that NCAM represents a major receptor for HSPGs and CSGPs, and that these ECM molecules may modulate neurite outgrowth, synaptogenesis, and synaptic plasticity. It is also noteworthy that the glial-cell line derived neurotrophic factor (GDNF) promotes neurite outgrowth in hippocampal and cortical neurons via binding to NCAM (Paratcha et al., 2003) (reviewed by (Ibanez, 2010)). The interaction between GDNF and NCAM requires the Ig3 module of NCAM (Sjostrand et al., 2007; Nielsen et al., 2009), and both NCAM140 and NCAM180 can induce GDNF-induced neurite outgrowth (Nielsen et al., 2009). In contrast to NCAM-mediated neurite outgrowth, GDNF-induced neurite outgrowth via NCAM does not require the presence of polySia (Nielsen et al., 2009).

The prion protein (PrP) associates with NCAM on the neuronal surface, and PrP has been shown to directly interact with NCAM (Santuccione et al., 2005). The PrP-NCAM interaction causes the recruitment of NCAM to lipid rafts, thereby stimulating NCAM-mediated neurite outgrowth via activation of the p59<sup>fyn</sup> nonreceptor tyrosine kinase (fyn) (Niethammer et al., 2002; Santuccione et al., 2005). In a posttranslational modification, NCAM140 and NCAM180 are palmitoylated at four cysteine residues, which are located in the juxta-membrane part of their transmembrane domain (Little et al., 1998). It is well known that palmitoylation of cytosolic and integral membrane proteins mediates their targeting to cholesterol- and sphingolipid-enriched microdomains of the cell membrane that are termed lipid rafts. Several studies have shown that palmitoylation plays an important role in synaptic morphology, clustering of ion channels, and synaptic strength (reviewed in (Huang and El-Husseini, 2005)). Mutation of the NCAM140 palmitoylation sites abrogates the association of NCAM to lipid rafts, reduces NCAM-mediated signaling via the focal adhesion kinase (FAK) and the extracellular signal-regulated kinase 1/2 (ERK 1/2), thereby blocking NCAM-dependent neurite outgrowth (Niethammer et al., 2002). Ponimaskin and colleagues (2008) have revealed that activation of the FGF receptor induces palmitoylation of NCAM140 and NCAM180 by the aspartate-histidine-histidine-cysteine

(DHHC) domain containing Zinc finger proteins (ZDHHC-3 and ZDHHC-7). This leads to the targeting of NCAM to lipid rafts and promotes neuronal outgrowth in hippocampal neurons (Ponimaskin et al., 2008). In a recent study, Lievens and colleagues (2016) demonstrated that the palmitoylating enzyme ZDHHC-3 is tyrosine phosphorylated by FGF receptor and src kinase. Specifically, the FGF receptor is responsible for the phosphorylation at Tyr18 of ZDHHC-3, whereas src kinase phosphorylates the ZDHHC-3 phosphorylation sites Tyr295 and Tyr297. Moreover, ablation of tyrosine phosphorylation leads to elevated autophosphorylation of ZDHHC-3, increased interaction between ZDHHC-3 and NCAM, and increased palmitoylation of NCAM. Consistently, expression of the tyrosine-mutated form of ZDHHC-3 in hippocampal neurons results in increased neuronal outgrowth compared with wild-type ZDHHC-3 (Lievens et al., 2016). Thus, this study shows that tyrosine phosphorylation of ZDHHC-3 has a physiological role in neuronal development.

The intracellular domain of NCAM180 can interact specifically with the cytoskeleton-membrane linker protein spectrin (Pollerberg et al., 1987). In this regard, Sytnik and colleagues (2006) have shown that spectrin represents a linker protein between NCAM, NMDARs, and CaMKII $\alpha$  in a postsynaptic signaling complex (Sytnyk et al., 2006). In particular, spectrin is known to interact with the GluN1, GluN2A, and GluN2B subunits of the NMDA receptor, and these interactions are modulated by calcium ions, calcium-binding protein calmodulin, and phosphorylation (Wechsler and Teichberg, 1998). Furthermore, the intracellular domain of NCAM140 shows a direct interaction with the intracellular domain of the receptor-like protein tyrosine phosphatase RPTP $\alpha$ , which is necessary for the NCAM-mediated activation of src family tyrosine kinase p59<sup>Fyn</sup> (Bodrikov et al., 2005). In response to NCAM stimulation, spectrin mediates the formation of a complex by NCAM and RPTP $\alpha$  in a Ca<sup>2+</sup>-dependent fashion. Subsequently, NCAM recruits RPTP $\alpha$  to lipid rafts to stimulate p59<sup>Fyn</sup>, thereby promoting neurite outgrowth (Bodrikov et al., 2005). The intracellular domain of NCAM can also interact with calmodulin in a Ca<sup>2+</sup>-dependent manner (Kleene et al., 2010a), the neurotrophin receptor TrkB, and the G-protein-coupled inwardly rectifying K<sup>+</sup> channel Kir3.3 (Kleene et al., 2010b). Of note, NCAM and TrkB regulate the cell membrane expression of Kir3.3 channels, and the level of Kir3.3 expression can influence NCAM-mediated neurite outgrowth. Thus, these data suggest that the interaction between NCAM, TrkB, and Kir3.3 has an important physiological role in brain development (Kleene et al., 2010b).

NCAM has been reported to restrain the expression level of G-protein-coupled inwardly rectifying K<sup>+</sup> (Kir3) channels in the cell membrane via lipid rafts (Delling et al., 2002). Kir3 channels are responsible for hyperpolarization of the postsynaptic membrane, leading to decreased cell excitability. Moreover, Kir3 channels are found presynaptically as well as postsynaptically, and the Kir3 family includes Kir3.1, Kir3.2, Kir3.3, and Kir3.4 subunits. These channels are known to form functional heterotetramers that require the presence of the Kir3.1 subunit (Wischmeyer et al., 1997), but there is also functional evidence for the existence of heterotetramers containing Kir3.2 and Kir3.3 (Jelacic et al., 2000), as well as homotetramers consisting of only Kir3.2 subunits identified postsynaptically in dopaminergic neurons of the substantia nigra, a region in the midbrain (Inanobe et al., 1999). Notably, Kir3 channels are known to interact with the serotonin 5-HT<sub>1A</sub> receptor (Luscher et al., 1997), and NCAM-deficient mice show elevated behavioral responses to agonists of the 5-HT<sub>1A</sub> receptor (Stork et al., 1999). In addition, NCAM-deficient mice exhibit elevated aggression between males due to increased activation of limbic brain regions during social interaction (Stork et al., 1997). Nevertheless, tissue concentration of serotonin and binding of 5-HT<sub>1A</sub> receptors are not altered in the brains of NCAM-deficient mice (Stork et al., 1999).

Interestingly, NCAM has been shown to directly interact with dopamine D<sub>2</sub> receptors (D<sub>2</sub>Rs), thereby promoting the internalization and degradation of D<sub>2</sub>Rs (Xiao et al., 2009). Consequently, NCAM-deficient mice display increased cell-surface expression of D<sub>2</sub>Rs and enhanced dopaminergic D<sub>2</sub>R signaling. Behavioral analysis has revealed that NCAM-deficient mice show increased sensitivity to the agonist of D<sub>1</sub>/D<sub>2</sub>Rs agonist apomorphine after dopamine depletion as well as elevated locomotor activity mediated by D<sub>2</sub>Rs (Xiao et al., 2009).

### **1.3.2. Interaction partners of polySia**

Similarly, polySia associated with NCAM has been implicated in interactions with several neurotrophic factors and neurotransmitters (reviewed in (Senkov et al., 2012)). Müller and colleagues (2000) have shown that the brain-derived neurotrophic factor (BDNF) can restore impaired synaptic plasticity in the CA1 region of hippocampal slices from NCAM-deficient mice (Muller et al., 2000). In addition, depletion of polySia causes suppressed BDNF-dependent survival and differentiation of cortical neurons, and BDNF signaling is decreased in the absence of polySia (Vutskits et al., 2001). These effects of polySia removal could be restored by the

addition of exogenous BDNF, suggesting that BDNF binds to polySia-NCAM. Indeed, a subsequent study by Kanato and co-workers has demonstrated that a BDNF dimer directly interacts with polySia under physiological conditions (Kanato et al., 2008). Intriguingly, this interaction requires a polySia with a minimum degree of polymerization of 12 (DP = 12). Likewise, polySia can form complexes with other neurotrophic factors, including nerve growth factor, neurotrophin-3, and neurotrophin-4 (Kanato et al., 2008). Furthermore, polySia-NCAM is involved in platelet-derived growth factor (PDGF)-induced migration of oligodendrocyte precursor cells, which plays an important role in myelin repair and formation in the central nervous system (Zhang et al., 2004). Thus, this finding indicates a possible interaction between PDGF and polySia. Recently, polySia has been reported to directly bind to fibroblast growth factor-2 (FGF2), and this interaction requires polySia chains with a degree of polymerization of at least 17 (DP = 17) (Ono et al., 2012). Moreover, FGF2-mediated cell growth is inhibited in polySia-NCAM-expressing murine fibroblast NIH-3T3 cells (Ono et al., 2012). In addition to neurotrophic factors, polySia is known to directly bind to the neurotransmitter dopamine and is involved in Akt-mediated signaling via dopamine receptor D2 in human neuroblastoma cells (Isomura et al., 2011). Therefore, Ono and colleagues (2012) have proposed the idea that polySia might serve as a “reservoir” for several neurotrophic factors and neurotransmitters.

Several studies have provided evidence indicating that polySia-NCAM might directly interact with glutamatergic receptors in the hippocampus. PolySia is known to potentiate  $\alpha$ -amino-3-hydroxy-5-methylisoxazole-4-propionic acid receptors (AMPA receptors) in a concentration-dependent manner in immature CA1 pyramidal cells, suggesting a direct interaction between polySia and AMPARs (Vaithianathan et al., 2004). Moreover, polysialylation of NCAM can alter the effects of NBQX, an AMPAR-selective competitive antagonist, on mouse behavior (Potschka et al., 2008). Accordingly, NCAM-deficient mice and ST8SIA4-deficient mice show higher levels of NBQX-induced ataxia and increased seizure thresholds compared with their wild-type littermates (Potschka et al., 2008).

In rats that have undergone induction of *in vivo* long-term potentiation (LTP) in the hippocampal dentate gyrus (DG) by tetanic stimulation of the perforant path, both NCAM180 and GluN2A-containing *N*-methyl-D-aspartate (NMDARs) have been detected at the edges of postsynaptic densities in rats. In contrast, NCAM180 and GluN2A are mainly located in the center of postsynaptic densities in the DG of control non-stimulated rats (Fux et al., 2003). Electron

microscopic analysis in the rat dentate gyrus has revealed that polySia is located perisynaptically in dendritic spines, where it associates with postsynaptic densities (Rodriguez et al., 2008). PolySia has been shown to specifically inhibit GluN2B-mediated currents induced by application of 3  $\mu$ M glutamate, but not by 30  $\mu$ M glutamate, in cultured hippocampal neurons (Hammond et al., 2006). Notably, such low glutamate concentrations have been reported for the extracellular space (Sherwin, 1999; Ueda et al., 2000). In line with these findings, polySia reduces open probability of recombinant heterodimeric GluN1/GluN2B- and heterotrimeric GluN1/GluN2A/GluN2B-NMDARs, which have been expressed in phospholipid bilayers and activated by 3  $\mu$ M glutamate (Kochlamazashvili et al., 2010).

Sialic acid-binding Ig superfamily lectins (Siglecs) represent type 1 membrane proteins that bind to sialic acid residues of glycoproteins. Recently, Siglec-11 has been discovered as a member of the CD33-related Siglecs superfamily of human Siglecs (Angata et al., 2002). Accordingly, Siglec-11 consists of five extracellular Ig-like domains, a transmembrane domain, and a cytosolic tail. Wang and Neumann (2010) have reported that human Siglec-11 expressed on murine microglia binds to polySia on neurons, thereby reducing inflammatory responses of microglia (Wang and Neumann, 2010). Recently, the same research group has demonstrated that polySia with a degree of polymerization 20 (DP = 20) has anti-inflammatory effects via interaction with Siglec-11 on human macrophages (Shahraz et al., 2015).

An extracellular pool of the histone H1, a nuclear protein responsible for the organization of nucleosomes in DNA packaging, can directly bind to polySia at the cell surface (Mishra et al., 2010). It is also noteworthy that histone H1 promotes neural outgrowth of Schwann cells *in vitro* as well as functional recovery of femoral nerve injury *in vivo* in a polySia-dependent fashion (Mishra et al., 2010).

#### **1.4. PolySia expression in the developing brain**

In the mouse embryonic brain, polySia is detectable starting from embryonic day E9 and is abundantly expressed over the time course of embryonic and early postnatal development. Similarly, expression of ST8SIA2 and ST8SIA4 mRNA becomes evident at embryonic day E8.5, which is the time point of neural tube closure. In the time period between E10.5 to E13.5, the mRNA expression of both polysialyltransferases strongly increases to reach a plateau phase that

persists until birth (Probstmeier et al., 1994; Ong et al., 1998). On the other hand, polySia synthesis is highest at E12 and thus coincides with the maximal expression of ST8SIA2 and ST8SIA4 transcripts. In line with the expression profiles for polysialyltransferases, NCAM mRNA expression is maximal between E11 and P10. These findings suggest that the synthesis of polySia is regulated at the level of ST8SIA2 and ST8SIA4 transcription (Ong et al., 1998).

During postnatal development, the expression of both polysialyltransferases strongly decreases. At postnatal day P1, ST8SIA2 mRNA is almost two-fold higher compared with ST8SIA4 mRNA, and the total pool of NCAM is polysialylated at this age (Galuska et al., 2006; Oltmann-Norden et al., 2008). ST8SIA2 mRNA displays a relatively steep reduction in a short period between P5 and P11 on the whole brain level, while ST8SIA4 mRNA decreases at a slower rate between P1 and P15 and becomes the predominant polysialyltransferase showing five-fold higher expression than ST8SIA2 in the third postnatal week. In agreement with the profiles of polysialyltransferases, polySia expression gradually decreases between P9 and P17 in whole brain lysates. The constant expression of NCAM and the parallel reduction of polySia synthesis during the first three postnatal weeks lead to the appearance of NCAM140 and NCAM180 that are negative for polySia (Oltmann-Norden et al., 2008). In the human dentate gyrus, polySia immunoreactivity has been reported to be maximal during the first three years of life and decreases between the second and third decades to a level that remains relatively constant with increasing age (Ni Dhuill et al., 1999).

During embryonic and early postnatal development, polySia has been identified on several cell types, such as olfactory interneuron precursors migrating tangentially from the anterior subventricular zone of the lateral ventricle to the olfactory bulb (Bonfanti and Theodosis, 1994; Rousselot and Nottebohm, 1995), precursors of interneurons in the cortex (Seki and Arai, 1991, 1993), and granule cells in the cerebellum (Hekmat et al., 1990). In the adolescent visual cortex, activity-dependent PolySia expression is involved in the maturation of perisomatic GABAergic inhibition by basket interneurons, which in turn regulate the onset and time course of ocular dominance plasticity, also known as the critical period (Di Cristo et al., 2007). In cortical slice cultures, maturation of GABAergic synapses is promoted by NCAM120/NCAM140-mediated activation of the Fyn kinase (Chattopadhyaya et al., 2013). Furthermore, polySia is expressed on radial glia of mesencephalon and cortex (Li et al., 2004; Schiff et al., 2009), Bergmann and Müller glia in the cerebellum and retina (Bartsch et al., 1990; Hekmat et al., 1990; Kustermann et

al., 2010), and axons of developing fiber tracts, including the corticospinal tract, optic nerve, and fibers connecting the thalamus and cortex (Bartsch et al., 1990; Seki and Arai, 1991; Daston et al., 1996; Chung et al., 2004).

### **1.5. Expression of NCAM and polySia in the adult brain**

In the rodent and human hippocampus, NCAM is intensively expressed in the hilus and inner molecular layer of the dentate gyrus (DG) and in the mossy fiber tract, which contains the axons of DG granule cells projecting to CA3 pyramidal neurons. Similarly, abundant immunohistochemical staining against NCAM has been reported in stratum radiatum and stratum oriens of the hippocampal CA1 subregion (Miller et al., 1993). In the aged human brain, polySia-NCAM is expressed in several areas, including the middle temporal gyrus, superior frontal gyrus, entorhinal cortex, hippocampal dentate gyrus, CA1 field, and subiculum (Mikkonen et al., 1999; Murray et al., 2016).

Mice constitutively deficient in all three main NCAM isoforms show various mild morphological changes, including reduced size of the olfactory bulb, abnormal lamination of mossy fibers in the hippocampal CA3 subregion, reduced total brain weight, and reduced body weight (Cremer et al., 1994; Cremer et al., 1997), severe hypoplasia of the corticospinal tract (Rolf et al., 2002), and impaired synaptic vesicle release at the neuromuscular junction (Polo-Parada et al., 2001). Likewise, mice with homozygous ablation of the NCAM180 isoform show reduced size of the olfactory bulb, decreased numbers and abnormal organization of granule cells in the olfactory bulb, and disorganized pyramidal cell layer in the CA3 subregion of the hippocampus (Tomasiewicz et al., 1993). These morphological defects suggest impaired cell migration, which is mainly attributed to the loss of polySia carried by NCAM180 in the mutant (Tomasiewicz et al., 1993).

Being highly expressed during embryonic development, polySia is strongly down-regulated during the first three weeks after birth in mice. Nevertheless, in the adult brain, expression of polySia is maintained in brain regions showing high levels of neurogenesis and neuronal plasticity. The neurogenic niche of the anterior subventricular zone of the lateral ventricle is derived from the embryonic lateral ganglionic eminence and persists into the adult brain (Pencea and Luskin, 2003). In the subventricular zone of the lateral ventricle, slowly dividing astrocytes



transform into rapidly dividing precursors that then generate polySia-positive olfactory interneuron precursors. These interneuron precursors migrate in the rostral migratory stream from the subventricular zone of the lateral ventricle to the olfactory bulb, in which they differentiate into periglomerular and glomerular interneurons (Bonfanti and Theodosis, 1994; Doetsch and Alvarez-Buylla, 1996; Doetsch et al., 1997). The second neurogenic niche revealing high levels of polySia expression in the adult brain is the subgranular zone of the dentate gyrus in the hippocampus. Here, astrocytic stem cells give rise to polySia-positive neuroblasts that migrate tangentially into the granule cell layer, where they differentiate into new granule cell neurons (Doetsch, 2003). In adult rodents, polySia-NCAM is particularly expressed in immature neurons located in the subventricular zone of the lateral ventricle, subgranular zone of the dentate gyrus, as well as in the layer II of the paleocortex (reviewed by (Nacher et al., 2013)).

Although ST8SIA2-deficient and ST8SIA4-deficient mice display normal morphology of the rostral migratory stream (RMS) and olfactory bulb (OB) (Eckhardt et al., 2000; Angata et al., 2004), a recent study found accumulations of calretinin (CR)-positive interneurons around the RMS in mice lacking ST8SIA2 at postnatal day P30. This implies that even a partial reduction in polySia levels in the RMS of ST8SIA2-deficient mice can impair the migration of SVZ-derived neuroblasts (Rockle and Hildebrandt, 2016). These changes were accompanied by significant reductions of calbindin (CB)-positive cells in the glomerular layer of the OB in both ST8SIA2-deficient and ST8SIA4-deficient mice at P30 (Rockle and Hildebrandt, 2016).

Apart from the neurogenic zones and the layer II of the paleocortex, polySia has also been identified in subsets of mature GABAergic interneurons in several brain regions, including hippocampus (Nacher et al., 2002a), entorhinal cortex (Gomez-Climent et al., 2011), prefrontal cortex (Varea et al., 2005; Varea et al., 2007; Gilabert-Juan et al., 2011; Gomez-Climent et al., 2011), piriform cortex (Nacher et al., 2002c), amygdala (Nacher et al., 2002b; Gilabert-Juan et al., 2011), and septum (Foley et al., 2003). In the prefrontal cortex, polySia-expressing interneurons have been reported to express the Ca<sup>2+</sup>-binding proteins calbindin and somatostatin, whereas hippocampal polySia-expressing interneurons are positive for cholecystokinin and calretinin (Gomez-Climent et al., 2011). This thus implies that the neurochemical phenotype of these interneurons can vary between brain regions. Notably, polySia-positive interneurons in the ventral hippocampus show decreased density of perisynaptic contacts, reduced dendritic arborization, and lower density of dendritic spines when compared with polySia-negative

interneurons, suggesting that polySia is involved in their structural plasticity (Gomez-Climent et al., 2011). Moreover, mice with genetic deletion of ST8SIA2, ST8SIA4, or both polysialyltransferases display decreased density of both parvalbumin- and somatostatin-expressing interneurons in the medial prefrontal cortex during adulthood (Krocher et al., 2014). Intriguingly, the spine density of hippocampal inhibitory interneurons is elevated two days after the enzymatic depletion of polySia using an *in vivo* injection of endosialidase N, but it is decreased when analyzed 7 days after injection (Guirado et al., 2014).

In the adult hippocampus, polySia is abundantly expressed in the mossy fibers of mature granule cells, while it is absent in their cell bodies located in the granule cell layer (Seki and Arai, 1993). This pattern can be observed also in the CA1 subregion, where polySia is identified at the dendrites and axons but not on the cell bodies of CA1 pyramidal cells (Becker et al., 1996). Besides the hippocampus and cortex, polySia is highly expressed in astrocytes and neurons in the hypothalamo-neurohypophysial system (Theodosis et al., 1999; Monlezun et al., 2005).

Adult mice lacking ST8SIA2 reveal reduced levels of polySia in the cerebral cortex, hippocampal dentate gyrus, and olfactory bulb. Similarly to NCAM-deficient mice, ST8SIA2 knockout mice display morphological deficits, including mistargeting of hippocampal infrapyramidal mossy fibers and formation of ectopic synapses (Angata et al., 2004). In contrast, ST8SIA4-deficient mice show normal brain development, which can be explained by the ability of ST8SIA2 to synthesize polySia during brain development, thereby compensating for the loss of ST8SIA4 in these knockout mice (Eckhardt et al., 2000).

The importance of polySia has been demonstrated by the finding that mice that simultaneously lack both polysialyltransferases (*St8sia2*<sup>-/-</sup> *St8sia4*<sup>-/-</sup>) die within four weeks of age (Weinhold et al., 2005). *St8sia2*<sup>-/-</sup> *St8sia4*<sup>-/-</sup> mice are entirely negative for polySia and exhibit severe morphological abnormalities, including progressive hydrocephalus, postnatal growth retardation, impaired corticospinal tract, agenesis of the anterior commissure, and hypoplasia of the internal capsule. In the healthy mouse brain, the internal capsule represents a prominent fiber tract to and from the cortex. Moreover, double-knockout mice are characterized by hypoplasia of the mammillothalamic tract, which projects from the mammillary bodies to thalamus and is part of the so called Papez' circuit in wild-type mice (Weinhold et al., 2005). This circuit includes

thalamus, cortex, hippocampus, and mammillary bodies, and is known to play a role in spatial working memory (Radyushkin et al., 2005).

There is converging evidence that polySia carried by NCAM plays a role in the regulation of endogenous circadian rhythms, which are synchronized with the daily light-dark cycles (Glass et al., 1994; Shen et al., 1997; Shen et al., 1999; Glass et al., 2000; Shen et al., 2001; Fedorkova et al., 2002; Prosser et al., 2003). Polysialylated NCAM is expressed in the hypothalamic suprachiasmatic nucleus, a brain region of key importance for the regulation of circadian rhythms (Glass et al., 1994; Shen et al., 1999). It has been demonstrated that mice lacking polySia-NCAM show impaired circadian functions (Shen et al., 1997; Shen et al., 2001). Consistent with this finding, similar disturbances of circadian rhythms are observed after the enzymatic depletion of polySia by injections of endoneuraminidase N (endoN) to the suprachiasmatic nucleus *in vivo* (Shen et al., 1997; Glass et al., 2000; Fedorkova et al., 2002). It has been shown that proteolytic fragments of NCAM, which consist of the intracellular domain, the transmembrane domain, and a part of the extracellular domain, can enter the nucleus in response to stimulation with function-inducing antibodies (Kleene et al., 2010a). A more recent study has revealed that polySia attached to a NCAM fragment is imported to the nucleus upon NCAM stimulation to interact with nuclear histone H1 in cultured hippocampal neurons. Furthermore, *in vitro* experiments in cerebellar neurons and *in vivo* analysis in several brain regions have shown that the nuclear import of polySia-NCAM is correlated with the expression of clock-related genes, thereby supporting the view that polySia might regulate circadian rhythm in mice (Westphal et al., 2016).

## 1.6. PolySia-NCAM in synaptic plasticity during adulthood

The role of polySia-NCAM in NMDA receptor-dependent synaptic plasticity in the hippocampal CA1 subregion has been extensively investigated using electrophysiological methods (for summary, see **Table 1.1**). Two main forms of synaptic plasticity have been described at excitatory synapses, namely, long-term potentiation (LTP) and long-term depression (LTD). LTP refers to the persisting (over several hours) potentiation of synaptic response that can be induced by application of high-frequency stimulation or other protocols resulting in co-activation of the pre- and postsynaptic neurons. In contrast, LTD represents the decrease of synaptic response after application of low-frequency stimulation (reviewed by (Malenka and Bear, 2004; Bliss and Collingridge, 2013)). Lüthi and coworkers have demonstrated that injection of polyclonal

antibodies against NCAM results in a strong decrease of LTP at Schaffer collateral-CA1 synapses in the hippocampus (Lüthi et al., 1994). Importantly, mice constitutively deficient in all three NCAM isoforms (*Ncam*<sup>-/-</sup>) (Cremer et al., 1994; Muller et al., 1996; Muller et al., 2000; Kochlamazashvili et al., 2010) as well as mice conditionally deficient in NCAM (*NCAMff+*) (Bukalo et al., 2004) show impairments in LTP and LTD in the CA1 subregion of the adult brain. Similarly, selective enzymatic removal of polySia by endosialidase N (Becker et al., 1996; Muller et al., 1996) or genetic ablation of the polysialyltransferase ST8SIA4 in mice (*St8sia4*<sup>-/-</sup>) (Eckhardt et al., 2000) lead to impaired LTP and LTD in the CA1 subregion of hippocampal slices. Of note, polySia-NCAM ablation affects neither basal synaptic transmission nor short-term potentiation, the plasticity measured within 2 min after application of theta-burst stimulation (Becker et al., 1996; Kochlamazashvili et al., 2010). It has been shown that injections of extracellular region of polySia-NCAM or soluble polySia (colominic acid) fully restore decreased LTP in the CA1 subregion, whereas injection of non-polysialylated NCAM had no effect on CA1 LTP induction (Senkov et al., 2006). Thus, these studies suggest that synaptic plasticity in the CA1 subregion depends on polySia rather than on its protein carrier NCAM.

Although polySia-NCAM is intensively expressed in the CA3 region and mossy fibers in wild-type mice, *in vivo* electrophysiological recordings have revealed that only adult *Ncam*<sup>-/-</sup> mice, but not *St8sia4*<sup>-/-</sup> mice, show reduced LTP levels in the dentate gyrus (Stoenica et al., 2006). Interestingly, *St8sia2*<sup>-/-</sup> mice show normal LTP, but abnormal basal synaptic transmission in the dentate gyrus (Stoenica et al., 2006). Moreover, LTP levels at mossy fibers–CA3 synapses are reduced in hippocampal slices from mature *Ncam*<sup>-/-</sup> mice (Cremer et al., 1998) but not in slices from *St8sia4*<sup>-/-</sup> mice (Eckhardt et al., 2000), indicating that synaptic plasticity in the CA3 subregion is modulated by NCAM rather than polySia (**Table 1.1**).

**Table 1.1. Functional impact of NCAM, polySia, and polysialyltransferases on synaptic plasticity in the hippocampus.** *Ncam*<sup>-/-</sup>, mice that are constitutively deficient in NCAM; *Ncamff+*, conditional deletion of NCAM in mice under the control of a calcium-calmodulin-dependent kinase II ( $\alpha$ CaMKII) promotor; CA, *Cornu Ammonis*; DG, dentate gyrus; LTP, long-term potentiation; LTD, long-term depression. ↓, reduced; =, unchanged; n.d., not determined. Adapted with modifications from (Hildebrandt and Dityatev, 2015).

Condition	CA1 LTP	CA1 LTD	CA3 LTP	DG LTP
<i>Ncam</i> <sup>-/-</sup>	↓	↓	↓	↓
<i>Ncam</i> <sup>ff+</sup>	↓	↓	=	n.d.
Endosialidase	↓	↓	=	n.d.
<i>St8siaIV</i> <sup>-/-</sup>	↓	↓	=	=
<i>St8siaII</i> <sup>-/-</sup>	=	n.d.	=	=

Recently, the downstream mechanisms underlying the deficits in synaptic plasticity in polySia-deficient hippocampus have been revealed (Kochlamazashvili et al., 2010) (reviewed by (Varbanov and Dityatev, 2016)). Notably, reduced LTP levels in the CA1 subregion of hippocampal slices from adult *Ncam*<sup>-/-</sup> mice were associated with increased activation of GluN2B-containing NMDARs in this region. Furthermore, GluN2B-NMDAR-mediated Ca<sup>2+</sup> transients in CA1 pyramidal neurons are increased after acute treatment with endosialidase NF (endoNF) to remove polySia, and elevated Ca<sup>2+</sup> transients can be restored to control levels by addition of polySia. It is noteworthy that the GluN2B-selective antagonist Ro 25-6981 fully restored abnormal CA1 LTP levels in slices from *Ncam*<sup>-/-</sup> mice and endoNF-treated slices (Kochlamazashvili et al., 2010); see also detailed overview in **Fig. 1.2**. Thus, these data suggest that NCAM-associated polySia might control the balance between predominantly extrasynaptic GluN2B- and synaptic GluN2A-mediated transmission in the CA1 subregion.

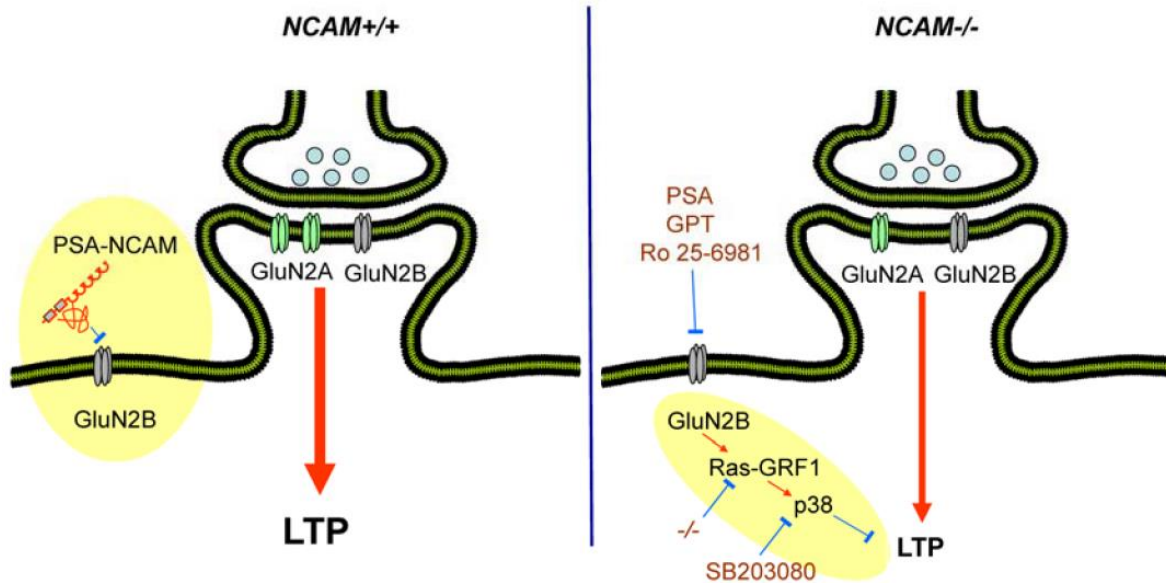


**Fig. 1.2. The role of polySia carried by the neural cell adhesion molecule (NCAM) in synaptic plasticity in the hippocampal CA1 subregion.** In wild-type mice, polySia (PSA)-NCAM restrains currents through extrasynaptic GluN2B-containing NMDARs and long-term potentiation (LTP) is promoted by synaptic GluN2A-containing NMDARs. In mice lacking NCAM (*Ncam*<sup>-/-</sup>), currents through GluN2B-containing NMDARs are elevated, leading to reduced LTP via increased activation of the calcium sensor Ras-GRF1 (guanine nucleotide exchange factor 1) and Rac effector p38 MAP (mitogen-activated protein) kinase. The abnormal LTP in *Ncam*<sup>-/-</sup> mice could be restored by application of soluble polySia, the GluN2B-specific antagonist Ro 25-6981, the glutamate scavenger glutamic-pyruvic transaminase (GPT), and the p38-specific antagonist SB203080. Note also that mice deficient in Ras-GRF1 show normal LTP. CA, Cornu Ammonis; adapted with modifications from (Kochlamazashvili et al., 2010).

Expression of NCAM and polySia-NCAM in neurons and astroglia has been reported to decrease with increasing age (Fox et al., 1995a; Kaur et al., 2008). In line with these findings, Kochlamazashvili and coworkers (2012) have demonstrated that NCAM-deficient mice show a steep and progressive decline in NMDA receptor-dependent LTP with age when measured at 3, 12, and 24 months, whereas age-matched wild-type mice revealed decreased LTP levels only at 24 months of age (Kochlamazashvili et al., 2012).

Transgenic mice that overexpress the extracellular domain of NCAM under the control of a neuron-specific enolase promoter (NCAM-EC mice) (Pillai-Nair et al., 2005) show a region-specific decrease in NMDAR-dependent LTP and short-term potentiation (STP) in the medial prefrontal cortex but normal STP and LTP in the hippocampal CA1 subregion (Brenneman et al., 2011). The expression levels of NCAM-EC in these mice reflect those obtained in postmortem samples from schizophrenic patients (Vawter, 2000). Notably, NCAM-EC mice exhibit reduced perisomatic puncta of  $\gamma$ -amino butyric acid (GABA) interneurons immunoreactive for glutamic acid decarboxylase (GAD)65, GAD67, and GABA transporter 1 (GAT-1) in the frontal cortex, cingulate cortex, and amygdala but not in the hippocampus (Pillai-Nair et al., 2005). GAD is the enzyme that is responsible for the biosynthesis of GABA. Its two isoforms, GAD65 and GAD67, are both expressed in GABAergic inhibitory interneurons, but they differ in their intraneuronal distribution. While GAD65 is mainly localized in nerve terminals, GAD67 is found throughout the soma and neuronal processes (Kaufman et al., 1991; Feldblum et al., 1993). Likewise, GAT-1 is localized in presynaptic nerve terminals of GABAergic interneurons in the neocortex (Minelli et al., 1995). The impaired GABAergic inhibition in NCAM-EC mice is consistent with studies showing altered expression levels of synaptic markers of GABAergic interneurons in the prefrontal cortex of schizophrenic patients (Akbarian et al., 1995; Volk et al., 2001). Further, NCAM-EC mice show reduced density of dendritic spines on pyramidal neurons in the cingulate cortex, indicating deficits in excitatory synapses (Pillai-Nair et al., 2005).

### 1.7. Role of polySia-NCAM in rodent models of learning and memory

Several behavioral studies in rodents have shown that polySia-NCAM plays a role in learning and memory. The Morris water maze is a hippocampus-dependent task, in which rodents have to find the spatial position of a hidden escape platform in a water tank over the course of several trials. Severe learning impairments in the Morris water maze have been demonstrated in *Ncam*<sup>-/-</sup> mice (Cremer et al., 1994; Stork et al., 2000), *St8sia4*<sup>-/-</sup> mice (Markram et al., 2007a; Zerwas et al., 2015), as well as in rats that have received intra-hippocampal injections of endosialidase N before behavioral testing (Becker et al., 1996). It is noteworthy that mice with postnatal conditional inactivation of the NCAM gene under the control of  $\alpha$ CaMKII in the hippocampus (*NCAM*<sup>ff+</sup>) display relatively mild behavioral deficits in the water maze task (Bukalo et al., 2004). In *St8sia4*<sup>-/-</sup> mice, impaired long-term memory in the spatial version of water maze task

could be restored by enriched environment (Zerwas et al., 2015). Altogether, these findings indicate that hippocampus-associated spatial learning is mediated by polySia carried by NCAM.

In fear conditioning, an animal is exposed to a conditioned stimulus (tone or context) paired with an unconditioned stimulus (footshock). After a few pairings of conditioned and unconditioned stimuli, healthy rodents quickly learn to associate the previously neutral conditioned stimulus with the aversive unconditioned stimulus. Consequently, even the neutral conditioned stimulus alone is sufficient to elicit fear-related responses such as freezing, which then can be quantified as a measure of fear memory acquisition (LeDoux, 2000). While so-called cued/auditory fear conditioning requires intact neural circuits in the amygdala, contextual fear conditioning depends on processing in both hippocampus and amygdala (LeDoux, 2000; Senkov et al., 2006). Notably, *Ncam*<sup>-/-</sup> mice show impaired learning in contextual fear conditioning as well as in cued/auditory fear conditioning (Stork et al., 2000; Senkov et al., 2006; Jurgenson et al., 2010). Similar deficits in both contextual and cued/auditory fear memory have been reported in *St8sia2*<sup>-/-</sup> mice (Angata et al., 2004). In *St8sia4*<sup>-/-</sup> mice, hippocampus- and amygdala-dependent contextual fear conditioning is reduced compared with wild-type control mice, whereas amygdala-dependent auditory fear conditioning is normal in *St8sia4*<sup>-/-</sup> mice (Senkov et al., 2006; Markram et al., 2007a).

When injected into the hippocampus before behavioral training, polySia-NCAM, but not NCAM, can partially rescue impaired contextual and cued fear memories in *Ncam*<sup>-/-</sup> mice (Senkov et al., 2006). In contrast, pretraining intrahippocampal injection of polySia-NCAM in control *Ncam*<sup>+/+</sup> mice reduces their contextual memory, but polySia-NCAM has no effect on their auditory fear memory (Senkov et al., 2006), suggesting that both lack and excess of polySia in the hippocampus lead to cognitive disturbances. Furthermore, a recent study has revealed that a pretraining injection of the selective GluN2B-NMDAR antagonist Ro 25-6981 into the hippocampus of *Ncam*<sup>-/-</sup> mice fully restores their abnormal contextual fear memory (Senkov et al., 2006). Thus, genetic ablation of polySia-NCAM might disrupt contextual fear conditioning via increased GluN2B-mediated neurotransmission.

The object recognition test comprises two sessions. In the first session (familiarization), an animal is allowed to explore two identical objects in an open field. In a second (test) session, one of the objects is replaced by a novel object. Because healthy rodents prefer exploring novel rather



than familiar objects, the exploration times for both objects in the test phase are measured and used to quantify object recognition memory for the novel object (Leger et al., 2013). Object recognition memory is known to depend on the hippocampus, medial prefrontal cortex, and perirhinal cortex (reviewed by (Warburton and Brown, 2015)). While homozygous *Ncam*<sup>-/-</sup> mice reveal impaired learning in object recognition tests (Jurgenson et al., 2010), heterozygous *Ncam*<sup>+/-</sup> mice are normal in this behavioral paradigm (Jurgenson et al., 2012). Moreover, both *St8sia2*<sup>-/-</sup> and *St8sia4*<sup>-/-</sup> mice display impaired learning in the object recognition test (Kröcher et al., 2015; Zerwas et al., 2015), indicating that polysialylated NCAM is involved in object recognition memory. Enriched environment has been shown to restore deficits in long-term object recognition memory in *St8sia4*<sup>+/-</sup> mice (Zerwas et al., 2015).

Interestingly, mice overexpressing the soluble extracellular domain fragment of NCAM (NCAM-EC) show impaired contextual and cued fear conditioning (Pillai-Nair et al., 2005), and they show impaired working memory in the prefrontal cortex-dependent delayed-non-match-to-sample task (Brenneman et al., 2011). These behavioral abnormalities imply that increased shedding of NCAM might lead to perturbation of synaptic circuits in the prefrontal cortex and amygdala (Brenneman et al., 2011) .

Several behavioral studies have shown that learning itself can alter the expression of polySia-NCAM in several brain regions. In the adult hippocampal dentate gyrus, levels of polySia-NCAM are increased when assessed 12–24 hours after learning in the spatial version of Morris water maze (Murphy et al., 1996; Venero et al., 2006) 12–24 hours after passive avoidance task (Doyle et al., 1992; Fox et al., 1995b), and 12–24 hours after contextual fear conditioning (Sandi et al., 2003; Lopez-Fernandez et al., 2007). In the amygdala, expression of polySia-NCAM has been shown to be increased 24 hours after auditory fear conditioning (Markram et al., 2007b). Similar upregulation of polySia expression has been demonstrated in the ventromedial prefrontal cortex, including the infralimbic, orbitofrontal and insular cortices of rats after Morris water maze training (Ter Horst et al., 2008). In contrast, passive avoidance conditioning induces a decrease in polySia in the dorsomedial prefrontal cortex, including cingulate and prelimbic cortices. These findings indicate that learning-associated changes in polySia expression in the prefrontal cortex may largely depend on the behavioral task and on the neural circuits that are involved in the behavior (Ter Horst et al., 2008).

## 1.8. *N*-methyl-D-aspartate receptors: structure and functions

As introduced above, polySia-NCAM might modulate signaling through glutamate receptors (reviewed by (Senkov et al., 2012; Hildebrandt and Dityatev, 2015)). In the central nervous system and the spinal cord, glutamate receptors mediate fast excitatory synaptic transmission and are expressed on both neurons and glia (reviewed by (Traynelis et al., 2010)). Glutamate receptors play a central role in activity-dependent synaptic plasticity and memory encoding (Malenka and Bear, 2004; Morris, 2013). Further, glutamate receptors have been implicated in several neuropsychiatric and neurological disorders, such as schizophrenia, major depression, Alzheimer's disease, Parkinson's disease, stroke, and neuropathic pain (Lau and Zukin, 2007; Zhuo, 2009; Traynelis et al., 2010). Ionotropic glutamate receptors represent ion channels that are activated by the excitatory neurotransmitter glutamate and they are permeable for cations. According to their pharmacology and structure, glutamate receptors can be subdivided into three main classes, including  $\alpha$ -amino-3-hydroxy-5-methyl-4-isoxazolepropionic acid receptors (AMPA), kainate receptors, and *N*-methyl-D-aspartate receptors (NMDARs).

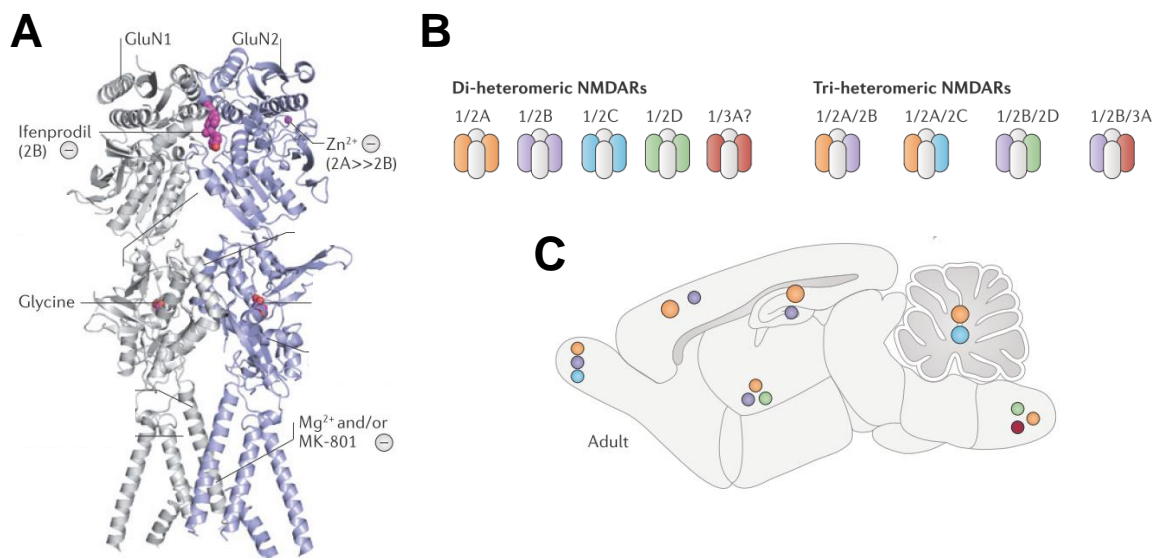


**Fig. 1.3. Structure and expression of NMDARs.** (A) Overview of NMDAR binding sites for extracellular small-molecule ligands that represent subunit-specific allosteric modulators. Binding sites that are not relevant for this doctoral thesis have been omitted for clarity. The picture shows a model of GluN1/GluN2 heterodimer that is prepared on the basis of X-ray crystal structures of GluN1/GluN2B N-

terminal domains (Karakas et al., 2011) and GluN1/GluN2A agonist binding domains (Furukawa et al., 2005). Positive and negative allosteric modulation are shown by + and – signs, respectively. **(B)** Subunit compositions of NMDARs in the central nervous system. Heterodimeric NMDARs contain the GluN1 subunit and an additional GluN subunit, while heterotrimeric NMDARs show a mixture of three different GluN subunits **(C)** Schematic diagram of the adult mouse brain showing the expression of different GluN subunits. Adapted with modifications from (Paoletti et al., 2013).

The NMDAR represents a heterotetramer that primarily consists of two obligatory GluN1 subunits and two GluN2 subunits (**Fig. 1.3B**) (reviewed by (Traynelis et al., 2010; Paoletti et al., 2013)). Four different types of GluN2 subunits have been reported, namely GluN2A, GluN2B, GluN2C, and GluN2D. The functional activation of NMDARs requires the collective presence of the NMDAR agonist glutamate and the NMDAR co-agonist glycine (Johnson and Ascher, 1987; Kleckner and Dingledine, 1988). Subsequent studies have revealed that D-serine (Mothet et al., 2000; Henneberger et al., 2010), another NMDAR co-agonist, can serve as a substitute for glycine. Glutamate binds to the GluN2 subunit, while glycine and D-serine bind to the strychnine-insensitive NMDAR glycine-binding site, which has been identified in the GluN1 and GluN3 subunits (Furukawa et al., 2005). In contrast to other types of ionotropic ligand-gated receptors, NMDARs exhibit a voltage-dependent block by extracellular  $Mg^{2+}$  ions, and they are highly permeable for  $Ca^{2+}$  ions. It is known that these properties are strongly governed by NMDAR subunit composition. Moreover, NMDARs show remarkably slow kinetics due to slow unbinding of glutamate (Paoletti et al., 2013). It is noteworthy that the gating properties of NMDARs largely depend on the type of GluN2 subunits. GluN1/GluN2A-containing NMDARs show the fastest decay of excitatory postsynaptic currents (EPSCs), a measure of glutamate deactivation kinetics, from all GluN2 subunits. In contrast, GluN1/GluN2B-NMDARs are characterized by their slow EPSC decay. Furthermore, the GluN2A subunit displays considerably lower sensitivity to glutamate and glycine compared to the GluN2B subunit (Paoletti et al., 2013).

During development, the expression of GluN2 subunits changes dramatically (Monyer et al., 1994). Whereas GluN2B and GluN2D subunits are highly expressed during embryonic stages and decrease with age, GluN2A expression begins following birth and gradually increases over the course of development. In the adult hippocampus and the cortex, postsynaptic NMDARs are composed of heterodimeric (GluN1/GluN2A and GluN1/GluN2B) or heterotrimeric

(GluN1/GluN2A/GluN2B) (**Fig. 1.3C**). It has been reported that heterotrimeric NMDARs account for 15% to >50% of the total receptor population in the adult cortex and hippocampus (Al-Hallaq et al., 2007; Rauner and Kohr, 2011).

In addition to synaptic sites, NMDARs are also expressed at perisynaptic and extrasynaptic sites, such as the spine neck and dendritic shaft. It has been shown that extrasynaptic NMDARs predominantly contain GluN2B rather than GluN2A subunits (Angulo et al., 2004; Fellin et al., 2004; Hardingham and Bading, 2010). Remarkably, the role of NMDAR subunit composition in synaptic plasticity is still not completely understood. It has been proposed that activation of GluN2A-containing NMDARs is involved in the induction of LTP, whereas activation of GluN2B-containing NMDARs promotes LTD in several brain regions (Liu et al., 2004; Massey et al., 2004; Zhao and Constantine-Paton, 2007; Papouin et al., 2012). Nevertheless, GluN2B-containing NMDARs might also play a role in LTP induction, and they are not always involved in LTD induction (Berberich et al., 2005; Weitlauf et al., 2005; Zhao et al., 2005; Morishita et al., 2007; von Engelhardt et al., 2008). Thus, the involvement of NMDAR subunit composition in synaptic plasticity might depend on animal's age, LTP/LTD induction protocols, brain region, and, possibly, type of the synapse.

Moreover, several studies indicate that activation of synaptic NMDARs supports neuronal health, whereas extrasynaptic NMDAR-induced signaling leads to neuronal cell death and have thus been implicated in neurodegenerative diseases, such as Huntington's disease and ischemic stroke (reviewed by (Hardingham and Bading, 2010)).

### **1.9. The NMDAR glycine-site as a therapeutic target in the treatment of schizophrenia**

Schizophrenia is a severe chronic neuropsychiatric disease that has a relatively high prevalence (approximately 1% of the world's population), and shows its onset during adolescence or early adulthood (Freedman, 2003). The clinical symptoms of schizophrenia can be subdivided into two main categories: psychotic (also known as positive) and deficit (negative). Psychotic symptoms include thought disorganization, auditory hallucinations, and delusions, such as persecution and megalomania, while negative symptoms involve withdrawal from social life, affect flattening, apathy, speech poverty, and anhedonia (i.e., the inability to experience pleasure) (Frankle et al.,

2003). In addition to the well-known positive and negative symptoms, schizophrenic patients show deficits in major cognitive processes mediated by the dorsolateral prefrontal cortex, including attention, working memory, and executive functions (Lewis and Lieberman, 2000; Lewis and Moghaddam, 2006). Importantly, these cognitive symptoms might occur several years before the onset of psychotic symptoms, and they are stable over the time course of the disorder, predicting long-term functional disability of the patients (Gold, 2004). Antipsychotic drugs, which act as antagonists of the dopamine D<sub>2</sub> receptor, represent the standard pharmacological treatment in schizophrenia. They have been shown to efficiently alleviate positive symptoms in schizophrenic patients (Howes and Kapur, 2009). However, it has to be emphasized that D<sub>2</sub> receptor antagonists have only limited effects on the negative and cognitive symptoms in schizophrenic patients (reviewed by (Beck et al., 2016)). In agreement with these findings, it has been shown that one third of schizophrenic patients do not respond to standard antipsychotic drugs (Beck et al., 2014). Therefore, there is an urgent need for the development of novel treatment strategies targeting receptor types involved in the cognitive and negative symptoms of schizophrenia. Extensive research in the last decades indicates that dysregulation of NMDARs in the prefrontal cortex and hippocampus plays an important role in the pathophysiology of schizophrenia (reviewed by (Kantrowitz and Javitt, 2010; Geddes et al., 2011)). Several early studies have demonstrated that non-competitive NMDAR antagonists, such as ketamine and phencyclidine (PCP), can induce schizophrenic symptoms in healthy humans (Krystal et al., 1994; Steinpreis, 1996). Consequently, these observations have led to the development of the NMDA hypothesis of schizophrenia (for recent reviews, see (Javitt, 2012; Moghaddam and Javitt, 2012)), which postulates that agents enhancing NMDAR function might improve schizophrenic symptoms that are resistant to standard antipsychotic treatment (Javitt and Zukin, 1991). Because the direct stimulation of NMDARs by agonists of the glutamate binding site on the GluN2 subunit results in several side effects, including seizures, cell death, and memory loss (Wolf et al., 1990; Misztal et al., 1996), subsequent studies have focused on strategies for the indirect enhancement of NMDARs (reviewed by (Danysz and Parsons, 1998; Balu and Coyle, 2015)). To date, one of the most promising targets for positive modulation of NMDARs is the strychnine-insensitive NMDAR glycine-binding site, which is located on the GluN1 subunit (Johnson and Ascher, 1987). In clinical studies, agonists of the NMDAR glycine site, such as glycine, D-serine, D-cycloserine, and the glycine transporter 1 (GlyT1) inhibitor sarcosine, have

been proposed to alleviate the negative and cognitive symptoms in schizophrenic patients, when used in combination with antipsychotic treatment (reviewed by (Shim et al., 2008; Javitt, 2012)).

Despite their therapeutic potential in schizophrenia (reviewed by (Danysz and Parsons, 1998)), the endogenous full NMDAR glycine site agonists glycine and D-serine are rapidly metabolized, and they thus require high daily doses to pass the blood-brain barrier and enter the brain in patients (Javitt, 2012). Therefore, GlyT1 inhibitors, including sarcosine and novel compounds with high specificity, are of particular interest for the current study. Their mechanism of action and effects on synaptic plasticity will be introduced in the following subchapters.

### **1.9.1. Glycine transporter 1 inhibitors in synaptic plasticity and learning**

An alternative strategy for NMDAR enhancement involves the inhibition of glycine transporters, which are responsible for glycine reuptake, thereby leading to increased levels of extracellular glycine in the vicinity of NMDARs located in the synaptic cleft (reviewed by (Harvey and Yee, 2013; Balu and Coyle, 2015)). Two main subtypes of specific glycine transporters have been reported, GlyT1 and GlyT2, which both belong the family of Na<sup>+</sup>/Cl<sup>-</sup>-dependent transporters of neurotransmitters (Supplisson and Bergman, 1997; Lopez-Corcuera et al., 1998). At the regional level, GlyT1 and GlyT2 are both expressed in spinal cord, brain stem, and cerebellum; however, GlyT1 is expressed additionally in forebrain regions, including prefrontal cortex, hippocampus, septum, and thalamus (Smith et al., 1992; Zafra et al., 1995b; Zafra et al., 1995a; Cubelos et al., 2005). At the cellular level, GlyT2 has been identified in presynaptic glycinergic terminals in the spinal cord, while GlyT1 is expressed mainly in glial cells (Zafra et al., 1995b), but also in pre- and postsynaptic terminals at excitatory glutamatergic synapses in close association with NMDARs (Cubelos et al., 2005; Harvey and Yee, 2013). According to these findings, GlyT2 regulates the extracellular glycine level mainly at inhibitory glycinergic synapses in the spinal cord, whereas GlyT1 is involved in glycine uptake predominantly at excitatory glutamatergic synapses in the forebrain. Although the glycine concentration in the mammalian cerebrospinal fluid is relatively high (approximately 6 μM) (McGale et al., 1977) compared with the dissociation constant ( $K_D$ ) of the NMDAR glycine-binding site, it has been assumed that the glycine-binding site is not saturated *in vivo* because the glycine concentration near NMDAR at the glutamatergic synapse is maintained at sub-saturating concentrations by the GlyT1 (Supplisson and Bergman, 1997; Bergeron et al., 1998).

Previous preclinical studies have demonstrated that the glial GlyT1 plays an important role in NMDA-dependent synaptic plasticity, leading to the development of several GlyT1 inhibitors (reviewed by (Javitt, 2012; Harvey and Yee, 2013)). The endogenous amino acid sarcosine (also known as N-methyl glycine) has been identified as a low-affinity competitive inhibitor of GlyT1 (Smith et al., 1992; Herdon et al., 2001; Zhang et al., 2009a; Zhang et al., 2009b). Another extensively studied compound is the sarcosine derivate NFPS (ALX 5407), which is a selective and potent inhibitor of the GlyT1 (Bergeron et al., 1998; Atkinson et al., 2001; Herdon et al., 2001). Electrophysiological studies in brain slices have shown that several GlyT1 inhibitors can enhance NMDAR-mediated excitatory postsynaptic currents from pyramidal cells in the CA1 subregion of the hippocampus (Bergeron et al., 1998; Martina et al., 2004; Depoortere et al., 2005; Boulay et al., 2008) and in the prefrontal cortex (Chen et al., 2003; Fossat et al., 2012). Furthermore, GlyT1 inhibitors are known to increase the magnitude of NMDAR-dependent LTP in the CA1 *in vitro* (Martina et al., 2004; Zhang et al., 2008; Alberati et al., 2012). *In vivo* studies in anesthetized rats have revealed that GlyT1 inhibitors can potentiate NMDAR-mediated responses in the prefrontal cortex (Chen et al., 2003) and increase the level of LTP in the hippocampal dentate gyrus (Kinney et al., 2003; Manahan-Vaughan et al., 2008).

Several behavioral studies have shown that GlyT1 inhibitors can attenuate cognitive disturbances in animal models of schizophrenia. GlyT1 inhibitors improve cognitive deficits in object recognition memory and social recognition memory in rats treated with the NMDAR antagonists MK-801 or phencyclidine (PCP) (Boulay et al., 2008; Chaki et al., 2015), and working memory in mice treated with MK-801 and/or the muscarinic acetylcholine receptors antagonist scopolamine (Harada et al., 2012). Furthermore, GlyT1 inhibitors are known to attenuate impaired reference memory in MK-801-treated rats (Manahan-Vaughan et al., 2008) and spatial learning in aged rats (Harada et al., 2012). In wild-type C57BL/6 mice, the selective GlyT1 inhibitor SSR504734 improves working memory in the continuous delayed alternation task (Singer et al., 2009). In animal models of epilepsy, GlyT1 inhibitors increase seizure threshold and decrease seizure duration (Zhang et al., 2008; Socala et al., 2010; Shen et al., 2015). Recently, it has been revealed that GlyT1 inhibitors can abrogate depression-like behavior in rats (Huang et al., 2013; Chaki et al., 2015). In humans, adjuvant therapy with GlyT1 inhibitors has been reported to ameliorate negative, cognitive, and depressive symptoms in schizophrenia (Lane et al., 2005) (reviewed by (Tsai and Lin, 2010; Javitt, 2012)), and improved symptoms in other

neuropsychiatric disorders, such as depression (Huang et al., 2013) and obsessive-compulsive disorder (Wu et al., 2011). In schizophrenia, a meta-analysis comparing the efficacy of several NMDAR glycine-site agonists concluded that glycine, D-serine, and sarcosine show more beneficial effects than D-cycloserine on the overall psychopathology in schizophrenic patients treated with antipsychotics (Tsai and Lin, 2010).

### **1.10. Involvement of NCAM and polySia in psychiatric and neurodegenerative diseases**

Changes in the expression of NCAM or polySia have been reported in several psychiatric and neurodegenerative diseases, such as bipolar disorder, schizophrenia, depression, and Alzheimer's disease (AD) (for reviews, see (Vawter, 2000; Brennaman and Maness, 2010; Hildebrandt and Dityatev, 2015)). Schizophrenic patients show decreased postmortem expression of polySia-NCAM in the hippocampal dentate gyrus (Barbeau et al., 1995) as well as in the dorsolateral prefrontal cortex (Gilabert-Juan et al., 2012). Similarly, postmortem levels of polySia-NCAM are reduced in the amygdala of patients suffering from depression, whereas polySia-NCAM is increased in the amygdala of bipolar disorder patients (Varea et al., 2012). NCAM180, the longest isoform of NCAM, is decreased in postmortem samples from the cerebellar cortex of autistic patients (Purcell et al., 2001). The secreted isoform of NCAM (115 kDa and 108 kDa) shows an increased 115 kDa/ 108 kDa ratio in the hippocampus of bipolar disorder patients (Vawter et al., 1999).

Levels of soluble NCAM fragments (105–115 kDa), which consist primarily of the extracellular domain of NCAM (NCAM-EC), are altered in the cerebrospinal fluid (Poltorak et al., 1995; van Kammen et al., 1998; Vawter et al., 1998a; Vawter et al., 2001) and in postmortem samples from hippocampus and prefrontal cortex (Honer et al., 1997; Vawter et al., 1998b) of patients diagnosed with schizophrenia. Recently, Piras and colleagues have shown that elevated polySia-NCAM levels in the blood serum of schizophrenic patients are correlated with negative symptoms, declarative memory impairment, and reduced volume of Brodmann area 46, which is located in the left PFC. Notably, serum polySia-NCAM levels are not associated with the dosages of antipsychotic medication (Piras et al., 2015).



Several genetic association studies have suggested that single nucleotide point mutations (SNPs) within *ST8SIA2* and *NCAM1* genes are associated with schizophrenia, bipolar disorder, and autism spectrum disorder (Arai et al., 2006; Atz et al., 2007; Sullivan et al., 2007; Tao et al., 2007; McAuley et al., 2012; Gilabert-Juan et al., 2013; Shaw et al., 2014) (reviewed by (Brenneman and Maness, 2010; Sato et al., 2016)). Interestingly, *ST8SIA2*, which is located on chromosome 15q26, has been shown to represent a common susceptibility locus for both schizophrenia and bipolar disorder (Vazza et al., 2007), whereas variations in the *ST8SIA4* gene are not associated with schizophrenia (Arai et al., 2006). Moreover, the expression mRNA level of *ST8SIA4* is not changed in schizophrenia patients (Volk et al., 2016).

In AD patients, polySia-NCAM expression in the hippocampal dentate gyrus is increased compared with healthy controls (Mikkonen et al., 1999; Jin et al., 2004; Perry et al., 2012); however, a recent study has revealed decreased expression of polySia-NCAM in the entorhinal cortex of AD patients (Murray et al., 2016). Levels of NCAM are reduced in the frontal and temporal cortex of AD patients (Yew et al., 1999; Aisa et al., 2010). Moreover, levels of NCAM are increased in serum samples from AD patients (Todaro et al., 2004). It is also noteworthy that soluble NCAM fragments in the cerebrospinal fluid are considerably increased in AD patients compared with healthy controls, but this increase remains below the significance level (Strekalova et al., 2006).

### **1.11. Objectives of the thesis**

Expression levels of polySia-NCAM are altered in the dorsolateral prefrontal cortex of schizophrenic patients (Brenneman and Maness, 2010), and both polySia and NCAM have been associated with impaired neurocognition in schizophrenia (Sullivan et al., 2007; Piras et al., 2015). Recently, it has been shown that LTP is reduced in the mPFC of mice overexpressing the extracellular domain fragment of NCAM (Brenneman et al., 2011). However, the role of polySia-NCAM in synaptic plasticity in the adult murine mPFC has remained unknown.

To determine whether acute removal of polySia may affect the activation of NMDARs and AMPARs in the mPFC, I carried out whole-cell patch-clamp recordings of AMPAR- and NMDAR-mediated currents from layer V pyramidal neurons in sham- and endoNF-treated mPFC

slices from adult C57BL/6 mice and mice deficient in the polySia-synthesizing enzyme ST8SIA4.

Because NCAM-deficient mice show increased activation of extrasynaptic GluN2B-containing NMDARs in the hippocampal CA1 subregion, we sought to determine whether endoNF treatment or genetic ablation of ST8SIA4 would change the sensitivity of NMDAR-mediated currents from mPFC pyramidal neurons to low concentration of the GluN2B-selective blocker Ro 25-6981 (Volianskis et al., 2013). Moreover, we aimed to assess whether tonic NMDAR-mediated currents, which reflect the activation of extrasynaptic NMDARs (Le Meur et al., 2007; Papouin et al., 2012), would be altered after enzymatic ablation of polySia or genetic abrogation of ST8SIA4 in the mPFC.

A previous study has shown that polySia with a degree of polymerization (DP) of 25–50 inhibits GluN2B-NMDAR-mediated currents in cultured hippocampal neurons (Hammond et al., 2006). However, the impact of oligomers of sialic acid and polySia with a low degree of polymerization on NMDAR currents has not been addressed. Thus, one of the major objectives of this thesis was to determine the effects of oligomers and short-chain polymers of sialic acid on NMDAR-mediated currents using whole-cell patch-clamp recordings in mPFC slices in control conditions and after endoNF treatment. In addition, we asked whether the recently described polySia mimetic tegaserod (Bushman et al., 2014) would have effects on NMDAR-mediated currents.

Importantly, we wondered whether acute enzymatic removal of polySia or genetic ablation of the polySia-synthesizing enzyme ST8SIA4 would affect basal synaptic transmission and synaptic plasticity in the mPFC. To this aim, I recorded LTP in sham- and endoNF-treated mPFC slices from C57BL6 mice, ST8SIA4-deficient mice (*St8sia4*<sup>-/-</sup>), and their wild-type littermates (*St8sia4*<sup>+/+</sup>). Moreover, I examined the impact of NCAM protein on synaptic plasticity in the mPFC by measuring the levels of LTP in mPFC slices from NCAM-deficient (*Ncam*<sup>-/-</sup>) mice.

In the mPFC, polySia is known to be predominantly expressed by a subpopulation of GABAergic interneurons (Gomez-Climent et al., 2011). To study the effects of polySia removal on the GABAergic input from interneurons to pyramidal neurons, I recorded GABA<sub>A</sub>-mediated currents from mPFC pyramidal cells during theta-burst stimulation, which is used to induce LTP, in sham- and endoNF-treated slices.

Finally, I tested several pharmacological strategies for restoration of abnormal synaptic plasticity in endoNF-treated slices and slices from *St8sia4*<sup>-/-</sup> mice, including application of oligomers and short-chain polymers of sialic acid, inhibition of GluN1/GluN2B-NMDARs, and two different inhibitors of the glial glycine transporter type 1 (GlyT1). In addition, I tested whether the glycine transporter type 1 sarcosine might restore reduced LTP levels in mPFC slices from *Ncam*<sup>-/-</sup> mice. We also asked whether a GluN2B-selective blocker or a GlyT1-selective inhibitor would change LTP in brain slices from C57BL6 mice, *St8sia4*<sup>+/+</sup>, and *Ncam*<sup>+/+</sup> mice.

## 2. MATERIALS AND METHODS

### 2.1. Animals

All treatments and behavioral procedures were conducted in accordance with animal research ethics standards defined by German law and approved by the Ethical Committee on Animal Health and Care of the State of Saxony-Anhalt.

Mice constitutively deficient in the polysialyltransferase ST8SIA4 (*St8Sia4*<sup>-/-</sup>) (Eckhardt et al., 2000) and their wild-type littermates (*St8Sia4*<sup>+/+</sup>) were backcrossed to C57BL/6J mice for >8 generations. *St8sia4*<sup>-/-</sup> and *St8sia4*<sup>+/+</sup> mice for experiments were obtained by mating male and female *St8sia4*<sup>+/-</sup> mice. Mice constitutively deficient for NCAM (*Ncam*<sup>-/-</sup>) (Cremer et al., 1994) and their wild-type littermates (*Ncam*<sup>+/+</sup>) were backcrossed to C57BL/6J mice for >10 generations. NCAM mice were kindly provided by Prof. Dr. Herbert Hildebrandt (Hannover Medical School). C57BL/6J, *St8sia4*<sup>-/-</sup>, and *St8sia4*<sup>+/+</sup> mice were bred at the animal facility of DZNE Magdeburg.

For electrophysiological experiments in acute brain slices, we used adult 2–4-month-old C57BL/6J, *St8sia4*<sup>-/-</sup>, and *St8sia4*<sup>+/+</sup> mice, and 4–9-month-old *Ncam*<sup>-/-</sup> and *Ncam*<sup>+/+</sup> mice from both sexes. Immunohistochemistry and confocal imaging of polySia were performed in 2–4-month-old *Thy1*-GFP mice (M line: Tg(Thy1-EGFP)MJrs/J; The Jackson Laboratory, Maine, USA).

Mice were kept in a reverse light-dark cycle (12:12 hours, light on at 9:00 pm) with food and water *ad libitum*. Electrophysiological experiments were carried out during the dark phase of the cycle, when mice are active.

### 2.2. Electrophysiological recordings in mPFC brain slices

#### 2.2.1. Preparation of acute brain slices

Each mouse was quickly sacrificed by cervical dislocation. Following rapid decapitation using large scissors, the head was placed in a Petri dish (on crushed ice) that was filled with ice-cold (0–4 °C) slicing artificial cerebrospinal fluid (aCSF) that was saturated with 95% O<sub>2</sub>/5% CO<sub>2</sub> (carbogen). The slicing aCSF contained the following (in mM): 250 sucrose, 24 NaHCO<sub>3</sub>, 25

glucose, 2.5 KCl, 1.25 NaH<sub>2</sub>PO<sub>4</sub>, 2 CaCl<sub>2</sub>, and 1.5 MgCl<sub>2</sub> (osmolality 345–350 mOsm/kg, pH 7.4) (Kochlamazashvili et al., 2010). To minimize ischemic death of the neural tissue, the time for brain removal was kept between 1 and 1.5 min. The mouse head was kept in place by holding it with a bent forceps (length 13.5 cm, Carl Roth, Karlsruhe, Germany) that was inserted into the eye sockets. A sagittal cut through the skin was made using fine scissors (Hardened Fine Iris Scissors, straight, length 8.5 cm, FST, Heidelberg, Germany), and the excess skin and muscle tissue were removed using a fine forceps (Dumont #2 Laminectomy Forceps, straight, length 12 cm, FST) to expose the parietal and frontal bones. Starting from the occipital bone, the parietal bones were cut along the sagittal sutures using fine scissors (**Fig. 2.1**, cut 1) and removed. To facilitate bone removal, two more parallel cuts were made laterally through the occipital and parietal bones (**Fig. 2.1**, cuts 2 and 3). Notably, special care was taken to prevent damage of the brain surface while using scissors and forceps. The remaining frontal bones were then removed using a fine forceps after applying two lateral cuts along the eye sockets using fine scissors (**Fig. 2.1**, cuts 4 and 5). These cuts were especially helpful when dissecting mice older than 2 months, because the thickness of skull bone increases with age. Following removal of the occipital, interparietal, parietal, and frontal bones using a fine forceps, the optic nerves were cut, and the whole brain was removed from the skull using a small metal spatula (width 3 mm, Carl Roth). The cerebellum was then trimmed away using a scalpel, thereby creating a clean flat surface that was necessary for glueing the brain on the magnetic specimen holder of a VT1200S vibratome (Leica, Nussloch, Germany) using Vetbond™ tissue adhesive (3M™, Germany). The specimen holder carrying the glued brain was quickly submerged and mounted in the buffer tray of the vibratome, which was pre-filled with slicing aCSF. The temperature of the slicing aCSF in the vibratome chamber was maintained at 0–4°C by filling the surrounding ice tray of the vibratome with crushed ice. Coronal slices containing the prelimbic and infralimbic cortices (1.9–1.3 mm anterior to bregma) (Franklin and Paxinos, 2007) were cut using the VT1200S vibratome equipped with double-edged Platinum+Teflon blades (Industrieklingen Nr. 13510, Martor, Solingen, Germany) while the slicing solution was continuously bubbled with 95% O<sub>2</sub>/5% CO<sub>2</sub>. The thickness of cortical slices was 400 μm for extracellular recordings and 350 μm for patch-clamp recordings. It is noteworthy that only two to three mPFC slices (350 or 400 μm) could be obtained from an adult mouse brain. Using a Pasteur pipette with a wide tip (broken and fire-polished, diameter 4–5 mm), the acute slices were transferred to a slice holding chamber (**Fig. 2.2**) filled with 200 ml of 95% O<sub>2</sub>/5% CO<sub>2</sub>-saturated recording aCSF (osmolality 300–305

mOsm/kg, pH 7.4) that contained 120 mM NaCl instead of sucrose (Eckhardt et al., 2000; Kochlamazashvili et al., 2010), where they were incubated for varying time periods and at different temperature depending on pharmacological treatment and mouse genotype (see below). For experiments including field excitatory postsynaptic potential (fEPSP) recordings or patch-clamp recordings in endosialidase NF (endoNF)-treated sections, slices from C57BL/6J mice were first allowed to recover for 20 min at room temperature (22–25°C) in recording aCSF. The slices were then incubated in 2 ml of sham solution (recording aCSF) or endoNF (10 µg/ml in aCSF) at 35°C for 2 hours. For sham/endoNF treatment, we used a 24-well plate that was installed in a water bath (ED, Julabo, Seelbach, Germany). For fEPSP recordings in knockout mice, mPFC slices were stored in recording aCSF for >2 hours at room temperature before recordings were initiated. For patch-clamp recordings in knockout mice, acute slices were first incubated at 35°C for 20 min in recording aCSF and then stored at room temperature for >30 min prior to recordings. During all incubation steps and recordings, solutions were continuously bubbled with 95% O<sub>2</sub>/5% CO<sub>2</sub>.

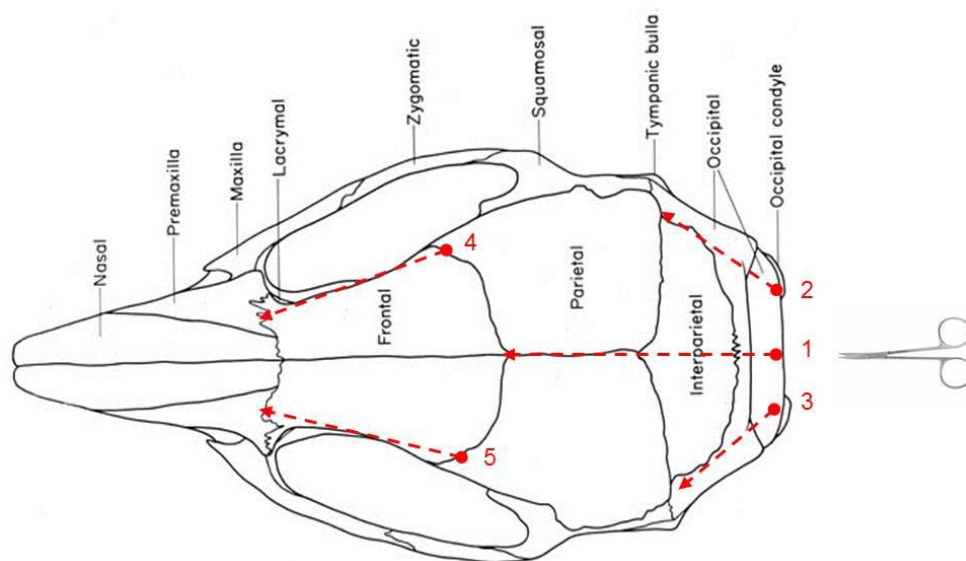


**Fig. 2.1. Dorsal view of the mouse skull.** Red dotted arrows with numbers denote the location and order of cuts that were made through the skull bones during laminectomy. Details are given in the text. The illustration was adapted with modifications from [www.informatics.jax.org](http://www.informatics.jax.org).

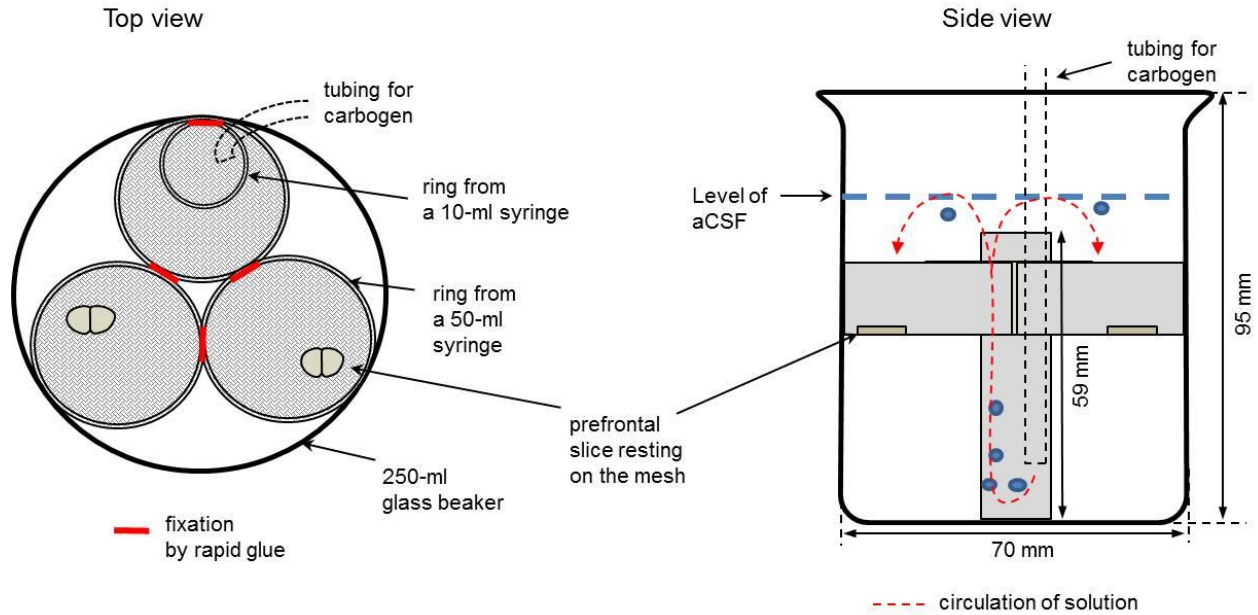


**Fig. 2.2. Chamber for incubation of acute brain slices.** Three plastic rings were prepared from a large syringe (capacity 50 ml). A fine mesh from standard cotton muslin was stretched and glued on each ring. A tube (length 59 mm) made from a small syringe (capacity 10 ml) was glued in one of the rings, and all three rings were glued together using rapid glue. This construction could be neatly fitted into a standard beaker (capacity 250 ml, Carl Roth). A silicon tubing (outer diameter 3.5 mm) with perforations in the lower third was used for bubbling with 95% O<sub>2</sub>/5% CO<sub>2</sub> (carbogen) and was inserted into the tube made from a 10 ml syringe. After their release from the carbogen tubing, the bubbles rise to the aCSF surface within the 10 ml syringe. Please note that it is important to protect the brain slices from mechanical disturbance by rising bubbles. The fine cotton mesh allows for sufficient oxygenation of the brain slices. In this way, the solution can reach both sides of the slices. The slice chamber can be stored either at room temperature or in a water bath at physiological temperature depending on the selected incubation protocol.

### 2.2.2. Extracellular LTP recordings

Each mPFC slice (400  $\mu$ m) was placed into a submerged-type recording MC membrane chamber (volume 2 ml; Scientific Systems Design Inc., Mississauga, Ontario, Canada), which was continuously perfused with 95% O<sub>2</sub>/5% CO<sub>2</sub>-bubbled recording ACSF using a perfusion system connected to a programmable peristaltic pump controlled by LinLab software (Scientifica, Uckfield, UK). In the recording chamber, the brain slice was secured using a HSG5F harp slice

grid, which was made of a steel ring and a fine nylon mesh (ALA Scientific Instruments, Inc., Farmingdale, NY, USA). The perfusion rate was maintained at 4 ml/min in all experiments, and fEPSP recordings were performed at room temperature (22–25°C) using a PTC03 proportional temperature controller (Scientific Systems Design Inc., Mississauga, Ontario, Canada). Some recordings were carried out at physiological temperature (35°C, as indicated in the Results section). The prefrontal cortex was visualized using a 4x objective of a SliceScope Pro 6000 upright fixed-stage microscope (Scientifica).

Glass pipettes for extracellular recordings were pulled on a DMZ universal electrode puller (Zeitz Instruments GmbH, Martinsried, Germany) using thin-walled borosilicate glass capillaries (wall thickness 0.188 mm; length 100 mm, outer diameter 1.5 mm, Hilgenberg, Malsfeld, Germany). Both recording and stimulating electrodes were filled with carbogen-saturated recording aCSF. The stimulating glass electrode (tip resistance 0.3–0.5 M $\Omega$ ) was carefully inserted into the slice surface in layers 2/3 of the prelimbic cortex using the low-speed mode of the PatchStar micromanipulator (Scientifica). Layer 2/3 was chosen for stimulation because it represents the location of the input fibers of pyramidal neurons in layer 5 (Huang et al., 2004). The recording glass electrode (tip resistance 2–2.5 M $\Omega$ ) was gently placed on layer 5 of the prelimbic cortex, which is the location of dendrites and cell bodies of pyramidal cells (Huang et al., 2004). Electrical stimuli (pulse duration 0.2 ms) to layer 2/3 input fibers were applied using an A385 stimulus isolator (WPI, Berlin, Germany), and the resulting evoked fEPSPs were recorded using a double patch-clamp EPC10 amplifier (HEKA, Lambrecht, Germany). First, the stimulation intensity was set to 70  $\mu$ A (every 10 s, frequency 0.1 Hz), and the recording electrode was slowly deepened in the slice until the maximal fEPSP amplitude was reached. To study the basal synaptic transmission in the brain slice, electrical stimuli with increasing intensity (40–85  $\mu$ A, step 5  $\mu$ A) were applied every 20 s (frequency 0.05 Hz), and the relationship between stimulation intensity and fEPSP slope was determined. The supramaximal stimulation intensity was defined as the stimulation strength necessary to elicit a population spike, a small upward-going peak occurring during the fEPSP decay due to increasing number of pyramidal cells that fire action potentials in response to increasing synaptic stimulation (Taube and Schwartzkroin, 1988). For LTP experiments, baseline fEPSPs were recorded at 0.05 Hz for at least 10 min at ~50% of the supramaximal stimulation intensity. In recordings with persisting population spikes, the stimulation intensity was reduced to ~40% of the supramaximal value. If the fEPSP slope was not



stable during these 10 min, the baseline recording was repeated or the slice exchanged. To induce LTP of fEPSPs in mPFC slices, five trains of theta-burst stimulation (TBS) were applied (inter-theta interval 20 s) (Brenneman et al., 2011). Each TBS train was composed of eight bursts of stimuli delivered at 5 Hz, while each burst consisted of four stimuli applied at 100 Hz (stimulus duration 0.2 ms). To calculate the magnitude of LTP in each slice, the mean fEPSP slope was measured during 0–10 min before TBS (baseline) and during 50–60 min after the delivery of TBS. Subsequently, the mean fEPSP slope obtained during 50–60 min after TBS was normalized to the mean fEPSP slope during 0–10 min before TBS. For reasons of clarity, stimulus artifacts in the representative examples of cortical fEPSPs in all figures were blanked.

### **2.2.3. Whole-cell patch-clamp recordings**

#### **2.2.3.1. Recordings of evoked EPSCs**

Each mPFC slice (thickness 350  $\mu\text{m}$ ) was transferred to a submerged-type recording MC membrane chamber (Scientific Systems Design Inc.) and was continuously perfused (flow rate 4 ml/min) with 95%  $\text{O}_2$ /5%  $\text{CO}_2$ -bubbled recording aCSF at room temperature (22–25°C). Pyramidal neurons located in layer 5 of the prelimbic cortex were identified based on their triangular cell bodies and long apical dendrites. They were visualized using 40x water-immersion objective (numerical aperture 0.8) mounted on a upright fixed-stage microscope Olympus microscope (Tokyo, Japan), which was part of a SliceScope Pro 6000 electrophysiology system (Scientifica). The microscope was equipped with infrared illumination and differential interference contrast (DIC) videomicroscopy (Dodt and Zieglansberger, 1990).

For synaptic stimulation, a thin-walled glass electrode (tip resistance 0.3–0.5  $\text{M}\Omega$ ) was filled with recording aCSF and was positioned in layer II/III of the prelimbic cortex. Recordings were carried out using an EPC10 double patch-clamp amplifier (HEKA), which was operated via the PatchMaster software (HEKA). Patch pipettes (tip resistance 3–5  $\text{M}\Omega$ ) were pulled using thick-walled borosilicate glass capillaries (wall thickness 0.315 mm, length 100 mm, outer diameter 1.5 mm, Hilgenberg) and a DMZ universal electrode puller (Zeitz Instruments GmbH) and were filled with an intracellular solution containing the following in (mM): 140.7 Cs-methanesulfonate, 5 NaCl, 1  $\text{MgCl}_2$ , 0.2 EGTA, 10 HEPES, 3 ATP-Mg, 0.3 Na-GTP, and 3.1 QX-314 (osmolarity 295 mOsm/kg, adjusted to pH 7.2 with CsOH).

Video microscopy-guided patch-clamp recordings were performed as described previously with small modifications (Blanton et al., 1989; Dodt and Zieglansberger, 1990). In brief, a healthy pyramidal neuron was selected as deep as possible in the slice because most superficial neurons and their dendrites had been damaged during slicing. To avoid clogging of the pipette tip in the tissue, positive pressure was applied to the patch pipette using a 5-ml syringe with a three-way stopcock that was connected to the electrode holder via thin tubing. The patch pipette was then slowly advanced into the brain slice using the low-speed mode of the micromanipulator. It was important to constantly monitor the pipette resistance measured by the amplifier using the PatchMaster software. After carefully placing the pipette tip immediately above the neuron membrane, the positive pressure in the syringe was released. As a result from the pressure change, the cell membrane was partially sucked into the pipette tip, and this event was reflected by a slow and steady increase in pipette resistance, leading to the formation of the so-called  $G\Omega$  seal (pipette resistance  $>1000\text{ M}\Omega$ ). To facilitate  $G\Omega$  seal formation in neurons from aged mice, it was necessary to apply slight negative pressure (continuously for 10–20 s) using a tubing-connected mouthpiece, which was made from a clean plastic pipette tip. When the membrane resistance reached  $>100\text{ M}\Omega$ , the holding membrane potential was gradually decreased to  $-60\text{mV}$ , near the resting membrane potential of pyramidal neurons ( $\sim-70\text{ mV}$ ) (Myme et al., 2003). Once the  $G\Omega$  seal was established (cell-attached configuration), the cell membrane was ruptured by applying short pulses of negative pressure via the mouthpiece. Thus, the whole-cell configuration was reached.

Recordings were initiated  $>5$  min after rupturing the cell membrane to allow complete dialysis of the intracellular pipette solution into the neuronal soma. Synaptic excitatory postsynaptic currents (EPSCs) from pyramidal cells were evoked every 30 s (frequency 0.033 Hz) by applying electrical pulses (duration 0.2 ms, intensity 50–150  $\mu\text{A}$ ) using an A385 stimulus isolator (WPI) that was controlled via the EPC10 amplifier. In normal recording aCSF at room temperature, evoked EPSCs were recorded at a holding membrane potential of  $-60\text{ mV}$  in whole-cell voltage-clamp mode for 10 min. These EPSCs revealed an early  $\alpha$ -amino-3-hydroxy-5-methyl-4-isoxazolepropionic acid receptor (AMPA)-mediated component (fast decay) that was followed by the late *N*-methyl-D-aspartate receptor (NMDAR)-mediated component (slow decay). For all neurons, the stimulation intensity was set at a level that was necessary to induce EPSCs with mean peak amplitude of  $\sim 300\text{ pA}$ .

To pharmacologically isolate NMDAR-mediated EPSCs, the slice perfusion medium was changed to modified aCSF that contained 0.1 mM  $Mg^{2+}$ , 3.2 mM  $Ca^{2+}$  (for adjustment of divalent cation concentrations), 10  $\mu$ M NBQX (specific antagonist of AMPAR/kainate receptors), and 2  $\mu$ M CGP-55845 (specific antagonist of  $\gamma$ -aminobutyric acid ( $GABA$ )<sub>B</sub> receptors) (Chen et al., 2003), and the amplitude of EPSCs was monitored. Because the washout of  $Mg^{2+}$  from the slice was relatively slow, the complete isolation of NMDAR-EPSCs was reached after 25–30 min perfusion in this modified aCSF containing 0.1 mM  $Mg^{2+}$ . To ensure that EPSCs were predominantly mediated by NMDARs, 50  $\mu$ M AP5 (specific competitive NMDAR antagonist) was applied to the perfusion medium in the end of each recording. In all voltage-clamp recordings, the series resistance ( $R_s$ , range 8–25 M $\Omega$ ) was monitored continuously throughout the experiment and was compensated by 20–30%. If  $R_s$  changed >20% during experiments, these recordings were excluded from data analysis. Recordings of evoked EPSCs were carried out at room temperature (22–25°C).

Since we aimed to test the effects of several subsequently applied drugs on NMDAR-mediated currents in slices from adult (2–4 months) mice, we performed recordings of evoked NMDAR-EPSCs at a holding potential (–60 mV) that is near the resting membrane potential of pyramidal cells. In our experience, this approach enables longer and more stable recordings compared with standard recordings of NMDAR-EPSCs at positive holding potentials (e.g., at +40 mV) for short time periods, which are sufficient for quick analysis of NMDAR/AMPA currents ratio. Voltage-clamp recordings of NMDAR-EPSCs at –60 mV were stable for >60–90 min.

### ***2.2.3.2. Recordings of NMDAR-mediated tonic currents***

For whole-cell recordings of tonic holding currents in mPFC slices, layer 5 pyramidal neurons were maintained at a holding potential of +40 mV in voltage-clamp mode (Papouin et al., 2012), and recordings were carried out at room temperature (22–25°C). To isolate the NMDAR-mediated component of the holding current, the AMPAR-specific antagonist NBQX (10  $\mu$ M), the  $GABA$ <sub>B</sub>-specific antagonist CGP-55845 (2  $\mu$ M), and the  $GABA$ <sub>A</sub>/glycine receptor-specific antagonist picrotoxin (50  $\mu$ M) were added to the recording aCSF >20 min prior to recordings. Patch pipettes were filled with the same intracellular solution containing Cs-methane-sulfonate that was used for evoked EPSCs (see above). Baseline recording for holding currents was initiated 20–25 min after obtaining the whole-cell configuration. Once a stable baseline holding current (>1.5 min)

was obtained, the competitive NMDAR antagonist AP5 (50  $\mu$ M) was applied to the perfusion medium for 5 min. In some experiments, Ro 25-6981 (0.3  $\mu$ M) was added to the perfusion medium >20 min before the recordings were started.

### ***2.2.3.3. Recordings of inhibitory postsynaptic currents***

Layer V pyramidal neurons were first maintained at  $-60$  mV and ten consecutive AMPAR-mediated EPSCs were recorded at 0.033 Hz in normal aCSF at room temperature in sham- and endoNF-treated mPFC slices. In all slices, stimulation strength was adjusted to evoke EPSCs with peak amplitude of  $\sim 100$  pA. Then, the neurons were voltage-clamped at a holding potential of 0 mV, which represents the reversal potential for NMDAR- and AMPAR-mediated currents. It has been shown that both NMDAR- and AMPAR-EPSCs in mPFC pyramidal neurons are not activated at 0 mV, the reversal potential for these receptors (Myme et al., 2003). GABA<sub>A</sub> receptor-mediated inhibitory postsynaptic currents (IPSCs) were evoked by delivering five trains of theta-burst stimulation (TBS; for details on protocol, see section Extracellular LTP recordings), which was used to induce LTP in the mPFC.

### **2.2.4. Chemicals used in electrophysiological experiments**

Sucrose, NaCl, NaHCO<sub>3</sub>, glucose, KCl, NaH<sub>2</sub>PO<sub>4</sub>\*H<sub>2</sub>O, CaCl<sub>2</sub>\*2H<sub>2</sub>O, and MgCl<sub>2</sub>\*6H<sub>2</sub>O, Cs-methane-sulfonate, EGTA, HEPES, ATP-Mg, Na-GTP, and CsOH were purchased from Sigma Aldrich. The membrane-impermeable quaternary derivate of lidocaine and antagonist of voltage-activated Na<sup>+</sup> channels N-(2,6-Dimethylphenylcarbamoylmethyl)triethylammonium chloride (QX 314 chloride) was purchased from Tocris Bioscience (Bristol, UK). The enzyme endosialidase NF (endoNF), which cleaves polySia specifically, was produced in the lab of Prof. Rita Gerardy-Schahn, Medical School Hannover (Stummeyer et al., 2005). In electrophysiological experiments, all antagonists and agonists were bath applied using the perfusion system, unless stated otherwise in Results. For pharmacological treatment during LTP recordings, drugs were added to the recording aCSF >20 min prior to fEPSP recordings. Solutions containing sarcosine (0.75 mM) or D-cycloserine (40  $\mu$ M) in oxygenated recording aCSF were freshly prepared on the day of experiment. For all other chemicals, stock solutions of appropriate concentrations were prepared using double-distilled water or dimethyl sulfoxide (DMSO) in accordance with manufacturer's recommendations, and these were stored at  $-20^{\circ}$ C.

For a detailed list of chemical compounds used in electrophysiological experiments, see **Table 2.1**.

**Table. 2.1. Drugs used for pharmacological treatment *in vitro* electrophysiology.**

<b>Compound name</b>	<b>Mechanism of action</b>	<b>Supplier (location)</b>
NANA12 (polySia consisting of twelve sialic acid residues) ( <b>Keys et al., 2014</b> )	Selective inhibitor of extrasynaptic GluN2B-NMDARs	Prof. Rita Gerardy-Schahn, Hannover
NANA1	No action on NMDARs (negative control for polySia)	EY Laboratories (San Mateo, CA, USA)
NANA5	Inhibits NMDARs via unknown mechanism	EY Laboratories (San Mateo, CA, USA)
1,2-diamino-4,5-methylenedioxy-benzene.2HCl (DMB)-labelled NANA12	Selective Inhibitor of GluN2B-NMDARs	Prof. Rita Gerardy-Schahn, Hannover
DMB-labelled NANA2	Negative control for DMB-NANA12	Prof. Rita Gerardy-Schahn, Hannover
$\alpha$ R, $\beta$ S)- $\alpha$ -(4-hydroxyphenyl)- $\beta$ -methyl-4-(phenylmethyl)-1-piperidinepropanol maleate (Ro 25-6981 maleate)	Selective antagonist of GluN2B-NMDARs	Tocris Bioscience (Bristol, UK)
D-(-)-2-amino-5-phosphonopentanoic acid (AP5)	Subtype-unselective antagonist of NMDARs	Tocris Bioscience (Bristol, UK)
2,3-dioxo-6-nitro-1,2,3,4-tetrahydrobenzo[f]quinoxaline-7-sulfonamide disodium salt (NBQX)	Selective antagonist of AMPARs	Tocris Bioscience (Bristol, UK)
Picrotoxin	Selective antagonist of GABA <sub>A</sub> and glycine receptors	Tocris Bioscience (Bristol, UK)
(2S)-3-[[[(1S)-1-(3,4-dichlorophenyl)ethyl]amino-2-hydroxypropyl] (phenylmethyl) phosphinic acid hydrochloride (CGP-55845)	Selective antagonist of GABA <sub>B</sub> receptor	Tocris Bioscience (Bristol, UK)
1-[4-amino-5-chloro-2-(3,5-dimethoxyphenyl)methoxy]-3-[1-[2-methylsulphonylamino]ethyl]piperidin-4-yl]propan-1-one hydrochloride (RS 39604 hydrochloride)	Selective antagonist of 5-HT <sub>4</sub> receptors	Tocris Bioscience (Bristol, UK)
N-methylglycine (sarcosine)	Selective antagonist of the glial glycine transporter 1 (GlyT1)	Sigma Aldrich (Taufkirchen, Germany)
(R)-4-Amino-3-isoxazolidone, 4-Amino-3-isoxazolidinone (D-cycloserine, DCS)	Partial agonist at the glycine modulatory site of NMDA receptors	Sigma Aldrich (Taufkirchen, Germany)
(2-chloro-N-[(S)-phenyl[(2S)-piperidin-2-yl] methyl]-3-trifluoromethyl benzamide (SSR 504734)	Selective antagonist of GlyT1	Axon Medchem (Groningen, Netherlands)
Tegaserod maleate ( <b>Bushman et al., 2013</b> )	Selective agonist of 5-HT <sub>4</sub> receptor/mimetic of polySia	Sequoia Research Products LTD (Pangbourne, UK)

### 2.3. Data analysis and statistical comparisons for *in vitro* electrophysiology

Electrophysiological data were acquired at a sampling rate of 10 kHz and low-pass filtered at 3 kHz using an EPC10 amplifier operated using the PatchMaster software (Heka Elektronik, Lambrecht, Germany). Data analysis and presentation were performed using PatchMaster, SigmaPlot 12 (Systat Software Inc., San Jose, CA, USA), Igor Pro 6.37 (WaveMetrics, Lake Oswego, OR, USA), and Adobe Illustrator CS5 (Adobe Systems Inc., San Jose, CA, USA).

Recordings of fEPSPs were low-pass filtered at 500 Hz using PatchMaster software. The rising slope of fEPSPs was measured within its early linear phase using PatchMaster. Relationships between stimulus intensity and fEPSP slope for each slice were obtained by plotting the average fEPSP slope of 3–5 consecutive fEPSPs against the stimulus intensity at which they were evoked. In each slice, the slopes of 30 consecutive fEPSPs recorded during baseline (0–10 min before TBS delivery) were averaged, and this mean value was used to normalize the slopes of fEPSPs recorded during 0–60 min after TBS. Since fEPSPs were evoked every 20 s, every three consecutive slope values were averaged to obtain one mean slope value per minute. To reflect the marked changes of fEPSP slope that occur immediately after TBS (short-term post-tetanic potentiation), normalized fEPSP slopes during 0–3 min after TBS were not averaged. If the mean amplitude of fiber volley measured 50–60 min after TBS delivery changed by >15% compared with its baseline mean value (0–10 min before TBS), fEPSP recordings were not included in data analysis.

Whole-cell recordings of synaptically evoked EPSCs were filtered at 1000 Hz, and measurements of peak current amplitude and decay time were carried out on EPSC averages of 8–10 consecutive traces using PatchMaster. The EPSC amplitude was defined as the difference between baseline current (measured during 20 s immediately before stimulus) and the maximal peak of the EPSC for each cell. The 20–80% decay time of EPSCs was measured after the EPSC peak, and it was defined as the time interval between the two time points measured at 80% and 20% from the peak EPSC amplitude. For analysis of drug effects on EPSCs, the amplitude or decay time measured 10–15 min after drug application was compared with those measured during the last 5 min before drug was added. The NMDAR/AMPA ratio was defined as the ratio between the mean peak amplitude of the pharmacologically isolated slow NMDAR-mediated

component and the fast AMPAR-mediated component that was recorded in normal aCSF in each neuron.

The amplitude of tonic currents was measured within five consecutive 2-s time intervals immediately before AP5 addition and 3 min after AP5 was applied, and mean amplitudes before and after AP5 were calculated for each neuron. The shift in holding currents was defined as the difference between mean current amplitude recorded before and 3 min after AP5 application. Recordings in which the amplitude of tonic current during the last 1.5 min before AP5 changed by >5% were not included in the data analysis.

The mean amplitude of each TBS-evoked IPSC burst was measured during the total burst duration (230 ms) in each neuron using the PatchMaster software. The IPSC/EPSC ratio for each TBS train was defined as the ratio between mean amplitude of IPSC burst during 230 ms and the mean EPSC peak amplitude (average of ten consecutive EPSCs recorded before TBS delivery).

Statistical analysis was performed using the SigmaPlot software. Differences in the mean of two independent groups (recorded from different cells/slices/mice) with normal distribution were assessed using unpaired Student's *t* test. If the data were not normally distributed, non-parametric Mann Whitney U test (two independent groups) or one-way ANOVA on ranks (three or more independent groups) was used for statistical comparison. For multiple (three or more) independent groups with normal distribution, differences in means were determined using one-way ANOVA followed by multiple comparisons using *post hoc* Holm-Sidak *t* test. For related groups (recorded from the same cell/slice/mouse), statistical comparison of means was performed using paired Student's *t* test (two groups) or repeated measures ANOVA (three or more groups). Statistical significance was reached, if  $P < 0.05$ . All data were presented as mean  $\pm$  standard error of the mean (SEM).

#### **2.4. Immunohistochemistry in brain slices**

Coronal 400- $\mu$ m-thick mPFC and hippocampal slices from *Thy1*-GFP mice were incubated in 2 ml of carbogenated aCSF (sham) or endoNF (10  $\mu$ g/ml in aCSF) for 2 hours at 35°C. The slices were then fixed for 3 hours in 4% paraformaldehyde in phosphate buffered saline (PBS, 0.24M, pH 7.2, room temperature) and cryoprotected in 30% sucrose in PBS overnight at 4°C. On the following day, 400- $\mu$ m-thick slices were mounted on the specimen disc of a CM1950 cryostat

(Leica Biosystems) using Jung tissue medium (Leica Biosystems), and 50- $\mu$ m-thick coronal subslices were prepared and stored in a cryo-protective solution containing 25% glycerin (Carl Roth, Karlsruhe, Germany) and 25% ethylene glycol (Carl Roth) in 0.24 M PBS. For immunohistochemistry, free floating sections were washed in PBS (3x 10 min, at room temperature on a shaker) and incubated for 1 hour in a blocking solution containing 10% normal goat serum (NGS, Gibco®, Thermo Fisher Scientific, New Zealand origin) and 0.2% Triton X-100 (Sigma Aldrich) in PBS at room temperature. Subsequently, slices were treated for 48 hours at 4°C with the primary mouse monoclonal antibody against polySia (clone 735 (Frosch et al., 1985)1:200 in PBS containing 5% NGS and 0.2% Triton X-100), as published previously (Eckhardt et al., 2000; Kochlamazashvili et al., 2010). The slices were then washed in PBS and incubated on a shaker for 3 hours in the secondary antibody (goat anti-mouse Alexa 546, Invitrogen, 1:250 in PBS containing 5% NGS and 0.2% Triton X-100) at room temperature. For imaging, sections were mounted on glass slides using Vectashield mounting medium (Vector Laboratories, Burlingame, CA, USA), and images of the mPFC and hippocampal mossy fibers (10x objective) were obtained using a confocal laser-scanning microscope (LSM 700, Carl Zeiss, Germany) operated by the Zen software (Carl Zeiss, Jena, Germany).

Imaging of spines was carried out on segments of proximal dendrites of EGFP-expressing layer V pyramidal neurons that were located in the prelimbic cortex of *Thy1*-GFP mice using an oil 63x objective. Z-stacks were acquired using a Z-step of 0.22  $\mu$ m and 3x optical zoom. ImageJ 1.46 software (NIH, USA) was used for image analysis and preparation of maximum-intensity projections from Z stacks. Spine images were deconvoluted using Huygens deconvolution software (Scientific Volume Imaging).



## 3. RESULTS

### 3.1. Loss of polySia in mPFC slices after endoNF treatment

To study the effects of acute polySia removal in mPFC, I used the enzyme endoNF that specifically removes polySia in neocortical and hippocampal slices (Eckhardt et al., 2000; Kochlamazashvili et al., 2010). To confirm the removal of polySia by endoNF in the hippocampus and cortex in my experiments, I first incubated hippocampal and mPFC slices in aCSF (sham) or aCSF containing endosialidase NF (endoNF, 10  $\mu$ g/ml) and performed immunohistochemical staining of polySia followed by confocal imaging in sham- and endoNF-treated slices from wild-type *Thy1*-EGFP mice. As expected, endoNF-incubated hippocampal slices showed reduced polySia immunoreactivity, whereas sham-treated hippocampal slices revealed strong polySia expression in the mossy fibers of mature granule cells and CA3 subfield, as reported previously (Eckhardt et al., 2000) (**Fig. 3.1**). No polySia staining could be detected in the absence of primary antibody against polySia (**Fig. 3.1**), indicating that this antibody was specific for polySia. In sham-treated mPFC slices, polySia was expressed in the neuropil of all cortical layers (**Fig. 3.1**). In contrast, endoNF-treated mPFC showed a strong decrease of polySia immunoreactivity (**Fig. 3.1**), suggesting that the endoNF treatment reliably removes polySia in these brain slices.

To investigate the distribution of polySia in relation to dendritic spines in the mPFC, I performed confocal imaging of proximal dendrites of layer 5 pyramidal neurons in sham- and endoNF-treated mPFC slices from *Thy1*-EGFP mice, which show expression of enhanced green fluorescent protein (EGFP) under the control of the *Thy1* promoter in a subset of cortical layer V pyramidal neurons (Feng et al., 2000). In sham-treated mPFC slices, polySia was expressed in close proximity of several EGFP-expressing dendritic spines (inset in **Fig. 3.2**). In endoNF-treated mPFC slices, polySia staining was markedly reduced compared to sham-treated slices (**Fig. 3.2**).

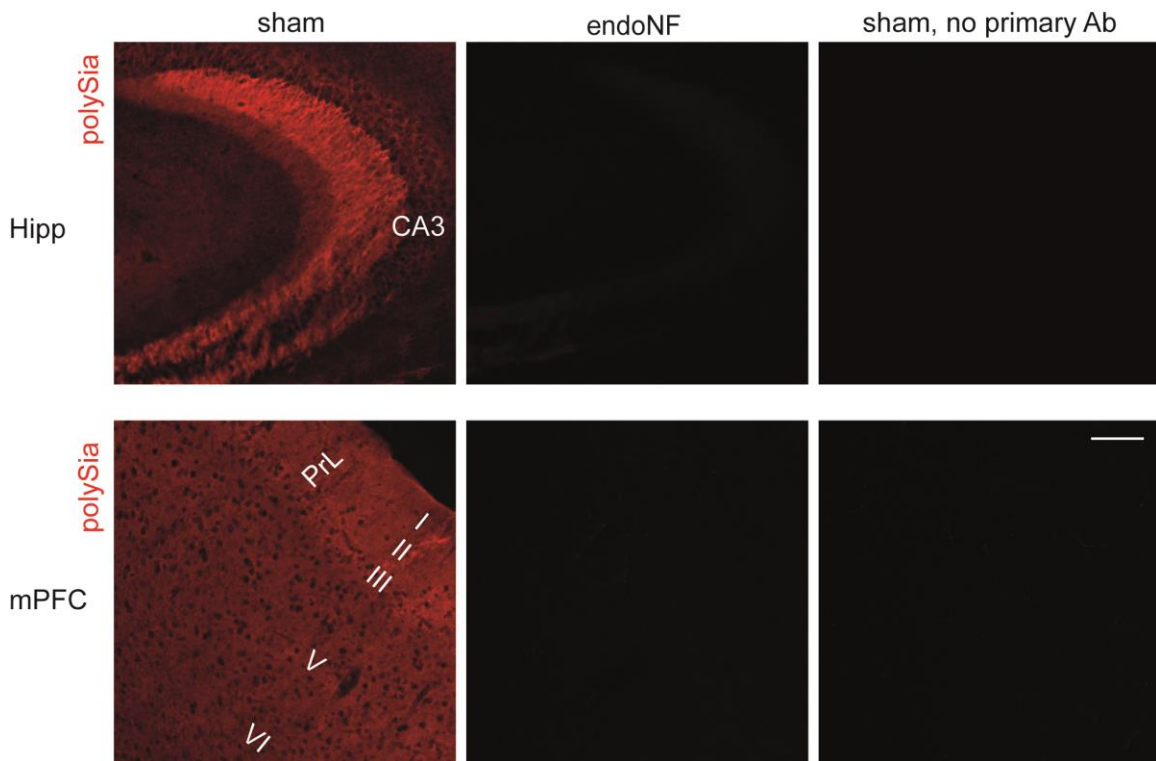


**Fig. 3.1. Enzymatic treatment with endoNF removes polySia in the hippocampus and mPFC of *Thy1-EGFP* mice.** Hippocampal (hipp) and mPFC (prelimbic cortex, PrL) brain slices were incubated in sham (aCSF) or endoNF (10  $\mu\text{g/ml}$  in aCSF) for 2 hours at 35°C. Representative single-plane confocal images revealing immunohistochemical staining of polySia (red) in sham- and endoNF-treated slices using a primary mouse monoclonal antibody (clone 735). After endoNF treatment, the polySia staining in both mPFC and hippocampus was strongly reduced compared with sham-treated slices. When the primary antibody against polySia was omitted in sham condition, no polySia staining was observed. Images of hippocampus and mPFC were taken using a 10x objective. Scale bar, 100  $\mu\text{m}$ . I–VI, cortical layers.

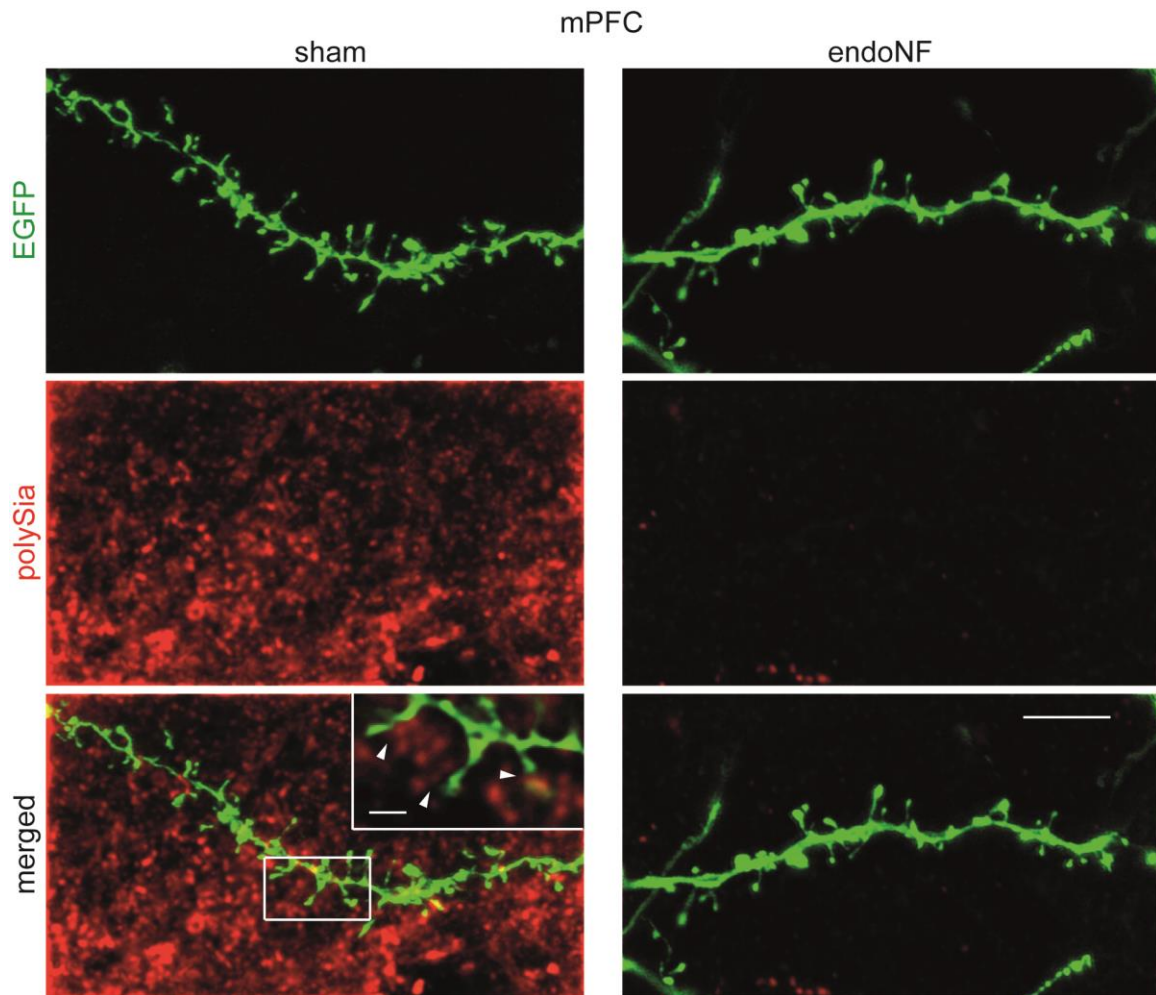


**Fig. 3.2. PolySia-NCAM surrounds dendritic spines in the mPFC.** Representative confocal images (maximal-intensity projections) of dendritic segments from EGFP-expressing proximal dendrites (green) of layer V pyramidal neurons in sham- (left) and endoNF-treated mPFC slices (right), from the same *Thy1-EGFP* mouse shown in **Fig. 3.1**. In sham-treated slices, the pyramidal dendrite was embedded in dense polySia staining (red). The inset shows a magnified view (single plane) of the boxed area in sham overlay. Please note that polySia surrounded some of the dendritic spines (arrow heads in inset). The polySia staining around spines was largely reduced in endoNF-treated slices compared with sham treatment. Spine imaging was performed using a 63x objective. Scale bars, 5  $\mu\text{m}$  and 1  $\mu\text{m}$  (inset).

### 3.2. Acute enzymatic removal of polySia increases GluN2B-NMDAR-mediated currents and extrasynaptic, tonic NMDAR-mediated currents in the mPFC

Previously, extracellular fEPSP recordings have shown that *Ncam*<sup>-/-</sup> mice, which also lack NCAM-associated polySia, exhibit no changes in NMDAR/AMPA ratio in the hippocampal CA1 subfield (Kochlamazashvili et al., 2010). To investigate the effects of endoNF treatment on synaptic signaling through AMPARs and NMDARs in the mPFC, I recorded electrically evoked AMPAR- and NMDAR-mediated excitatory postsynaptic potentials (EPSCs) in whole-cell voltage clamp mode from layer 5 pyramidal neurons in sham- and endoNF-treated mPFC slices. After initial recording (>5 min) of AMPAR-EPSCs in normal aCSF at -60 mV holding potential, the aCSF was exchanged with modified recording solution containing low concentration of Mg<sup>2+</sup> (0.1 mM), the AMPAR-specific antagonist NBQX (10 μM) and the GABA<sub>B</sub>-specific antagonist CGP-55845 (2 μM), which allowed us to isolate NMDAR-EPSCs at -60 mV (**Fig. 3.3B**), a potential near the resting membrane potential of pyramidal neurons (Chen et al., 2003). NMDAR-EPSCs were almost completely blocked after bath application of the NMDAR-specific antagonist AP5 (**Fig. 3.3B**), suggesting that these isolated EPSCs are mediated through NMDARs. The stimulation intensity was set to elicit AMPAR-EPSCs with an amplitude of ~300 pA. Thus, we normalized the amplitude of NMDAR-EPSCs to the fixed amplitude of AMPAR-EPSCs. The ratio of NMDAR/AMPA current in endoNF-treated slices (0.31 ± 0.03) was not different from that in sham-treated slices (0.30 ± 0.05; *P* = 0.92, unpaired Student's *t* test; **Fig. 3.3C**), suggesting that the total synaptic NMDAR-mediated currents are similar in both conditions.

In a previous study, field EPSP recordings have indicated that GluN2B-mediated currents are increased in the CA1 subregion of *Ncam*<sup>-/-</sup> mice (Kochlamazashvili et al., 2010). To determine the effects of polySia removal on GluN2B subunit contribution in the mPFC, I compared evoked NMDAR-EPSCs recorded for 5 min before and for >15 min after bath application of the specific GluN2B antagonist Ro 25-6981 in sham- and endoNF-treated mPFC slices (**Fig. 3.3D**). Because polySia has been demonstrated to inhibit GluN1/GluN2B-NMDARs in hippocampal neurons at low glutamate concentrations, which are characteristic of the extracellular space (Hammond et al., 2006), we wondered whether endoNF would affect the activation of heterodimeric GluN1/GluN2B-NMDARs. To this aim, I used a relatively low concentration (0.3 μM) of Ro 25-6981, which has been reported to block mainly GluN1/GluN2B-NMDARs while leaving heterotrimeric GluN1/GluN2A/GluN2B-NMDARs largely intact in hippocampal pyramidal neurons (Volianskis et al., 2013). In sham-treated control slices, I observed no significant

changes in Ro 25-6981 (0.3  $\mu$ M)-mediated inhibition of mean amplitude ( $-4.22 \pm 4.68\%$ ; **Fig. 3.3D, E**) or mean decay time ( $-4.05 \pm 6.41\%$ ; **Fig. 3.3D, F**) of NMDAR-EPSCs from mPFC pyramidal neurons. However, endoNF-treated slices showed significantly increased Ro 25-6981 (0.3  $\mu$ M)-mediated inhibition of mean amplitude ( $25.06 \pm 5.19\%$ ; **Fig. 3.3D, E**,  $P < 0.001$ , unpaired Student's  $t$  test) and mean decay time ( $19.78 \pm 5.08\%$ ; **Fig. 3.3D, F**,  $P < 0.05$ , Mann-Whitney rank sum test) of NMDAR-EPSCs.

Similar conclusions could be drawn when recorded NMDAR-EPSCs were expressed as absolute values (in pA, **Fig. 3.3G**). In sham-treated slices, mean amplitude of NMDAR-EPSCs during basal recording was  $98.86 \pm 15.50$  pA, compared with  $100.45 \pm 13.98$  pA after the addition of Ro 25-6981. In endoNF-treated slices, mean amplitude of NMDAR-EPSCs during basal recording was  $106.56 \pm 6.23$  pA compared with  $81.74 \pm 8.72$  pA in the presence of Ro 25-6981.

A two-way repeated measures ANOVA showed a significant effect of Ro 25-6981 treatment ( $F_{(1,18)} = 13.990$ ,  $P = 0.001$ ), no effect of endoNF ( $F_{(1,18)} = 0.128$ ,  $P = 0.725$ ), but a significant endoNF x Ro 25-6981 interaction ( $F_{(1,18)} = 18.103$ ,  $P < 0.001$ ). A Holm-Sidak *post hoc* test revealed no significant difference in mean amplitude between basal and Ro 25-6981 treatment within sham-incubated slices ( $P = 0.733$ ), but it showed a significant difference in mean amplitude between basal and Ro 25-6981 treatment within endoNF-incubated slices ( $P < 0.001$ , **Fig. 3.3G**).

When analyzed in pyramidal cells in sham-treated slices, the mean decay time during basal recording was  $93.35 \pm 19.48$  ms, compared with  $92.92 \pm 17.24$  ms after Ro 25-6981. In endoNF-treated slices, the basal mean decay time was  $122.32 \pm 12.42$  ms, compared with  $99.24 \pm 13.41$  ms in the presence of Ro 25-6981 (**Fig. 3.3H**).

A two-way repeated measures ANOVA showed a significant effect of Ro 25-6981 treatment ( $F_{(1,18)} = 6.259$ ,  $P = 0.022$ ), no effect of endoNF ( $F_{(1,18)} = 0.680$ ,  $P = 0.420$ ), and a significant endoNF x Ro 25-6981 interaction ( $F_{(1,18)} = 5.812$ ,  $P = 0.027$ ). A Holm-Sidak *post hoc* test showed no significant differences in mean decay time between basal and Ro 25-6981 treatment within sham-incubated slices ( $P = 0.952$ ); however, it revealed a significant decrease in mean decay time after Ro 25-6981 treatment, compared with basal values, within endoNF-incubated slices ( $P = 0.002$ , **Fig. 3.3H**). Altogether, these results suggest that activation of GluN2B-containing NMDARs (presumably extrasynaptic GluN1/GluN2B) in the mPFC is elevated after

endoNF treatment. To further confirm whether endoNF has an effect on extrasynaptic NMDARs in the mPFC, I used whole-cell patch-clamp to record tonic holding currents at +40 mV membrane potential from layer V pyramidal neurons in sham- and endoNF-treated slices. To pharmacologically isolate NMDAR-mediated tonic currents, recordings were performed in normal aCSF (1.5 mM  $Mg^{2+}$ ) containing the AMPAR-specific antagonist NBQX (10  $\mu$ M), GABA<sub>A</sub>-specific antagonist picrotoxin (50  $\mu$ M), and the GABA<sub>B</sub>-specific antagonist CGP-55845 (2  $\mu$ M).

Previous electrophysiological studies have shown that, at depolarizing membrane potentials, the NMDAR-specific antagonist AP5 causes a shift in the holding current, which reflects the activation of extrasynaptic NMDARs by ambient glutamate in CA1 pyramidal neurons of the hippocampus (Sah et al., 1989; Le Meur et al., 2007; Papouin et al., 2012). After recording a stable baseline of holding tonic current at +40 mV, the NMDAR antagonist AP5 (50  $\mu$ M) was bath applied, and the shift in the holding current induced by AP5 was then measured. The mean shift in sham-treated control slices was  $33.40 \pm 2.51$  pA (**Fig. 3.4**), which is comparable with the shift reported in hippocampal neurons (Papouin et al., 2012). In endoNF-treated slices, the mean shift in NMDAR-mediated holding current after AP5 application reached  $-60.93 \pm 6.66$  pA. A two-way ANOVA revealed a significant effect of endoNF ( $F_{(1,26)} = 14.861$ ,  $P < 0.001$ ). A Holm-Sidak *post hoc* test showed a significant difference in amplitude of tonic current between the sham- and endoNF-treated slices ( $P < 0.01$ , **Fig. 3.4B**), suggesting that acute polySia removal led to increased activation of extrasynaptic NMDARs in mPFC slices.

Because extrasynaptic NMDARs are thought to be enriched in heterodimeric GluN1/GluN2B-NMDARs (Angulo et al., 2004; Fellin et al., 2004) (reviewed by (Papouin and Oliet, 2014)), we repeated these recordings of tonic NMDAR-mediated currents in the presence of low concentration of Ro 25-6981. A two-way ANOVA revealed no significant effect of Ro 25-6981 ( $F_{(1,26)} = 3.684$ ,  $P = 0.066$ ) and no significant endoNF x Ro 25-6981 interaction ( $F_{(1,26)} = 0.831$ ,  $P = 0.37$ ). When Ro 25-6981 (0.3  $\mu$ M) was present in the recording chamber, the NMDAR-mediated tonic current was still significantly higher in endoNF- compared with sham-treated slices ( $27.58 \pm 7.21$  pA in sham+Ro 25-6981;  $44.58 \pm 3.74$  pA in endoNF+Ro 25-6981;  $P = 0.046$ , Holm-Sidak *post hoc* test, **Fig. 3.4**). However, Ro 25-6981 significantly reduced the amplitude of NMDAR-mediated tonic current in endoNF-treated slices ( $P = 0.041$ , Holm-Sidak *post hoc* test for endoNF+Ro 25-6981 vs. endoNF), suggesting that GluN1/GluN2B-NMDARs

might contribute to the increased NMDAR-tonic currents in endoNF-treated slices. Moreover, mean amplitude of tonic current was similar in sham-treated slices without and with Ro 25-6981 (0.3  $\mu$ M) ( $P = 0.509$ , Holm-Sidak *post hoc* test, **Fig. 3.4**), which indicates that GluN1/GluN2B-NMDARs constitute only a minor fraction of extrasynaptic NMDARs in basal conditions.

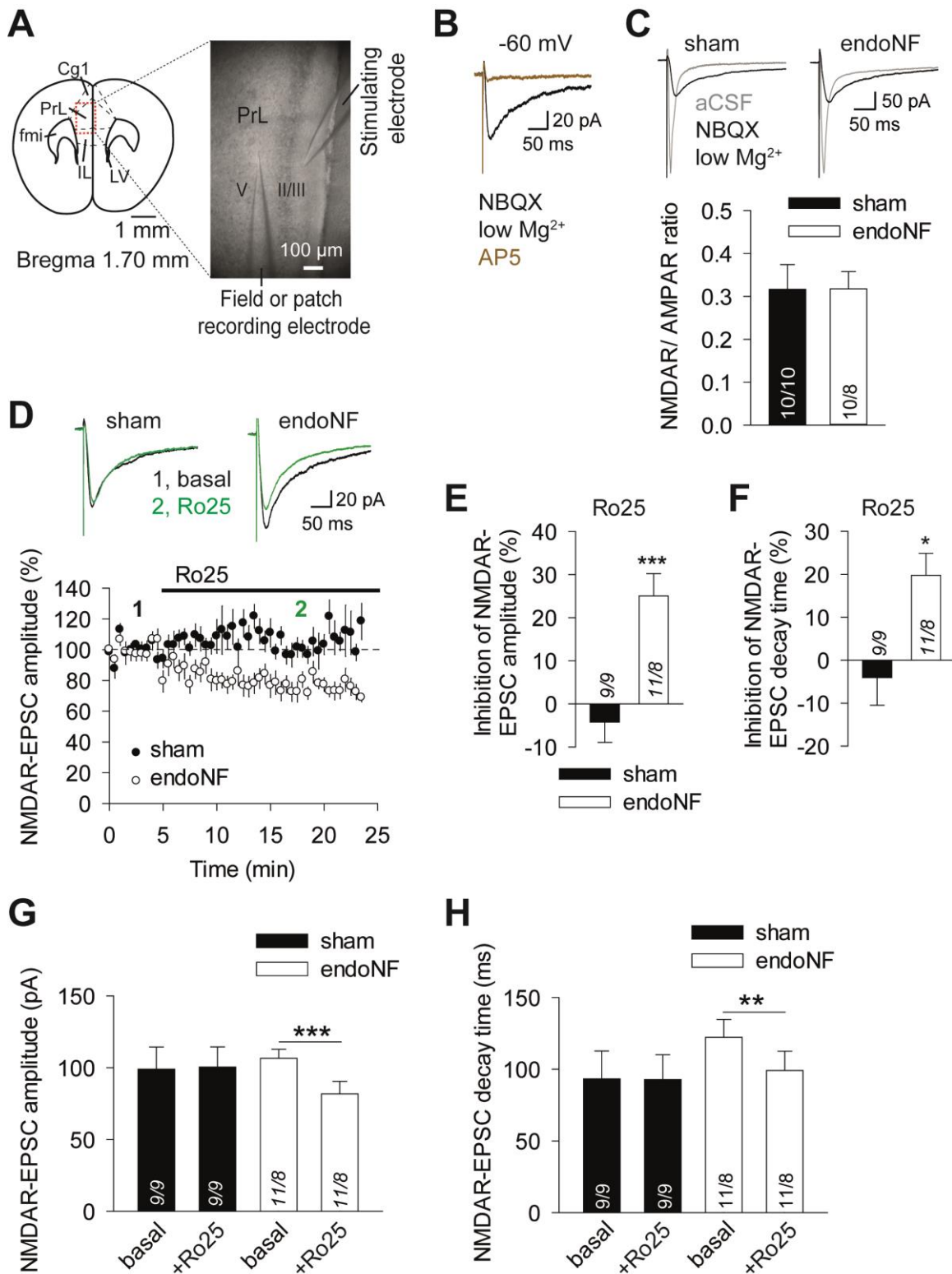


**Fig. 3.3. Increased GluN2B-NMDAR-mediated currents in mPFC slices after endoNF treatment.** (A) A coronal view of the mPFC (left) (Franklin and Paxinos, 2007) and a photomicrograph (4x objective) showing the positions of electrodes for evoked EPSCs recordings (right). Cg1, cingulate; PrL, prelimbic;



IL, infralimbic cortex; II/III, V, cortical layer; fmi, forceps minor of the corpus callosum; LV, lateral ventricle. **(B)** Representative examples (averages of 8–10 traces) of evoked NMDAR-EPSCs from layer V pyramidal neurons in aCSF containing  $Mg^{2+}$  (0.1 mM), NBQX (10  $\mu$ M), and CGP-55845 (2  $\mu$ M) (black trace). These EPSCs were completely inhibited after bath application of AP5 (50  $\mu$ M, brown trace). **(C)** Representative examples (top, averages of 8–10 traces) of fast AMPAR-EPSCs recorded in normal aCSF (gray) and slow NMDAR-EPSCs (black), which were subsequently isolated in the presence of  $Mg^{2+}$  (0.1 mM), NBQX (10  $\mu$ M), and CGP-55845 (2  $\mu$ M). A bar graph (bottom) showing unaltered NMDAR/AMPA ratio in endoNF- treated slices compared with sham treatment. **(D)** Examples (top, averages of 8–10 traces) and time courses of normalized amplitudes (bottom) of evoked NMDAR-EPSCs before (basal, black) and after bath application of Ro 25-6981 (Ro25, 0.3  $\mu$ M, green). The amplitude of EPSCs was presented as the percentage of the mean amplitude recorded within a 5-min time window of basal recording before the addition of Ro 25-6981. **(E, F)** Bar graphs showing increased inhibition of NMDAR-EPSCs amplitude **(E)** and increased inhibition of NMDAR-EPSC decay time **(F)** by Ro 25-6981 (0.3  $\mu$ M) in endoNF-treated slices compared with sham-treated slices. Evoked EPSCs were recorded in voltage-clamp mode at a holding membrane potential of  $-60$  mV. **(G, H)** Absolute values of peak amplitude **(G)** and decay time **(H)** of evoked NMDAR-EPSCs were measured during a 5-min time interval before (basal) and 10–15 min after application of Ro 25-6981 (Ro25, 0.3  $\mu$ M). The cells analyzed are the same as in **D–F**. Please note that Ro 25-6981 significantly inhibited both the amplitude **(G)** and the decay time **(H)** of NMDAR-EPSCs in endoNF-treated slices, whereas Ro 25-6981 had no effects on amplitude or decay time in sham-treated slices. Experimental design and representative examples of NMDAR-EPSCs in both treatments are shown in **Fig. 3.3D**. Numbers of cells recorded (n) and mice used (N) are shown in bars as n/N. \* $P < 0.05$ , \*\* $P < 0.01$ , \*\*\* $P < 0.001$ , for description of statistical analysis, please see the text. Data are presented as mean  $\pm$  SEM.

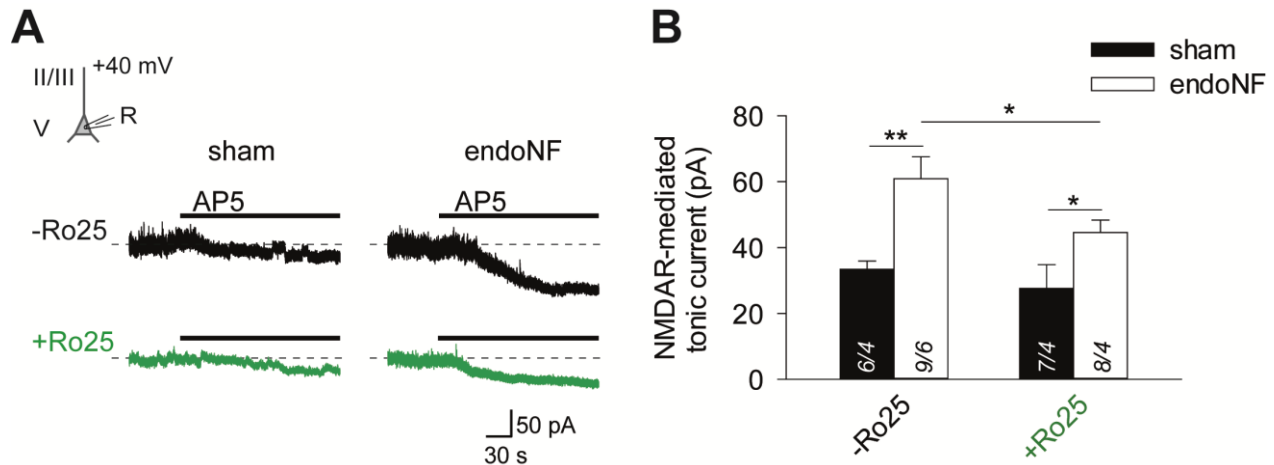


**Fig. 3.4. Increased tonic NMDAR-mediated currents after acute removal of polySia.** (A) Representative traces of NMDAR-mediated holding currents (holding potential +40 mV) recorded from layer V pyramidal neurons before and after bath application of the NMDAR-specific antagonist AP5 (50 μM) in sham- and endoNF-treated mPFC slices. The inset (left) illustrates the experimental design for whole-cell voltage-clamp recordings of tonic currents. Please note that the recorded cell was not stimulated synaptically. Tonic currents were recorded in aCSF containing NBQX (10 μM), picrotoxin (50 μM), and CGP-55845 (2 μM). Horizontal dotted lines denote the basal level of holding current before the addition of AP5. II/III, V, cortical layer; R, recording electrode. (B) A bar graph showing the mean amplitude of tonic NMDAR-mediated currents (measured as shift in holding current) recorded in the presence (+) or absence (-) of Ro 25-6981 (0.3 μM). The amplitude of tonic currents was increased in endoNF-treated slices compared with sham controls. Numbers of cells recorded (n) and mice used (N) are shown in bars as n/N. \* $P < 0.05$ , \*\* $P < 0.01$ , for description of statistical analysis, please see the text. Data are presented as mean  $\pm$  SEM.

### 3.3. PolySia fragments inhibit evoked NMDAR-mediated currents in the mPFC

The polymer chains of polySia are composed of 8 to >90 sialic acid residues, and this number is also known as degree of polymerization (DP) (Hildebrandt and Dityatev, 2015). A previous study has revealed that polymers of sialic acid with a relatively high degree of polymerization (DP = 25–50) inhibit GluN2B-NMDAR-mediated currents elicited by glutamate at concentrations in the low micromolar range (Hammond et al., 2006). However, the functional effects of short polySia fragments or sialic acid oligomers (oligoSia) have not been studied thus far. To determine the

impact of short polySia fragments with DP = 12 (NANA12) on NMDAR-mediated currents in the mPFC, I recorded evoked NMDAR-EPSCs in sham- and endoNF-treated mPFC slices. To compare the effect of NANA12 (1 µg/ml) with the inhibition mediated by a specific GluN2B antagonist, Ro 25-6981 (0.3 µM) was added to the recording solution 15 min after NANA12 application (**Fig. 3.5A**). In sham-treated slices, NANA12 did not change significantly basal NMDAR-EPSC amplitude (reduction by  $2.95 \pm 4.14\%$ ;  $P = 0.61$ , paired Student's *t* test), and Ro 25-6981 further reduced the amplitude by  $5.96 \pm 5.04\%$  ( $P = 0.28$ , paired Student's *t* test) (**Fig. 3.5A**). This result is consistent with the low inhibition after Ro 25-6981 in sham-treated slices, where Ro 25-6981 was applied immediately after basal recording (**Fig. 3.3D, E**).

In contrast, in endoNF-treated slices, NANA12 (1 µg/ml) significantly reduced the mean NMDAR-EPSC amplitude by  $24.80 \pm 4.42\%$  ( $P = 0.0002$ , paired Student's *t* test), whereas Ro 25-6981 significantly inhibited NMDAR-EPSC amplitude by  $19.01 \pm 4.71\%$  ( $P = 0.012$ , paired Student's *t* test, **Fig. 3.5A**), suggesting that NANA12 only partially occluded the inhibitory effect of Ro 25-6981 in endoNF-treated slices. **Fig. 3.5B** shows a summary of the mean inhibition levels of basal amplitude in both conditions. A two-way repeated measures ANOVA for level of inhibition showed significant effects of endoNF pre-incubation ( $F_{(1,15)} = 15.81$ ,  $P < 0.001$ ) and drug treatment ( $F_{(1,15)} = 10.842$ ,  $P = 0.005$ ), but no significant endoNF x drug treatment interaction ( $F_{(1,15)} = 1.81$ ,  $P = 0.19$ , **Fig. 3.5B**). In sham-treated slices, the Holm-Sidak *post hoc* test revealed that the mean inhibition level of basal amplitude after Ro 25-6981 addition was not significantly different from this produced by NANA12 alone ( $P = 0.177$ ). In contrast, in endoNF-treated slices, the mean inhibition level of basal amplitude after Ro 25-6981 addition was significantly higher than this measured after NANA12 ( $P = 0.006$ , Holm-Sidak *post hoc* test, **Fig. 3.5B**). Importantly, the level of inhibition caused by NANA12 in endoNF-treated slices was significantly higher than this in sham-treated slices ( $P = 0.005$ , Holm-Sidak *post hoc* test, **Fig. 3.5B**).

To assess whether the effect of NANA12 on NMDARs was specific, I performed recordings of evoked NMDAR-EPSCs before and after addition of sialic acid monomers with DP = 1 (NANA1) followed by addition of Ro 25-6981 (0.3 µM) in endoNF-treated mPFC slices (**Fig. 3.5C, D**). We used NANA1 as a control compound for NANA12 because sialic acid is also negatively charged, but unlike polySia, it has been previously shown to have no effect on NMDAR-mediated currents in hippocampal neurons (Hammond et al., 2006). In line with this

study, NANA1 (10  $\mu\text{g/ml}$ ) did not change the mean NMDAR-EPSC amplitude (reduction of basal amplitude by  $-1.29 \pm 4.90\%$ ,  $P = 0.62$ , paired Student's  $t$  test, **Fig. 3.5C**), whereas the subsequent addition of Ro 25-6981 significantly inhibited the NMDAR-EPSC amplitude by  $21.43 \pm 5.37\%$  ( $P = 0.020$ , paired Student's  $t$  test). Consistent with these results, the mean inhibition of basal amplitude measured after Ro 25-6981 was significantly higher than this caused by NANA1 alone ( $P = 0.013$ , paired Student's  $t$  test, **Fig. 3.5D**). Thus, these results indicate that NANA12 specifically inhibits NMDAR-mediated currents.

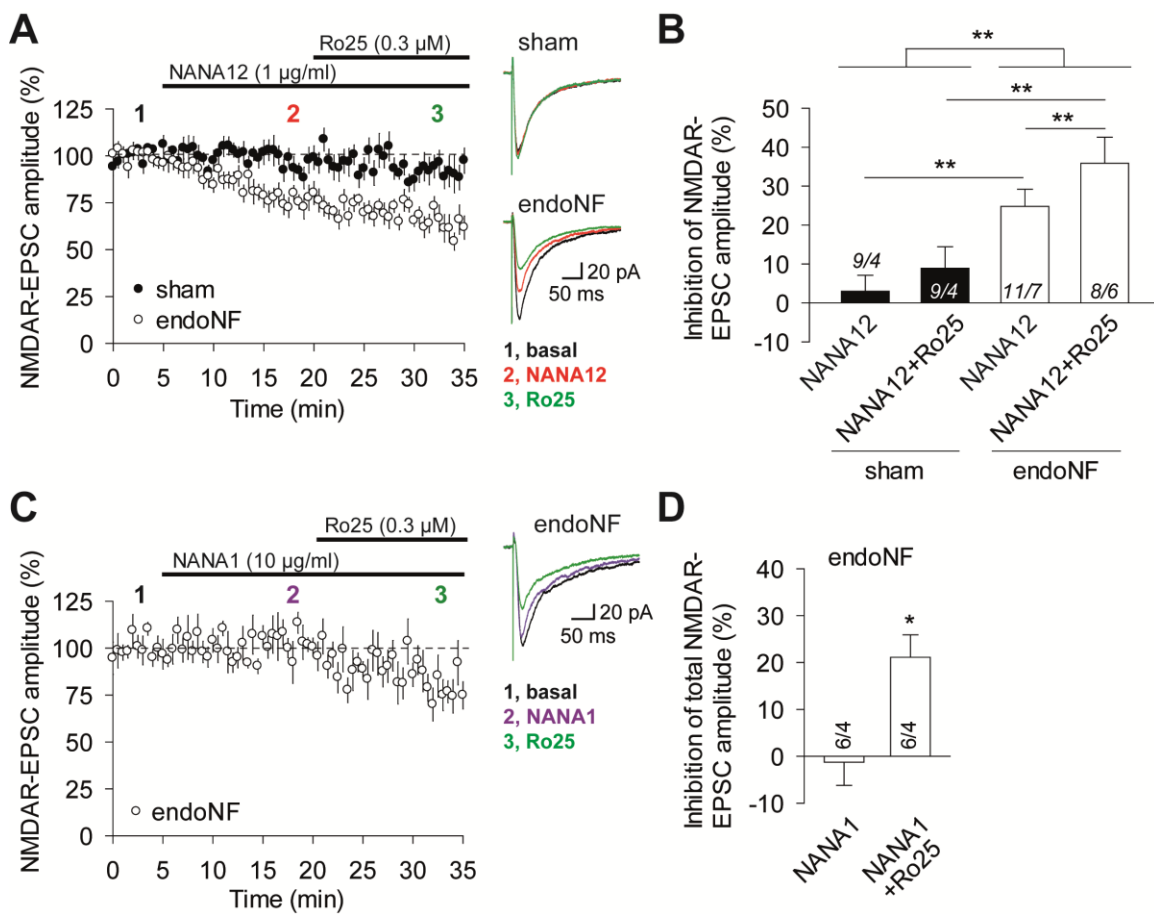


**Fig. 3.5. Short polySia NANA12 inhibits evoked NMDAR-EPSCs in endoNF-treated mPFC slices from C57BL/6 mice.** (A, C) Time courses of normalized amplitudes of evoked NMDAR-EPSCs (holding potential of  $-60$  mV) during basal recording followed by successive bath application of NANA12 (1  $\mu\text{g/ml}$ ) (A) or NANA1 (10  $\mu\text{g/ml}$ , control compound) (C) and Ro 25-6981 (0.3  $\mu\text{M}$ ) in sham- and endoNF-treated mPFC slices. Representative examples of NMDAR-EPSCs for each treatment (color-coding and sequence number 1–3) are shown in the right panels of A and C. (A, B) In endoNF-incubated

slices, NANA12 reduced the mean amplitude of NMDAR-EPSCs, whereas in sham-incubated slices, NANA12 had no effect. The experimental design in **A** and **C** was analogous to **Fig. 3.3A, D**. (**B**) Bar graph showing mean inhibition of basal amplitude (cells shown in **Fig. 3.5A**). (**C, D**) The control compound NANA1 had no effect on NMDAR-EPSC amplitude, but the subsequent addition of Ro 25-6981 significantly reduced NMDAR-EPSCs in endoNF-treated slices. (**D**) Bar graph summarizing mean inhibition of basal amplitude (cells shown in **C**). NMDAR-EPSCs were recorded in whole-cell voltage-clamp mode at  $-60$  mV in aCSF containing  $Mg^{2+}$  (0.1 mM), NBQX (10  $\mu$ M), and CGP-55845 (2  $\mu$ M). Numbers of cells recorded (n) and mice used (N) are shown in bars as n/N. \* $P < 0.05$ , \*\* $P < 0.01$ , for description of statistical analysis, please see the text. Data are presented as mean  $\pm$  SEM.

Next, we wondered whether oligoSia NANA5 (DP = 5) would exert similar inhibitory effects on NMDARs in endoNF-treated slices. Low concentration of NANA5 (0.1  $\mu$ g/ml) did not inhibit significantly the basal mean NMDAR-EPSC amplitude (reduction by  $10.60 \pm 5.87\%$ ,  $P = 0.104$ , paired Student's  $t$  test, **Fig. 3.6A**), whereas the subsequent application of Ro 25-6981 (0.3  $\mu$ M) significantly inhibited NMDAR-EPSCs amplitude by  $15.83 \pm 2.90\%$  ( $P = 0.013$ , paired Student's  $t$  test, **Fig. 3.6A**) in endoNF-treated slices. Consistently, the mean inhibition level after Ro 25-6981 was significantly higher than this after NANA5 (0.1  $\mu$ g/ml) alone ( $P = 0.012$ , paired Student's  $t$  test, **Fig. 3.6B**).

When a relatively high concentration of NANA5 (10  $\mu$ g/ml) was tested, it significantly inhibited mean NMDAR-EPSC amplitude by  $18.04 \pm 2.86\%$  ( $P = 0.0004$ , paired Student's  $t$  test), and Ro 25-6981 (0.3  $\mu$ M) further inhibited EPSC amplitude by  $11.06 \pm 4.45\%$ , which did not reach significance ( $P = 0.052$ , paired Student's  $t$  test, **Fig. 3.6C**). Moreover, the mean inhibition of basal amplitude after addition of Ro 25-6981 (0.3  $\mu$ M) was significantly higher, compared with that produced by NANA5 alone ( $P = 0.046$ , paired Student's  $t$  test, **Fig. 3.6D**).

The concentration-response curve summarizing the effects of NANA5 on NMDAR-EPSCs in endoNF-treated slices (concentrations 0.01  $\mu$ g/ml, 0.1  $\mu$ g/ml, 1  $\mu$ g/ml, 5  $\mu$ g/ml, and 10  $\mu$ g/ml) (**Fig. 3.6E**) shows that its inhibitory effect is concentration-dependent, reaching saturation at 1  $\mu$ g/ml.

To compare the effects of the tested compounds in relation to the GluN2B-selective antagonist Ro 25-6981, the inhibition levels caused by NANA1, NANA5, and NANA12 were plotted (bar

graph in **Fig. 3.6F**) after normalization to Ro 25-6981-induced inhibition of NMDAR-EPSCs in the same time-window in endoNF-treated slices (as measured in **Fig. 3.3E**). One-way ANOVA revealed significant differences between inhibition levels after NANA1 (10  $\mu\text{g/ml}$ ), NANA5 (1  $\mu\text{g/ml}$ ), and NANA12 (1  $\mu\text{g/ml}$ ) ( $F_{(3,30)} = 6.86$ ,  $P = 0.001$ ). The Holm-Sidak *post hoc* test showed that the inhibitory effect of low concentration of NANA5 (1  $\mu\text{g/ml}$ ) was not significantly different from this of NANA1 (10  $\mu\text{g/ml}$ ) (~50% of Ro 25-6981-mediated effect,  $P = 0.383$ , **Fig. 3.6F**), but high concentration of NANA5 (10  $\mu\text{g}$ ) reached significant difference compared with control NANA1 (~70% of Ro 25-6981-mediated effect,  $P = 0.02$ , Holm-Sidak *post hoc* test). The highest mean inhibition was produced by NANA12 at 1  $\mu\text{g/ml}$  (~90% of Ro 25-6981-mediated effect), and it was significantly higher than this measured after NANA1 ( $P < 0.001$ , Holm-Sidak *post hoc* test). Taken together, these data indicate that both polySia NANA12 and oligoSia NANA5 are able to inhibit NMDARs in the mPFC to a similar extent as Ro 25-6981 (0.3  $\mu\text{M}$ ).

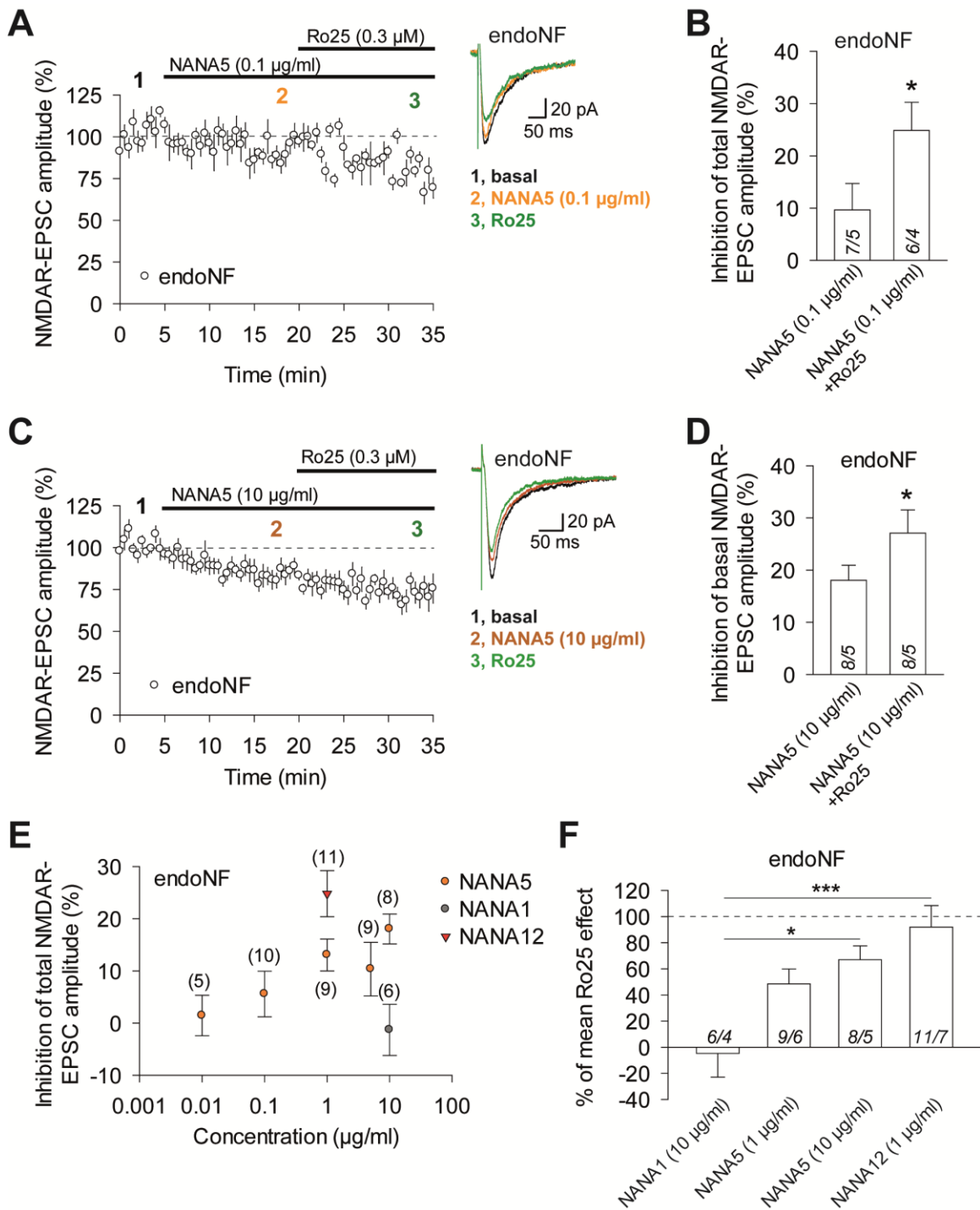


**Fig. 3.6. OligoSia NANA5 inhibits evoked NMDAR-EPSCs in mPFC slices from C57BL/6 mice.** (A) Time courses of normalized amplitudes of evoked NMDAR-EPSCs (holding potential of  $-60$  mV) during basal recording followed by successive bath application of NANA5 ( $0.1$   $\mu\text{g/ml}$ ) (A) or NANA5 ( $10$   $\mu\text{g/ml}$ ) (C) and Ro 25-6981 ( $0.3$   $\mu\text{M}$ ) in endoNF-treated mPFC slices. Representative examples of evoked NMDAR-EPSCs for each treatment (color-coding and sequence number 1–3) are shown in the right panels of A and C.

(A, B) NANA5 (0.1  $\mu\text{g/ml}$ ) produced only weak inhibition of mean NMDAR-EPSC amplitude in endoNF-treated slices. Please note that the subsequent bath addition of Ro 25-6981 significantly inhibited the mean NMDAR-EPSC (bar graph in B). (C, D) NANA5 (10  $\mu\text{g/ml}$ ) significantly reduced mean NMDAR-EPSC amplitude in endoNF-treated slices. The inhibition level of EPSC amplitude was significantly increased after addition of Ro 25-6981 (bar graph in D). NMDAR-EPSCs were recorded in whole-cell voltage-clamp mode at  $-60$  mV in aCSF containing  $\text{Mg}^{2+}$  (0.1 mM), NBQX (10  $\mu\text{M}$ ), and CGP-55845 (2  $\mu\text{M}$ ). (E) Concentration-response relationship showing the mean level of inhibition of NMDAR-EPSC amplitude by NANA1, NANA5, and NANA12 measured in endoNF-treated mPFC slices. (F) A summary bar graph showing mean inhibition of NMDAR-EPSC amplitude by NANA1, NANA5, and NANA12 in endoNF-incubated mPFC slices (presented as the percentage of mean Ro 25-6981-mediated inhibition of amplitude in endoNF slices shown in Fig. 3.3D, E). Numbers of cells recorded (n) and mice used (N) are shown in bars as n/N. \* $P < 0.05$ , \*\*\* $P < 0.001$ , for description of statistical analysis, please see the text. Data are presented as mean  $\pm$  SEM.

### 3.4. The polySia mimetic tegaserod inhibits NMDAR-mediated currents in mPFC slices

Mimetics of polySia, molecules mimicking polySia's structure and function, represent an alternative option for restoration of functional impairments after polySia removal. A recent study has shown that the small organic compound tegaserod acts as a polySia mimetic (Bushman et al., 2014). Tegaserod is a clinically approved drug for therapy of irritable bowel syndrome (Muller-Lissner et al., 2001), and it is known to activate of 5-HT<sub>4</sub> receptors on enteric neurons (Liu et al., 2005). Tegaserod has been shown to stimulate neurite extension of Schwann cells, motoneurons, and dorsal root ganglion neurons *in vitro*. Notably, this effect is independent of tegaserod's activity as 5-HT<sub>4</sub> receptor agonist (Bushman et al., 2014). Moreover, tegaserod improves functional recovery and histological measures after femoral nerve injury (Bushman et al., 2014) as well as after spinal cord injury in mice (Pan et al., 2014). To assess whether tegaserod would modulate NMDARs, I recorded evoked NMDAR-EPSCs from layer V pyramidal neurons before and after the addition of tegaserod in sham- and endoNF-treated slices. Since tegaserod is a 5-HT<sub>4</sub> receptor antagonist, whole-cell patch-clamp recordings were performed in the presence of the 5-HT<sub>4</sub> receptor antagonist RS 39604 (10  $\mu\text{M}$ ).



In sham-treated mPFC slices, tegaserod (0.1  $\mu\text{M}$ ) significantly inhibited basal NMDAR-EPSC amplitude by  $45.64 \pm 7.39\%$  ( $P = 0.0007$ , paired Student's  $t$  test) (**Fig. 3.7A**). Since neither NANA12 nor Ro 25-6981 had effects on NMDAR-EPSCs in sham-treated slices (**Fig. 3.3D** and **5A**), this finding indicates that tegaserod does not inhibit selectively GluN2B-containing NMDARs.

Similarly, in endoNF-treated slices, tegaserod (0.1  $\mu\text{M}$ ) significantly inhibited basal NMDAR-EPSC amplitude by  $30.19 \pm 4.52\%$  ( $P = 0.0045$ , paired Student's  $t$  test). Unpaired Student's  $t$  test showed that the level of basal NMDAR-EPSC amplitude inhibition in endoNF-treated slices was not significantly different from this measured in sham-treated controls (**Fig. 3.7B**), suggesting that tegaserod inhibits NMDAR-mediated currents in a manner that is independent of its action as 5-HT<sub>4</sub> receptor agonist, but tegaserod's effect on NMDARs is different from that underlying the action of polySia.

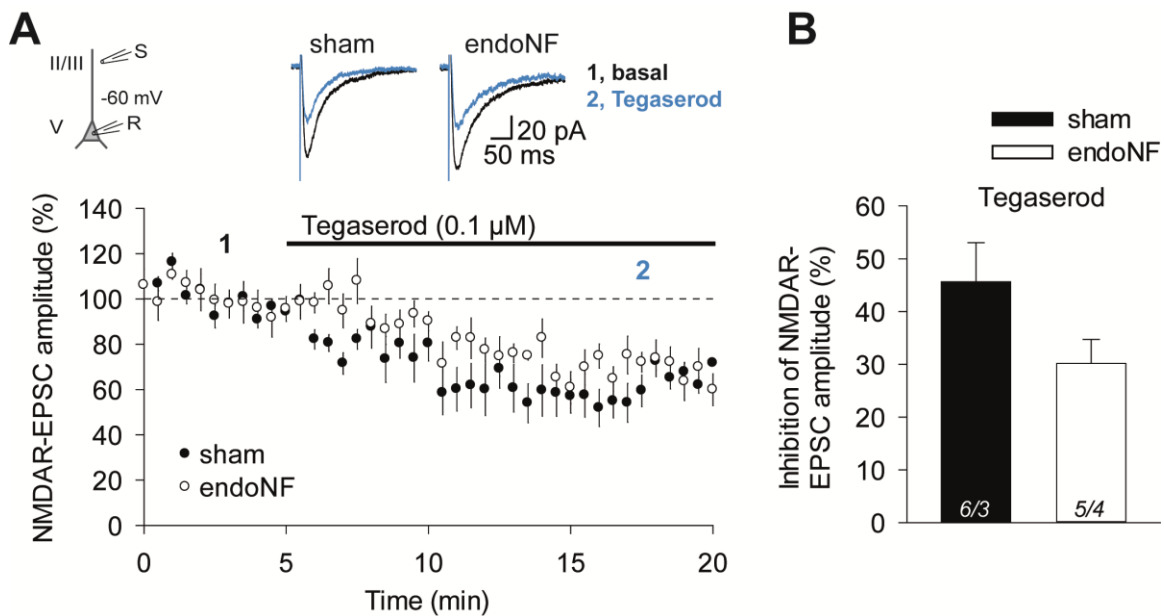


**Fig. 3.7. PolySia mimetic tegaserod inhibits evoked NMDAR-mediated currents in mPFC slices.** (A) Examples (top, averages of 8–10 traces) and time courses of normalized amplitudes (bottom) of evoked NMDAR-EPSCs recorded from layer V pyramidal neurons during basal recording (black traces) and after the addition of tegaserod (0.1  $\mu\text{M}$ , blue traces) in sham- and endoNF-treated mPFC slices from C57BL/6 mice. Please note that tegaserod inhibited NMDAR-EPSCs not only in sham- but also in endoNF-treated slices. The experimental design (inset, top left) was analogous to **Fig. 3.3A, D**. NMDAR-EPSCs were

recorded in whole-cell voltage-clamp mode at  $-60$  mV in aCSF containing  $Mg^{2+}$  (0.1 mM), NBQX (10  $\mu$ M), CGP-55845 (2  $\mu$ M), and RS 39604 (10  $\mu$ M). II/III, V, cortical layer; R, recording electrode. **(B)** A bar graph showing similar levels of mean inhibition of basal NMDAR-EPSCs after tegaserod application in sham- and endoNF-treated slices. Numbers of cells recorded (n) and mice used (N) are shown in bars as n/N. Data are presented as mean  $\pm$  SEM.

### 3.5. Pharmacological restoration of abnormal long-term potentiation in mPFC slices by Ro 25-6981, sarcosine, or NANA12

Several studies have shown that activation of GluN2B-containing NMDARs supports the induction of long-term depression (LTD) (Liu et al., 2004; Massey et al., 2004; Papouin et al., 2012). Furthermore, it has been proposed that synaptic NMDARs mediate the induction of long-term potentiation (LTP), whereas both synaptic and extrasynaptic NMDARs promote LTD (Rusakov et al., 2004; Papouin et al., 2012). Because endoNF treatment increased GluN1/GluN2B-mediated component of synaptic currents (**Fig. 3.3**) and tonic currents mediated by extrasynaptic NMDARs (**Fig. 3.4**), we asked whether acute removal of polySia using endoNF would alter LTP in mPFC slices. To this aim, I recorded theta-burst stimulation (TBS)-induced LTP at layer II/III–layer V synapses in sham- and endoNF-treated mPFC slices from C57BL/6 mice. Induction of LTP in the mPFC is NMDAR-dependent, as shown previously (Fossat et al., 2012). In sham-treated slices, delivery of TBS reliably induced stable LTP of fEPSPs ( $144.82 \pm 6.71\%$ , **Fig. 3.8A, D**). In contrast, mean LTP level in endoNF-treated slices ( $101.31 \pm 5.06\%$ ) was markedly impaired in comparison with sham-treated slices (**Fig. 3.8A, D**). One-way ANOVA revealed significant differences in LTP levels between treatment groups ( $F_{(7,65)} = 15.390$ ,  $P < 0.001$ ). A Holm-Sidak *post hoc* test showed a significant difference between sham- and endoNF-treated slices ( $P < 0.001$ ). Notably, the relationship between fEPSP slope and stimulation intensity (input-output curve) in endoNF-treated slices was similar to this in sham-treated controls ( $F_{(1,89)} = 0.0293$ ,  $P = 0.866$ , two-way repeated measures ANOVA, **Fig. 3.9**), suggesting that reduced LTP levels in endoNF-treated slices are not mediated through changes in basal synaptic transmission. Since basal fEPSPs are mediated mainly through AMPARs (Myme et al., 2003), the unaltered input-output curves confirm the lack of changes in NMDAR/AMPA ratio in endoNF-treated slices as shown using whole-cell recordings (**Fig. 3.3C**).

Because endoNF-treated slices exhibited elevated GluN2B-mediated currents (**Fig. 3.3D–F**) and since the GluN2B-selective antagonist Ro 25-6981, polySia NANA12, and oligoSia NANA5 inhibited a similar fraction of evoked NMDAR-EPSCs, we sought to determine whether these compounds could restore impaired LTP via inhibition of GluN2B-NMDARs. Indeed, both Ro 25-6981 (0.3  $\mu$ M) and NANA12 (1  $\mu$ g/ml) led to increased mean LTP levels in endoNF-treated mPFC slices ( $140.04 \pm 9.05\%$  in endoNF+Ro 25-6981;  $130.26 \pm 4.67\%$  in endoNF+NANA12, **Fig. 3.8B, D**). A Holm-Sidak *post hoc* test showed that LTP levels in endoNF-treated slices perfused with Ro 25-6981 or NANA12 were significantly higher than those in endoNF-treated slices in normal aCSF ( $P = 0.005$  for endoNF vs. endoNF+Ro 25-6981;  $P = 0.027$  for endoNF vs. endoNF+NANA12, Holm-Sidak *post hoc* test, **Fig. 3.8D**). Further, mean LTP levels in endoNF-treated slices perfused with Ro 25-6981 or NANA12 were not significantly different from those in sham-treated slices ( $P = 0.951$  for sham vs. endoNF+Ro 25-6981;  $P = 0.590$  for sham vs. endoNF + NANA12, Holm-Sidak *post hoc* test, **Fig. 3.8D**). Mean LTP levels in Ro 25-6981 and NANA12 were similar ( $P = 0.917$ , Holm-Sidak *post hoc* test, **Fig. 3.8D**). Thus, these results suggest that both Ro 25-6981 and NANA12 can fully restore impaired synaptic plasticity in the mPFC.

Ro 25-6981 (0.3  $\mu$ M) had no effect on LTP in sham-treated mPFC slices compared with sham-treated controls perfused in normal aCSF ( $129.23 \pm 6.37\%$  in sham+Ro 25-6981;  $129.16 \pm 4.34\%$  in sham;  $P = 0.993$ , unpaired Student's *t* test, **Fig. 3.10**), indicating that, under our recording conditions, the GluN1/GluN2B-NMDARs blocked at this low concentration of Ro 25-6981 are not involved in the induction of mPFC LTP in normal brains.

In contrast, neither NANA5 (1  $\mu$ g/ml) nor NANA5 (10  $\mu$ g/ml) were able to restore LTP in endoNF-treated slices ( $74.45 \pm 8.60\%$  in endoNF+NANA5 (1  $\mu$ g/ml);  $100.86 \pm 5.89\%$  in endoNF+NANA5 (10  $\mu$ g/ml)). The LTP level in endoNF-treated slices perfused in NANA5 (1  $\mu$ g/ml) was significantly lower than that in sham-treated slices in normal aCSF ( $P < 0.001$ , Holm-Sidak *post hoc* test, **Fig. 3.8D**) but similar to that in endoNF-treated slices ( $P = 0.104$ , Holm-Sidak *post hoc* test). The mean LTP level in endoNF-treated slices perfused in NANA5 (10  $\mu$ g/ml) was still significantly lower than this in sham-treated slices in normal aCSF ( $P < 0.001$ , Holm-Sidak *post hoc* test) and comparable to this in endoNF-treated slices in normal aCSF ( $P = 0.964$ , Holm-Sidak *post hoc* test). These data thus indicate that, in contrast to NANA12, NANA5 does not improve LTP induction, although both compounds could inhibit NMDAR-EPSCs.

Moreover, application of NANA5 (1  $\mu\text{g/ml}$ ) had no effect on the basal fEPSP slope in sham-treated slices (reduction by  $15.16 \pm 9.96\%$ ;  $P = 0.203$ , paired Student's  $t$  test **Fig. 3.11**), suggesting that a lack of NANA5's support of LTP is not mediated via changes in basal synaptic transmission. Other possible side effects of NANA5 were not investigated in the frame of this study.

In our search for further pharmacological treatments of LTP deficits, we tested whether abnormal LTP can be restored by the inhibitor of glycine transporter type 1 (GlyT1) sarcosine. Importantly, glycine is an endogenous agonist of the NMDAR glycine site. Under normal physiological conditions, the glycine site is not saturated because glycine concentration in the synaptic cleft is maintained at relatively low levels by the glial GlyT1. Accordingly, inhibitors of GlyT1 block the uptake of glycine, thus leading to increased concentration of glycine near synaptic NMDARs (Bergeron et al., 1998; Chen et al., 2003; Martina et al., 2004). Previous studies have shown that GlyT1 inhibitors potentiate NMDAR-mediated currents and increase LTP levels in the hippocampal CA1 subregion (Bergeron et al., 1998; Martina et al., 2004; Depoortere et al., 2005) and mPFC (Chen et al., 2003). In the presence of sarcosine (0.75 mM), the mean magnitude of LTP in endoNF-treated slices was  $137.66 \pm 3.38\%$ , a level similar to that measured in sham-treated slices in normal aCSF ( $P = 0.869$ , Holm-Sidak *post hoc* test, **Fig. 3.8C, D**). Of note, the mean LTP in endoNF-treated slices in sarcosine (0.75 mM) was significantly higher than that in endoNF-treated slices in normal aCSF ( $P = 0.001$ , Holm-Sidak *post hoc* test).

Recently, several novel inhibitors with improved specificity and affinity for GlyT1 have shown positive effects on NMDAR-mediated cognitive functions in rodent models (reviewed by (Javitt, 2012; Harvey and Yee, 2013)). Therefore, I next tested the effects of the highly potent and specific GlyT1 inhibitor SSR 504734 on synaptic plasticity in the mPFC. In line with sarcosine's positive effect, the magnitude of LTP in endoNF-treated slices in the presence of SSR 504734 (3  $\mu\text{M}$ ) was fully restored to sham level ( $157.22 \pm 10.87\%$  in endoNF+SSR 504734; endoNF+SSR 504734 vs. sham,  $P = 0.751$ , Holm-Sidak *post hoc* test, **Fig. 3.8C, D**). Furthermore, LTP magnitude in endoNF-treated slices perfused in SSR 504734 was significantly higher than this in endoNF-treated slices in normal aCSF ( $P < 0.001$ , Holm-Sidak *post hoc* test). Thus, these results suggest that GlyT1 inhibitors can reliably rescue abnormal synaptic plasticity caused by polySia removal.

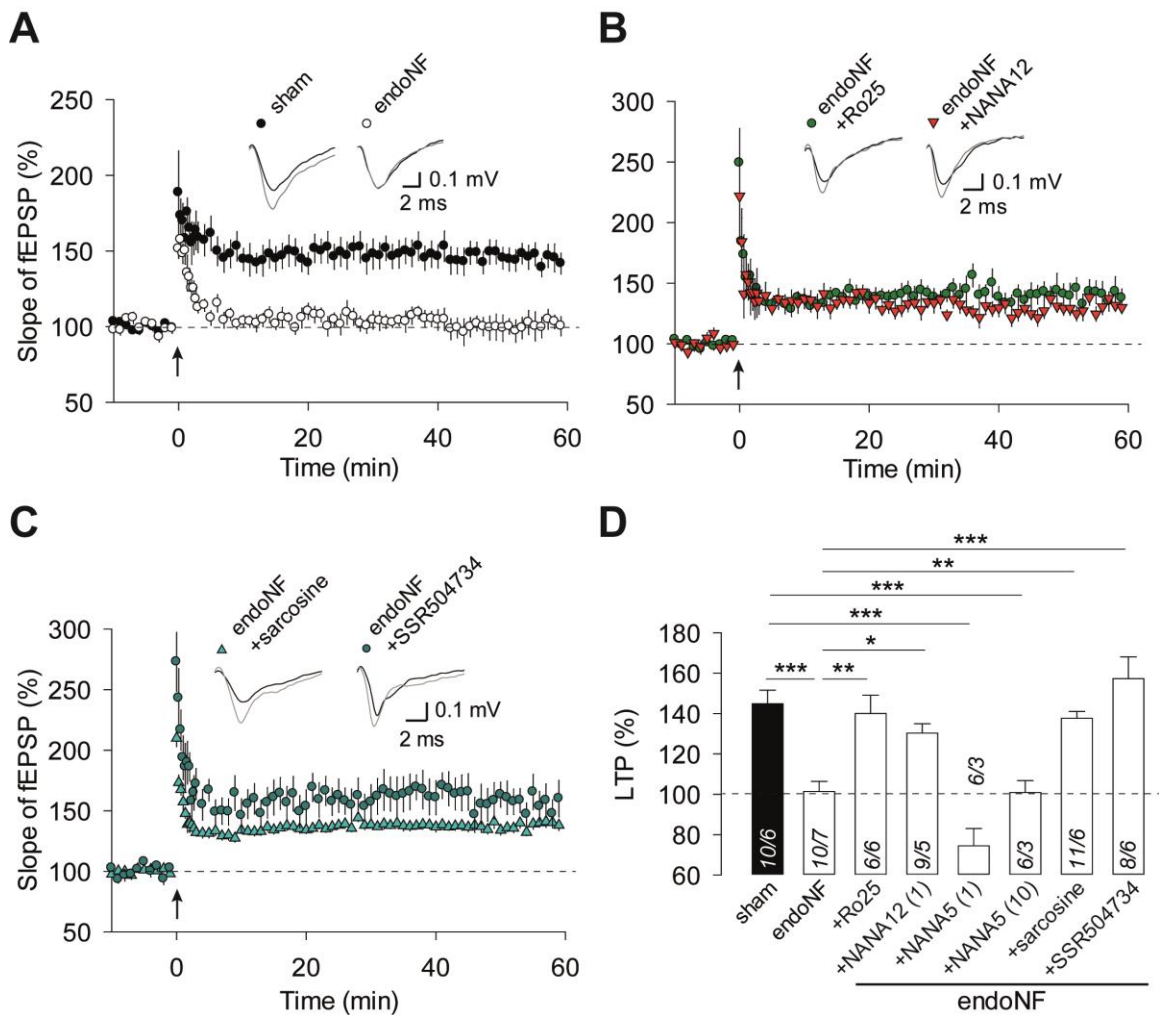


**Fig. 3.8. Impaired long-term potentiation (LTP) of fEPSPs in mPFC slices after endoNF treatment and its restoration by GluN2B-specific antagonist Ro 25-6981, NANA12, and GlyT1 inhibitors. (A–C)** Time courses of normalized mean slopes and representative examples (insets) of field excitatory postsynaptic potentials (fEPSPs) recorded before and after induction of LTP by theta-burst stimulation (TBS) in endoNF- and sham-treated mPFC slices from C57BL/6 mice. **(A)** In endoNF-treated slices, mean LTP magnitude in the mPFC was strongly reduced compared with sham-treated slices. Recordings of fEPSPs in **A** were performed in normal aCSF. **(B)** In the presence of Ro 25-6981 (Ro25, 0.3  $\mu$ M) or NANA12 (1  $\mu$ g/ml), mean LTP levels in endoNF-treated slices were similar to those measured in sham-treated slices in **A**. **(C)** In the presence of the glycine transporter type 1 inhibitors sarcosine (0.75 mM) or SSR 504734 (3  $\mu$ M), mean LTP levels in endoNF-treated slices were restored to the level of those in sham-treated slices in **A**. **(A–C)** Arrows indicate the time points at which five trains of TBS were applied

via stimulation electrode. Example fEPSPs (insets) represent averages of 30 fEPSPs recorded during a 10-min time interval before TBS (basal recording, black trace) and 50–60 min after TBS (gray trace) in each condition. Slopes of fEPSPs are presented as the percentage of mean fEPSP slope measured during basal recording. **(D)** A bar graph showing mean levels of LTP measured 50–60 min after TBS delivery in **A–C**. Please note that NANA12 was continuously perfused at concentration of 1  $\mu\text{g/ml}$  (1). NANA5 was perfused at 1  $\mu\text{g/ml}$  (1) and 10  $\mu\text{g/ml}$  (10). \* $P < 0.05$ , \*\* $P < 0.01$ , \*\*\* $P < 0.001$ , for description of statistical analysis, please see the text. Numbers of slices recorded (n) and mice used (N) are shown in bars as n/N. Data are presented as mean  $\pm$  SEM.

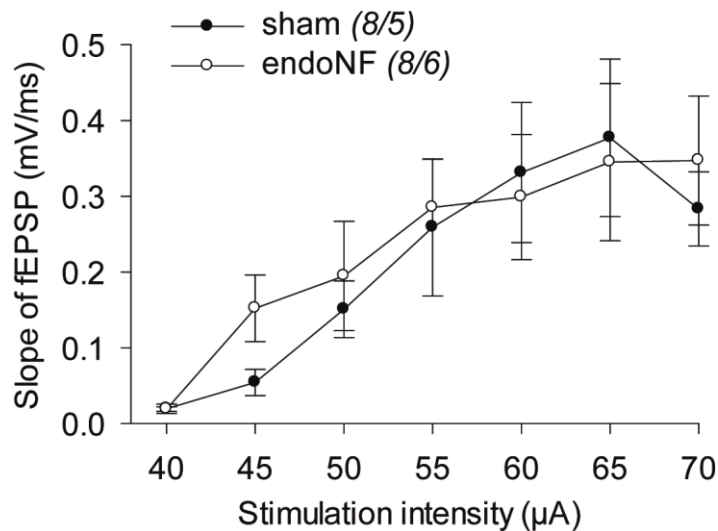


**Fig. 3.9. Normal basal synaptic transmission in endoNF-treated slices.** Input-output curves showing relationship between fEPSP slope and stimulation intensity in sham- and endoNF-treated slices. Recordings of fEPSPs were performed in normal aCSF. Numbers of slices recorded (n) and mice used (N) are shown as n/N. Data are presented as mean  $\pm$  SEM.

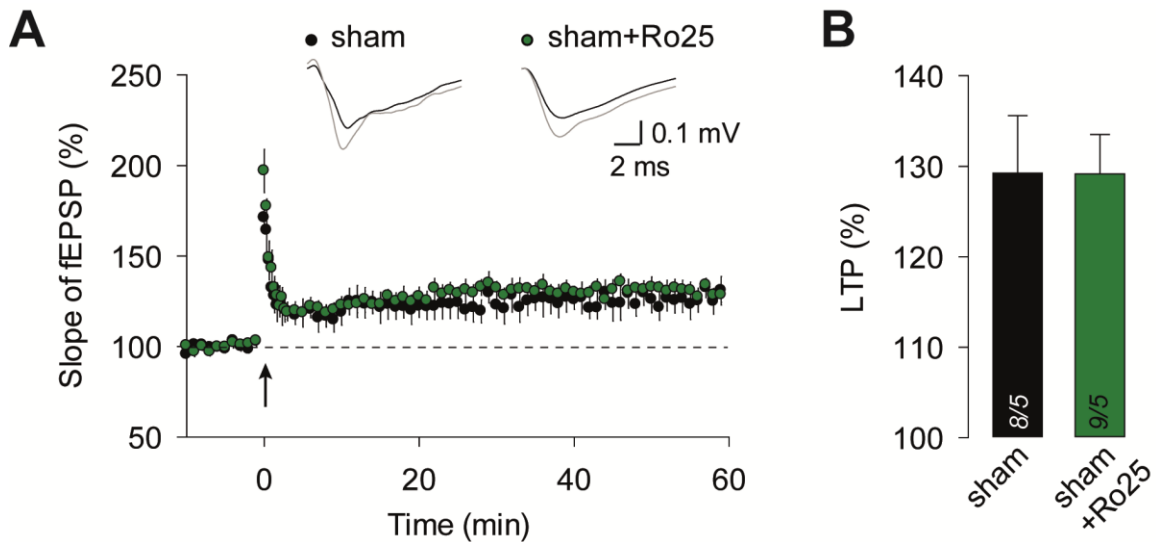


**Fig. 3.10. Unaltered long-term potentiation (LTP) of fEPSPs in the mPFC in the presence of GluN2B-NMDAR antagonist Ro 25-6981.** (A) Time courses and representative examples (inset) of TBS-induced changes in fEPSP slope in sham-incubated mPFC slices from C57BL/6 mice without and with bath perfusion of Ro 25-6981 (Ro25, 0.3  $\mu$ M). Please note that Ro 25-6981 did not alter LTP magnitude in sham-treated slices. An arrow indicates the time point at which five trains of TBS were applied via stimulation electrode. Example fEPSPs represent averages of 30 fEPSPs recorded during a 10-min time interval before TBS (basal recording, black trace) and 50–60 min after TBS (gray trace) in each condition. Slopes of fEPSPs are presented as the percentage of mean fEPSP slope measured during basal recording. (B) A bar graph (right) showing mean LTP levels measured 50–60 min after TBS in Ro 25-6981-treated sham-incubated slices compared with untreated (in normal aCSF) sham-incubated slices. Numbers of slices recorded (n) and mice used (N) are shown as n/N in parentheses. Data are presented as mean  $\pm$  SEM.

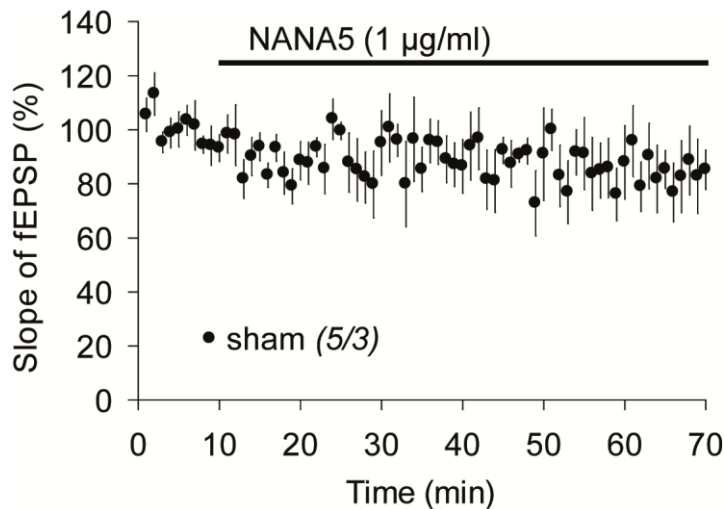


**Fig. 11. Unchanged basal synaptic transmission in mPFC after oligoSia NANA5.** Time course of normalized fEPSP slope showing no changes in fEPSP slope after application of NANA5 (1  $\mu\text{g/ml}$ ) in sham-treated slices. The slopes of fEPSPs were presented as the percentage of the mean fEPSP slope measured during a 10-min basal recording before adding NANA5. Numbers of slices recorded (n) and mice used (N) are shown as n/N. Data are presented as mean  $\pm$  SEM.

### 3.6. EndoNF treatment does not alter theta-burst stimulation-evoked inhibitory postsynaptic currents

Several immunohistochemical studies have demonstrated that polySia is expressed in a subset of mature interneurons in the adult prefrontal cortex (Varea et al., 2005; Varea et al., 2007; Castillo-Gomez et al., 2011; Gomez-Climent et al., 2011). Consequently, it is possible that removal of polySia would result in elevated activation of GluN2B-NMDARs on polySia-positive interneurons, leading to reduced LTP levels via increased excitation of these interneurons. To test the involvement of GABAergic interneurons during our LTP-inducing theta-burst stimulation (TBS) protocol, I recorded isolated TBS-evoked inhibitory postsynaptic currents (IPSCs) in normal aCSF at a holding potential of 0 mV, the reversal potential for postsynaptic currents through glutamatergic AMPAR and NMDAR receptors. These receptors are cation non-selective channels that are permeable for both  $\text{Na}^+$  and  $\text{K}^+$ . At  $\sim 0$  mV, their reversal membrane potential (also known as equilibrium potential), influx of  $\text{Na}^+$  and efflux of  $\text{K}^+$  across the postsynaptic membrane are balanced; thus, no postsynaptic current flows through the channel pore upon binding of the neurotransmitter glutamate to the glutamate receptor (Myme et al., 2003; Purves et al., 2008). Since this approach excludes AMPAR- and NMDAR-mediated currents, the remaining fraction of postsynaptic current at 0 mV is predominantly mediated through  $\text{GABA}_A$  receptors.

To normalize the level of excitation before the induction of TBS, I recorded basal AMPAR-mediated EPSCs at a holding potential of  $-60$  mV and amplitude of  $\sim 100$  pA in each cell. In



summary, whole-cell recordings showed that the ratio between TBS-evoked IPSC amplitude and basal EPSC amplitude was not changed in endoNF-treated slices compared with sham-treated slices (**Fig. 3.12**). Two-way repeated measures ANOVA revealed no significant effects of endoNF in TBS trains 1–5 (for TBS 1,  $F_{(1,98)} = 0.316$ ,  $P = 0.583$ ); for TBS 2 ( $F_{(1,98)} = 0.058$ ,  $P = 0.812$ ); for TBS 3 ( $F_{(1,98)} = 0.004$ ,  $P = 0.949$ ); for TBS 4 ( $F_{(1,98)} = 0.00001$ ,  $P = 0.997$ ); for TBS 5 ( $F_{(1,98)} = 0.0544$ ,  $P = 0.819$ , **Fig. 3.12E**). These findings indicate that inhibition of pyramidal cells mediated by GABAergic interneurons was not affected by endoNF treatment during LTP induction.

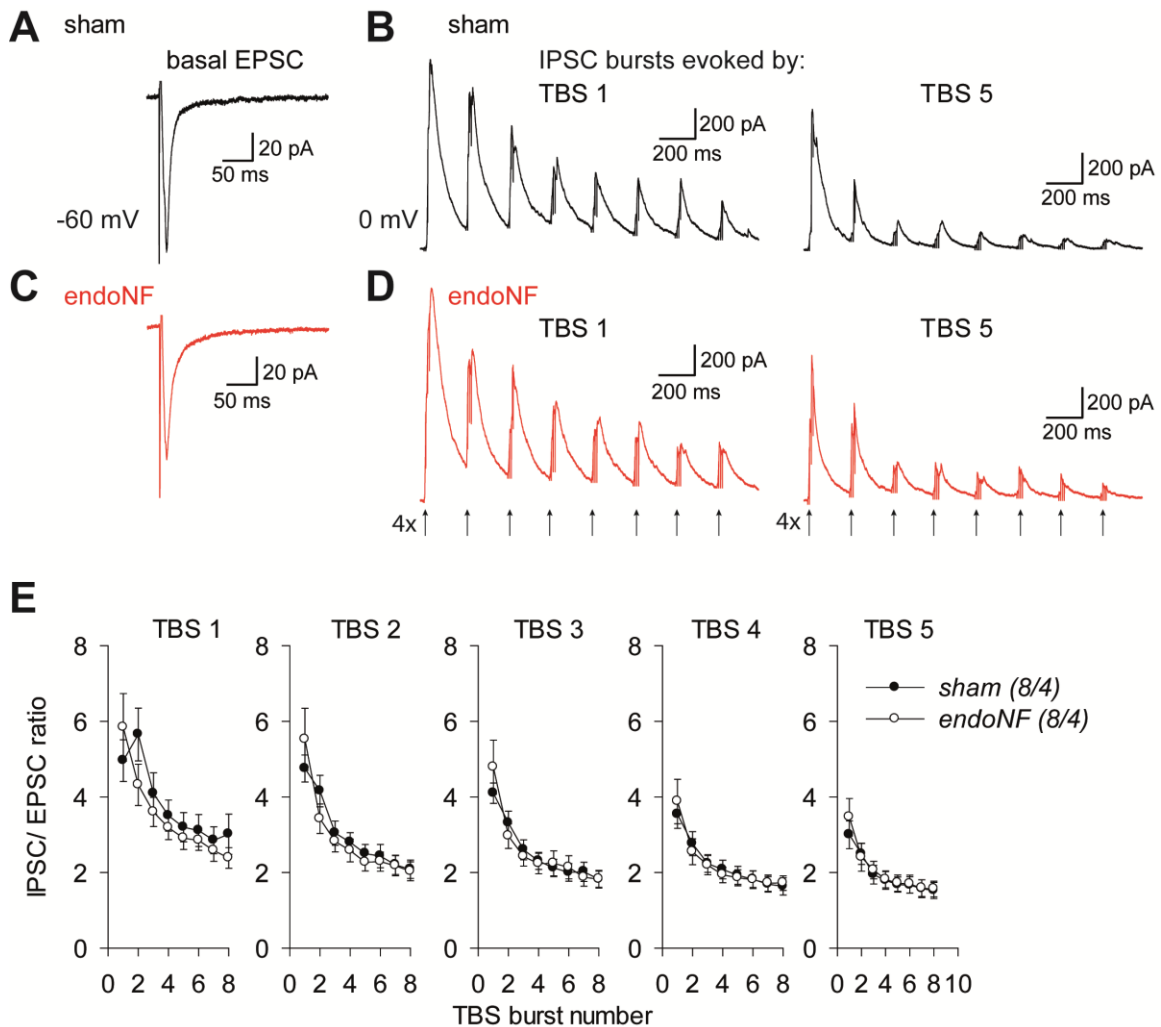


**Fig. 3.12. Unaltered theta-burst stimulation (TBS)-evoked inhibitory postsynaptic currents (IPSCs) mediated by  $\gamma$ -aminobutyric acid type A ( $GABA_A$ ) receptors in endoNF-treated mPFC slices from C57BL/6 mice.** (A, C) Representative examples (averages of 10 traces) of synaptically evoked AMPAR-mediated basal excitatory postsynaptic currents (EPSCs), which were recorded before TBS in sham- (A) and endoNF-treated slices (C). EPSCs were evoked by single electrical pulses at a frequency of 0.033 Hz at a holding potential of  $-60$  mV. (B, D) Representative traces of TBS-evoked IPSCs bursts recorded during the first train of TBS (TBS 1) and the fifth train of TBS (TBS 5) in sham- and endoNF-treated slices. Please note that these IPSCs were recorded at a holding potential of 0 mV. Recordings of both EPSCs and IPSCs were performed in whole-cell voltage-clamp mode in normal aCSF. Arrows (lower panel in D) show the time points at which a burst consisting of four electrical stimuli at 100 Hz (4x) was delivered. (E) Plots showing the ratio between mean amplitudes of TBS-evoked IPSCs during each TBS train (TBS 1–5) and peak amplitude of basal EPSCs, which were recorded before TBS in sham- and endoNF-treated slices. Of note, in all five TBS trains, endoNF-treated slices showed unchanged

IPSC/basal EPSC ratio compared with those in sham-treated slices. Numbers of cells recorded (n) and mice used (N) are shown as n/N in parentheses. Data are presented as mean  $\pm$  SEM.

### 3.7. Increased GluN2B-mediated currents in ST8SIA4-deficient mice

Adult mice deficient in the polysialyltransferase ST8SIA4 (*St8sia4*<sup>-/-</sup>) show no polySia in the mPFC ((Eckhardt et al., 2000; Nacher et al., 2010). To investigate the effects of genetic ST8SIA4 ablation on NMDARs, I recorded AMPAR- and NMDAR-mediated currents from layer V pyramidal neurons in mPFC slices from *St8sia4*<sup>-/-</sup> mice and their wild-type littermates (*St8sia4*<sup>+/+</sup> mice) using whole-cell patch-clamp recordings. Consistent with results in endoNF-treated slices (**Fig. 3.3C**), the NMDAR/AMPA ratio in *St8sia4*<sup>-/-</sup> mice ( $0.33 \pm 0.02$ ) was similar to that in their wild-type *St8sia4*<sup>+/+</sup> littermates ( $0.35 \pm 0.04$ ,  $P = 0.429$ , unpaired Student's *t* test, **Fig. 3.13B**).

Because GluN2B-mediated currents in mPFC pyramidal neurons from endoNF-treated slices were increased (**Fig. 3.3D**), we asked whether this change would be present in mPFC pyramidal cells in polySia-deficient *St8sia4*<sup>-/-</sup> mice. To this aim, I performed whole-cell recordings of isolated NMDAR-EPSCs from pyramidal cells in mPFC slices from *St8sia4*<sup>-/-</sup> and *St8sia4*<sup>+/+</sup> mice and examined the contribution of GluN1/GluN2B-NMDARs by applying low concentration of the GluN2B-selective antagonist Ro 25-6981 (0.3  $\mu$ M). Inhibition of NMDAR-EPSC amplitude by Ro 25-6981 in *St8sia4*<sup>-/-</sup> mice ( $10.32 \pm 1.49\%$ ) was not significantly different from this in *St8sia4*<sup>+/+</sup> mice ( $6.71 \pm 3.46\%$ ,  $P = 0.536$ , Mann-Whitney rank sum test, **Fig. 3.13D**). However, inhibition of NMDAR-EPSC decay time was significantly higher in *St8sia4*<sup>-/-</sup> mice ( $10.07 \pm 3.42\%$ ) compared to that in *St8sia4*<sup>+/+</sup> mice ( $2.82 \pm 2.33\%$ ;  $P = 0.007$ , Mann-Whitney rank sum test, **Fig. 3.13E**). These data suggest that genetic ablation of polySia-synthesizing polysialyltransferase ST8SIA4 leads to increased contribution of the GluN2B-mediated currents (presumably GluN1-GluN2B) in the mPFC, which is in agreement with GluN2B changes observed in endoNF-treated slices.

Analysis of absolute amplitude (pA) and decay time (ms) of the same NMDAR-EPSCs showed similar results (**Fig. 3.13F, G**). In wild-type *St8sia4*<sup>+/+</sup> mice, the mean amplitude of NMDAR-EPSCs was  $99.30 \pm 12.45$  pA during basal recording compared with  $92.96 \pm 12.88$  pA after Ro

25-6981. In *St8sia4*<sup>-/-</sup> mice, the mean NMDAR-EPSC amplitude was 94.93 ± 9.21 pA during basal recording compared with 85.95 ± 9.56 pA in the presence of Ro 25-6981 (**Fig. 3.13F**). A two-way repeated measures ANOVA revealed a significant effect of Ro 25-6981 on amplitude ( $F_{(1,17)} = 18.187$ ,  $P < 0.001$ ), no effect of genotype on amplitude ( $F_{(1,17)} = 0.139$ ,  $P = 0.714$ ), and no drug x genotype interaction ( $F_{(1,17)} = 0.541$ ,  $P = 0.472$ ). In *St8sia4*<sup>+/+</sup> mice, Holm-Sidak *post hoc* test revealed significant differences between mean amplitude during basal recording and in the presence of Ro 25-6981 ( $P = 0.033$ , Holm-Sidak *post hoc* test), which is in contrast with the analysis of Ro 25-6981-mediated inhibition levels that showed no effect of Ro 25-6981 on amplitude in wild-type mice (**Fig. 13.3D**). It is noteworthy that GluN2B contribution predominantly influences the decay time of the NMDAR-EPSC but not necessarily its amplitude (reviewed by (Paoletti et al., 2013)). In *St8sia4*<sup>-/-</sup> mice, Ro 25-6981 significantly inhibited mean amplitude during basal recording and in the presence of Ro 25-6981 ( $P = 0.001$ , Holm-Sidak *post hoc* test).

In wild-type *St8sia4*<sup>+/+</sup> mice, mean decay time of NMDAR-EPSCs during basal recording was 123.42 ± 10.84 ms compared with 119.47 ± 9.87 ms after the addition of Ro 25-6981. In *St8sia4*<sup>-/-</sup> mice, mean decay time of NMDAR-EPSCs during basal recording was 98.72 ± 11.27 ms versus 86.01 ± 9.36 ms after Ro 25-6981 (**Fig. 3.13G**).

A two-way repeated measures ANOVA revealed a significant effect of Ro 25-6981 on decay time ( $F_{(1,17)} = 13.656$ ,  $P = 0.002$ ), and a tendency for the effect of genotype ( $F_{(1,17)} = 3.822$ ,  $P = 0.067$ ), as well as for drug x genotype interaction ( $F_{(1,17)} = 3.789$ ,  $P = 0.068$ ). In wild-type *St8sia4*<sup>+/+</sup> mice, Holm-Sidak *post hoc* test revealed no significant difference in decay time between basal recording and Ro 25-6981 ( $P = 0.266$ ); however, in *St8sia4*<sup>-/-</sup> mice, Ro 25-6981 significantly reduced decay time compared with that during basal recording ( $P < 0.001$ ), confirming that GluN2B-mediated transmission is increased in *St8sia4*<sup>-/-</sup> mice.

Because tonic NMDAR-mediated currents were strongly increased in endoNF-treated slices, I also recorded whole-cell holding currents before and after NMDAR-selective antagonist AP5 (50 μA) in layer V pyramidal neurons in mPFC slices from *St8sia4*<sup>-/-</sup> and *St8sia4*<sup>+/+</sup> mice. These recordings revealed that the mean NMDAR-tonic current in *St8sia4*<sup>-/-</sup> mice (35.75 ± 2.35 pA) was similar to that recorded in *St8sia4*<sup>+/+</sup> mice (33.42 ± 5.72 pA;  $P = 0.792$ , Mann-Whitney rank

sum test, **Fig. 3.14**), suggesting a compensatory mechanism for tonic currents in these knockout mice, in contrast to the increase in tonic currents after acute enzymatic depletion of polySia.

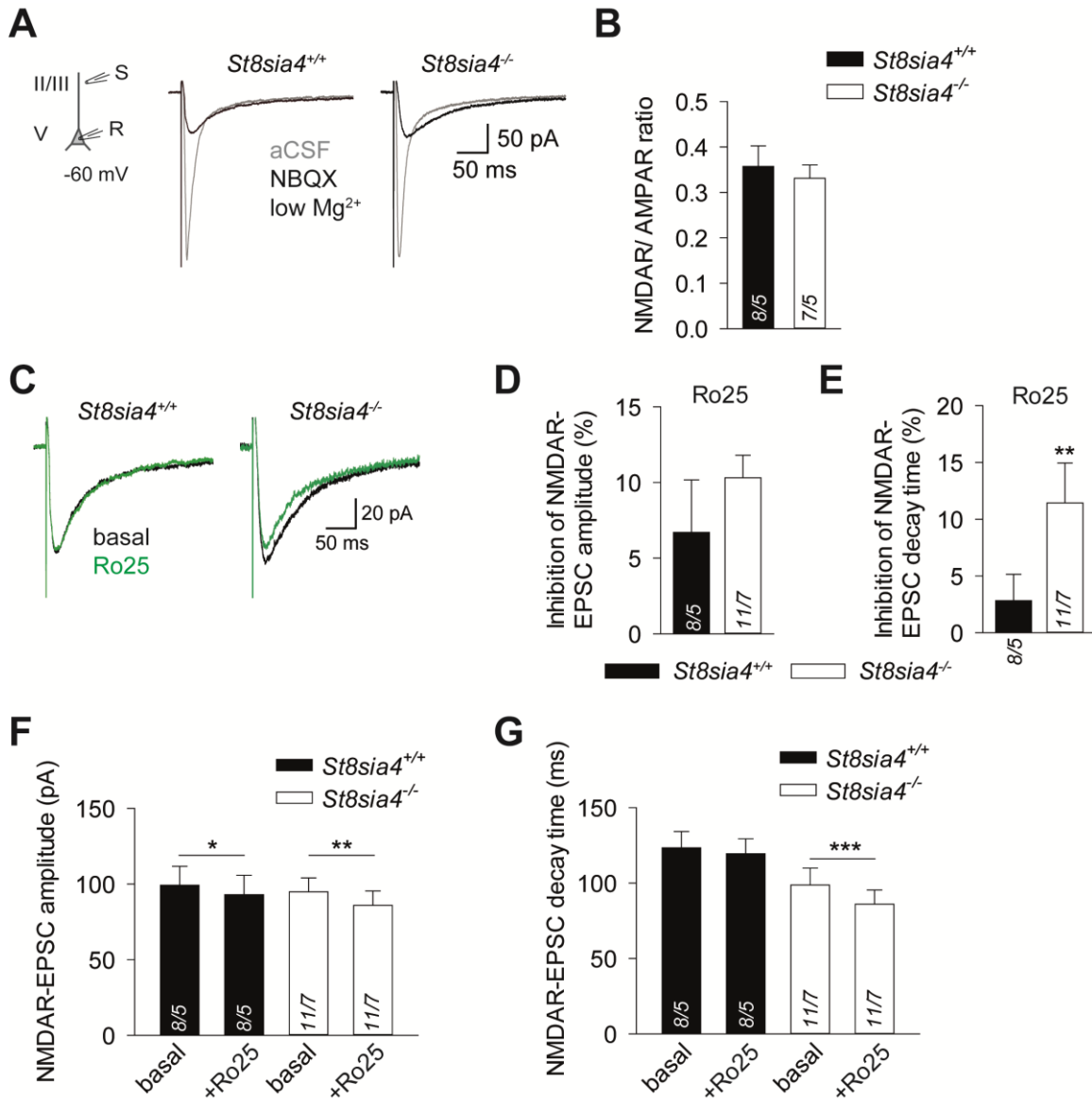


**Fig. 3.13. Unchanged NMDAR/AMPA ratio and increased GluN2B-mediated currents in ST8SIA4-deficient mice.** (A) Representative examples (averages of 8–10 traces) of fast, evoked AMPAR-mediated EPSCs recorded in normal aCSF (gray traces) and slow NMDAR-EPSCs (black traces; isolated in Mg<sup>2+</sup> (0.1 mM), NBQX (10 μM), and CGP-55845 (2 μM)) from layer V pyramidal neurons in mPFC slices from *St8sia4*<sup>+/+</sup> and *St8sia4*<sup>-/-</sup> mice. The experimental design for evoked EPSCs in whole-cell voltage-clamp mode at a holding potential of –60 mV is shown in inset (left). II/III, V, cortical layer; R, recording electrode. (B) A bar graph showing similar mean NMDAR/AMPA ratio in *St8sia4*<sup>-/-</sup> and

*St8sia4*<sup>+/+</sup> mice. (C) Representative examples (averages of 8–10 traces) of evoked NMDAR-EPSCs during 5-min basal recording (black traces) and 10–15 min after addition of Ro 25-6981 (Ro25, 0.3  $\mu$ M, green traces) in layer 5 pyramidal neurons in mPFC slices from *St8sia4*<sup>-/-</sup> and *St8sia4*<sup>+/+</sup> mice. (D, E) Summary bar graphs showing unaltered inhibition of NMDAR-EPSC peak amplitude (D) but significantly increased inhibition of NMDAR-EPSC decay (E) after application of Ro 25-6981 in neurons from *St8sia4*<sup>-/-</sup> mice compared with *St8sia4*<sup>+/+</sup> mice. (F, G) Absolute values of peak amplitude (F) and decay time (G) of evoked NMDAR-EPSCs were measured during a 5-min time interval before (basal) and 10–15 min after application of Ro 25-6981 (Ro25, 0.3  $\mu$ M). The cells analyzed are the same as in C–E. (F) Ro 25-6981 significantly reduced amplitude of NMDAR-EPSCs in pyramidal neurons from both *St8sia4*<sup>-/-</sup> and *St8sia4*<sup>+/+</sup> mice. (G) Please note that Ro 25-6981 significantly inhibited decay time of NMDAR-EPSCs in *St8sia4*<sup>-/-</sup> mice but not in wild-type *St8sia4*<sup>+/+</sup> mice. \* $P < 0.05$ , \*\* $P < 0.01$ , \*\*\* $P < 0.001$ , for description of statistical analysis, please see the text. Numbers of cells recorded (n) and mice used (N) are shown in bars as n/N. Data are presented as mean  $\pm$  SEM.

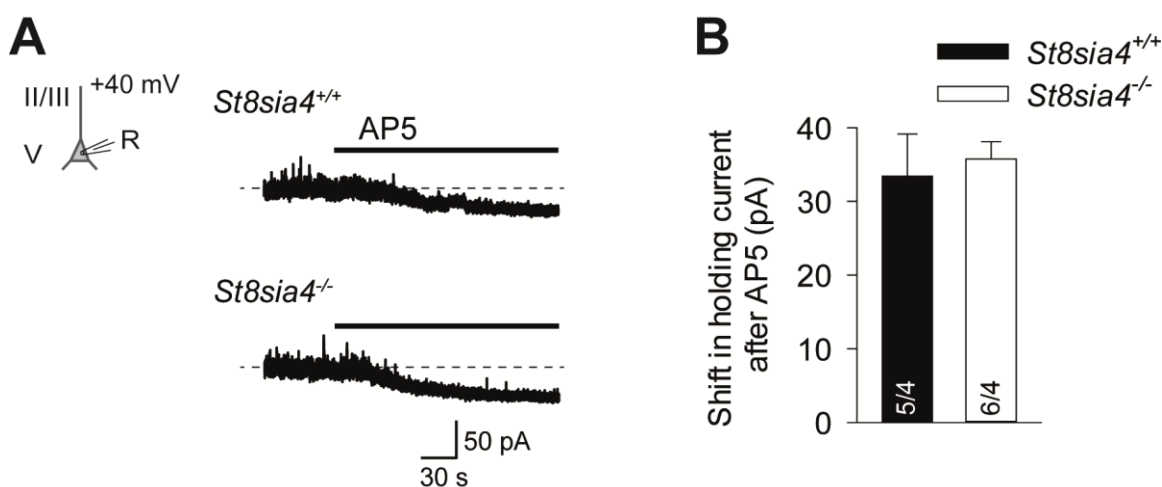


**Fig. 3.14. Unaltered tonic NMDAR-mediated currents in ST8SIA4-deficient mice.** (A) Representative traces of NMDAR-mediated holding currents (holding potential +40 mV) recorded from layer V pyramidal neurons before and after bath application of the NMDAR-specific antagonist AP5 (50  $\mu$ M) in mPFC slices from *St8sia4*<sup>+/+</sup> and *St8sia4*<sup>-/-</sup> mice. The inset (left) illustrates the experimental design for whole-cell voltage-clamp recordings of tonic currents. The recorded cell was not stimulated synaptically. Tonic currents were recorded in aCSF containing the AMPAR-specific antagonist NBQX (10  $\mu$ M), GABA<sub>A</sub> receptor-specific antagonist picrotoxin (50  $\mu$ M), and the GABA<sub>B</sub> receptor-specific antagonist CGP-55845 (2  $\mu$ M). Horizontal dotted lines show the basal level of holding current before the addition of

AP5. II/III, V, cortical layer; R, recording electrode. **(B)** A bar graph summarizing the mean amplitude of tonic NMDAR-mediated currents (measured as shift in holding current) recorded in pyramidal neurons in slices from *St8sia4<sup>+/+</sup>* and *St8sia4<sup>-/-</sup>* mice. The amplitude of tonic currents in *St8sia4<sup>-/-</sup>* mice was not changed compared with that in wild-type *St8sia4<sup>+/+</sup>* mice. Numbers of cells recorded (n) and mice used (N) are shown presented in bars as n/N. Data are presented as mean  $\pm$  SEM.

### 3.8. Impaired long-term potentiation in the mPFC of ST8SIA4-deficient mice and its pharmacological rescue

Because endoNF treatment led to reduced LTP in the mPFC (**Fig. 3.8**), we next sought to determine whether LTP induction is also affected in the mPFC of polySia-deficient *St8sia4<sup>-/-</sup>* mice. To this end, I recorded TBS-induced LTP of fEPSPs at mPFC layer II/III–layer V synapses in slices from *St8sia4<sup>-/-</sup>* mice and their wild-type littermates (*St8sia4<sup>+/+</sup>*). In agreement with results in endoNF-treated slices, the level of LTP in slices from *St8sia4<sup>-/-</sup>* mice ( $87.10 \pm 4.21\%$ ) was significantly reduced compared with *St8sia4<sup>+/+</sup>* mice ( $128.96 \pm 6.99\%$ ; two-way ANOVA, significant effect of genotype ( $F_{(1,68)} = 15.623$ ,  $P < 0.001$ ); Holm-Sidak *post hoc* test for untreated *St8sia4<sup>-/-</sup>* vs. untreated *St8sia4<sup>+/+</sup>*,  $P < 0.001$ ; **Fig. 3.15A, G**), indicating that both acute polySia removal and genetic ablation of polySia-synthesizing ST8SIA4 lead to abnormal synaptic plasticity in this brain region.

Previous studies have suggested that glutamate spillover activating extrasynaptic NMDARs is stronger at room temperature (21–23°C) than at physiological temperature (35–37°C) because glutamate clearance from the extrasynaptic space is improved at 35–37°C (Asztely et al., 1997; Kullmann and Asztely, 1998). To test whether the impairment of LTP in polySia-deficient mice depends on recording temperature, I repeated LTP recordings in mPFC slices from *St8sia4<sup>-/-</sup>* mice and their wild-type littermates at 35°C. In agreement with recordings at room temperature (**Fig. 3.15A**), fEPSP recordings revealed that the strong reduction in LTP levels in *St8sia4<sup>-/-</sup>* compared with *St8sia4<sup>+/+</sup>* mice persisted at physiological temperature ( $95.93 \pm 10.00\%$  in *St8sia4<sup>-/-</sup>* at 35°C;  $147.00 \pm 7.54\%$  in *St8sia4<sup>+/+</sup>* at 35°C; Holm-Sidak *post hoc* test for *St8sia4<sup>-/-</sup>* at 35°C vs. *St8sia4<sup>+/+</sup>* at 35°C,  $P < 0.001$ ; **Fig. 3.15B, G**). In slices from *St8sia4<sup>-/-</sup>* mice, Holm-Sidak *post hoc* test revealed no significant difference in LTP levels between physiological and room temperature (Holm-Sidak *post hoc* test for *St8sia4<sup>-/-</sup>* at 35°C vs. *St8sia4<sup>-/-</sup>* untreated,  $P =$

0.384, **Fig. 3.15G**), suggesting that the activation of extrasynaptic NMDARs by TBS (in contrast to a single pulse) at physiological temperature is similar to that measured at room temperature.

Since the GluN2B-selective antagonist Ro 25-6981, short-chain polySia NANA12, and the GlyT1 inhibitor sarcosine restored LTP in endoNF-treated mPFC slice, we wondered whether these pharmacological treatments would improve LTP in *St8sia4*<sup>-/-</sup> mice.

In the presence of Ro 25-6981 (0.3 μM), LTP levels in mPFC slices from *St8sia4*<sup>-/-</sup> mice (125.86 ± 6.73%) were fully restored to the level of wild-types (128.15 ± 4.83%; two-way ANOVA, significant effect of treatment,  $F_{(4,68)} = 7.781$ ,  $P < 0.001$ ; significant genotype x treatment interaction,  $F_{(4,68)} = 7.042$ ,  $P < 0.001$ ; Holm-Sidak *post hoc* test for *St8sia4*<sup>-/-</sup> + Ro 25-6981 vs. *St8sia4*<sup>+/+</sup> + Ro 25-6981,  $P = 0.967$ ). It is noteworthy that LTP levels in *St8sia4*<sup>-/-</sup> slices perfused in Ro 25-6981 were significantly higher than those in untreated *St8sia4*<sup>-/-</sup> slices (Holm-Sidak *post hoc* test for *St8sia4*<sup>-/-</sup> + Ro 25-6981 vs. *St8sia4*<sup>-/-</sup> untreated,  $P < 0.001$ ; **Fig. 3.15C, G**).

Consistent with the effects of Ro 25-6981, NANA12 (1 μg/ml) increased LTP magnitude in *St8sia4*<sup>-/-</sup> mice to 135.41 ± 7.85%, a level significantly higher than that in untreated *St8sia4*<sup>-/-</sup> slices (Holm-Sidak *post hoc* test for *St8sia4*<sup>-/-</sup> +NANA12 vs. *St8sia4*<sup>-/-</sup> untreated,  $P < 0.001$ , **Fig. 3.15D, G**). Moreover, LTP levels in *St8sia4*<sup>-/-</sup> slices perfused with NANA12 were not significantly different from those in NANA12-treated *St8sia4*<sup>+/+</sup> slices (136.96 ± 6.19%; Holm-Sidak *post hoc* test for *St8sia4*<sup>-/-</sup> +NANA12 vs. *St8sia4*<sup>+/+</sup> +NANA12,  $P = 0.873$ ). Thus, these data suggest that LTP induction in ST8SIA4-deficient mice was restored by NANA12 via inhibition of GluN1/GluN2B-NMDARs, which is in line with LTP restoration by NANA12 in endoNF-treated slices.

Similarly, LTP levels in mPFC slices from *St8sia4*<sup>-/-</sup> mice perfused in sarcosine (0.75 mM) (146.63 ± 3.20%) were significantly higher than those measured in untreated *St8sia4*<sup>-/-</sup> slices (Holm-Sidak *post hoc* test for *St8sia4*<sup>-/-</sup> + sarcosine vs. *St8sia4*<sup>-/-</sup> untreated,  $P < 0.001$ ; **Fig. 3.15E, G**). In line with the effects of Ro 25-6981 and NANA12, LTP levels in sarcosine-treated *St8sia4*<sup>-/-</sup> slices and sarcosine-treated wild-type slices (140.09 ± 8.09%) were similar (Holm-Sidak *post hoc* test for *St8sia4*<sup>-/-</sup> +sarcosine vs. *St8sia4*<sup>-/-</sup> +sarcosine,  $P = 0.548$ ), indicating that potentiating synaptic NMDARs by GlyT1 inhibitors can compensate for the GluN2B-mediated disturbance of LTP.



It has to be noted that neither Ro 25-6981, NANA12, or sarcosine had effects on LTP induction in *St8sia4<sup>+/+</sup>* mice (Holm-Sidak *post hoc* test for *St8sia4<sup>+/+</sup>* +Ro 25-6981 vs. *St8sia4<sup>+/+</sup>* untreated,  $P = 0.776$ ; for *St8sia4<sup>+/+</sup>* +NANA12 vs. *St8sia4<sup>+/+</sup>* untreated,  $P = 0.852$ ; for *St8sia4<sup>+/+</sup>* +sarcosine vs. *St8sia4<sup>+/+</sup>* untreated,  $P = 0.856$ ; **Fig. 15C–E**), consistent with the unaltered LTP recorded in the presence of Ro 25-6981 in sham-treated slices from C57BL/6 mice (**Fig. 3.10**).

In line with the inability of oligoSia NANA5 to rescue LTP in endoNF-treated slices (**Fig. 3.8**), NANA5 (10  $\mu\text{g/ml}$ ) had a tendency to impair LTP induction in slices from *St8sia4<sup>+/+</sup>* mice ( $101.09 \pm 15.66\%$  in *St8sia4<sup>+/+</sup>* +NANA5), although the difference between NANA5-treated *St8sia4<sup>+/+</sup>* slices and untreated wild-type slices did not reach statistical significance (unpaired Student's *t* test for *St8sia4<sup>+/+</sup>* +NANA5 vs. *St8sia4<sup>+/+</sup>* untreated,  $P = 0.147$ ; **Fig. 3.15F, G**). This finding hence indicates that, in contrast to NANA12, the shorter NANA5 does not enhance and may even inhibit synaptic plasticity.

In summary, these findings indicate that the low concentration of the GluN2B antagonist Ro 25-6981, short polySia fragments NANA12, and the GlyT1 inhibitor sarcosine could normalize deficits in cortical synaptic plasticity in polySia-deficient mice, whereas oligoSia NANA5 had detrimental effects on LTP.

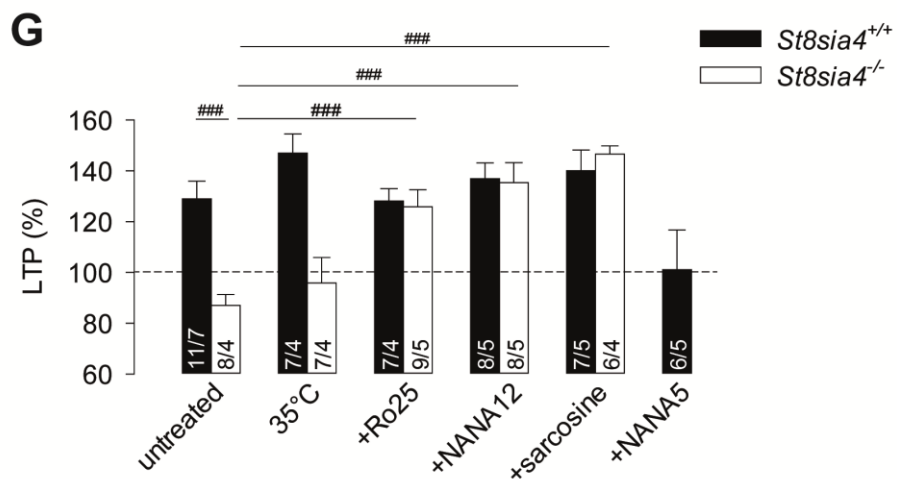
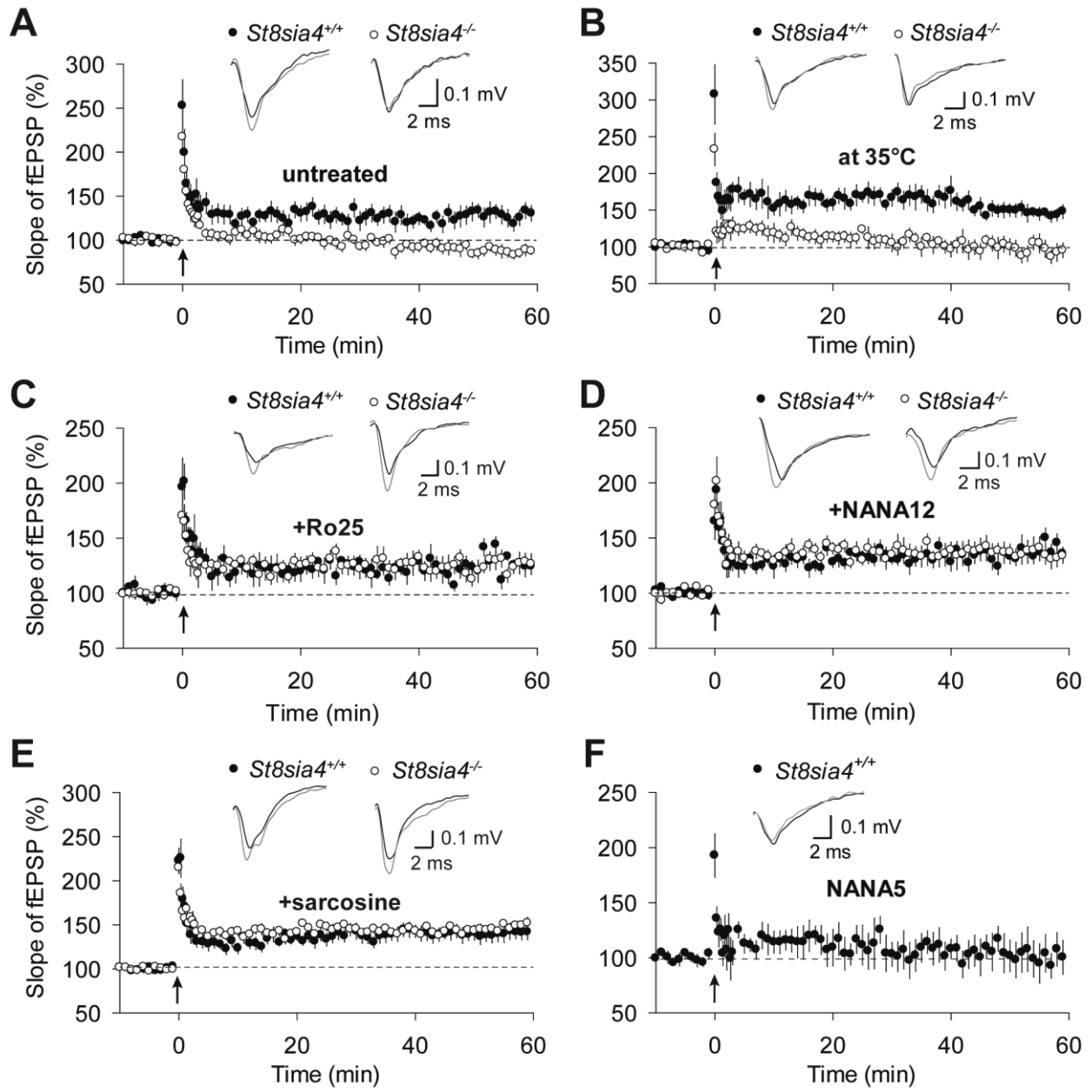


**Fig. 3.15. Impaired long-term potentiation (LTP) in the mPFC of ST8SIA4-deficient mice and its restoration by Ro 25-6981, NANA12, and sarcosine.** (A–F) Time courses of normalized mean slopes and representative examples of field excitatory postsynaptic potentials (fEPSPs, insets) in mPFC slices from *St8sia4*<sup>-/-</sup> mice and their wild-type littermates (*St8sia4*<sup>+/+</sup> mice). (A) Decreased levels of theta-burst stimulation (TBS)-induced LTP recorded in normal aCSF (untreated) in mPFC slices from *St8sia4*<sup>-/-</sup> mice compared with *St8sia4*<sup>+/+</sup> mice. (B) At physiological temperature (35°C), reduced levels of LTP in mPFC slices from *St8sia4*<sup>-/-</sup> mice compared with *St8sia4*<sup>+/+</sup> mice persist. Recordings in A and B were performed in normal aCSF. (C–E) In slices from *St8sia4*<sup>-/-</sup> mice, the levels of LTP were fully restored to the level of wild-type *St8sia4*<sup>+/+</sup> mice in the presence of either Ro 25-6981 (Ro25, 0.3 μM) (C), short-chain polySia NANA12 (1 μg/ml) (D), or sarcosine (0.75 mM) (E). Please note that LTP levels in slices from *St8sia4*<sup>+/+</sup> mice remained unchanged in the presence of either Ro 25-6981 (0.3 μM) (C), NANA12 (1 μg/ml) (D), or sarcosine (0.75 mM) (E). (F) In the presence of oligoSia NANA5 (10 μg/ml), LTP induction in wild-type *St8sia4*<sup>+/+</sup> mice was impaired. Arrows indicate the time points at which five trains of TBS were applied via stimulation electrode. Example fEPSPs (insets) represent averages of 30 fEPSPs recorded during a 10-min time interval before TBS (basal recording, black trace) and 50–60 min after TBS (gray trace) in each condition. Slopes of fEPSPs are presented as the percentage of mean fEPSP slope measured during basal recording. (G) A bar graph summarizing LTP levels measured 50–60 min after TBS delivery in slices from *St8sia4*<sup>-/-</sup> and *St8sia4*<sup>+/+</sup> mice in A–F. <sup>###</sup>*P* < 0.001, for description of statistical analysis, please see the text. Numbers of slices recorded (n) and mice used (N) are shown in bars as n/N. Data are presented as mean ± SEM.

### 3.9. Decreased mPFC LTP levels in NCAM-deficient mice can be restored by sarcosine

Previous studies have demonstrated that constitutively NCAM-deficient (*Ncam*<sup>-/-</sup>) mice show impaired LTP in the CA1 subregion of the hippocampal slices (Kochlamazashvili et al., 2010; Kochlamazashvili et al., 2012). Importantly, *Ncam*<sup>-/-</sup> mice show a nearly total loss of both NCAM and polySia in the hippocampus and mPFC (Cremer et al., 1994). To assess whether NCAM deficiency would affect synaptic plasticity in the mPFC and to test the effects of GlyT1 inhibitors on LTP, I recorded TBS-induced LTP of fEPSPs at mPFC layer II/III–layer V synapses in slices from *Ncam*<sup>-/-</sup> mice and their wild-type littermates in normal aCSF and then repeated these recordings in the presence of sarcosine (0.75 mM). In normal aCSF, mean LTP levels in slices from *Ncam*<sup>-/-</sup> mice (106.62 ± 3.67%) were significantly lower compared with those from

wild-type *Ncam*<sup>+/+</sup> mice ( $129.38 \pm 4.40\%$ ; **Fig. 3.16A, C**). Importantly, in the presence of sarcosine, the LTP magnitude in *Ncam*<sup>-/-</sup> mice ( $131.96 \pm 4.69\%$ ) was similar to that measured in *Ncam*<sup>+/+</sup> mice ( $129.19 \pm 4.41\%$ ; **Fig. 3.16B, C**). A two-way ANOVA revealed significant effects of mouse genotype ( $F_{(1,35)} = 4.246$ ,  $P = 0.047$ ), drug treatment ( $F_{(1,35)} = 6.702$ ,  $P = 0.014$ ), and a significant genotype x treatment interaction ( $F_{(1,35)} = 6.811$ ,  $P = 0.013$ ). A Holm-Sidak *post hoc* test showed a significant reduction of mean LTP magnitude in *Ncam*<sup>-/-</sup> mice compared with *Ncam*<sup>+/+</sup> mice ( $P < 0.001$ , **Fig. 3.16A, C**), which is in line with the impaired LTP in endoNF-treated mPFC slices as well as in *St8sia4*<sup>-/-</sup> slices.

In slices from *Ncam*<sup>+/+</sup> mice, sarcosine did not alter LTP levels compared with untreated *Ncam*<sup>+/+</sup> slices ( $P = 0.990$ , Holm-Sidak *post hoc* test, **Fig. 3.16B, C**). In slices from *Ncam*<sup>-/-</sup> mice, however, sarcosine significantly increased mean LTP levels ( $P < 0.001$ , Holm-Sidak *post hoc* test, **Fig. 3.16B, C**), thus confirming the efficacy of sarcosine in restoring impaired LTP in endoNF-treated slices and *St8sia4*<sup>-/-</sup> slices without altering synaptic plasticity in sham-treated or wild-type slices.

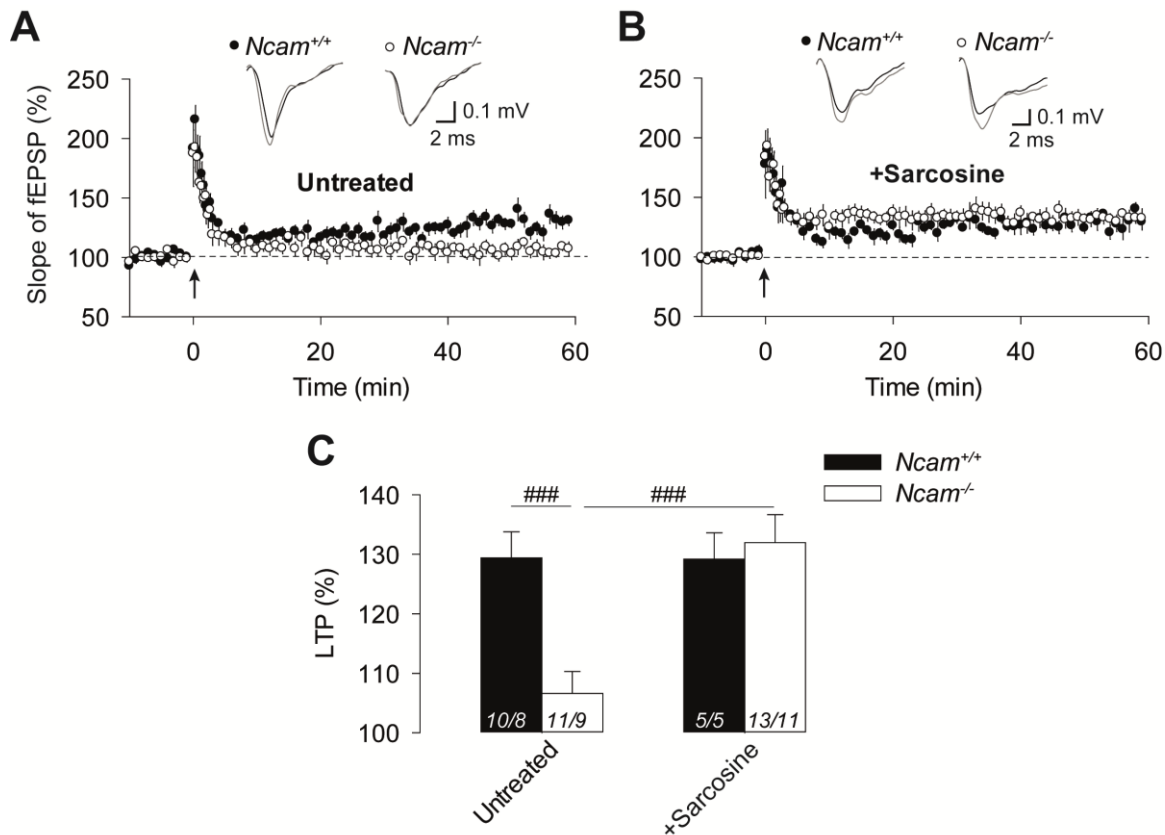


**Fig. 3.16. Impaired long-term potentiation (LTP) in mPFC slices from NCAM-deficient mice and its restoration by sarcosine.** (A, B) Time courses of normalized mean slopes and representative examples of field excitatory postsynaptic potentials (fEPSPs, insets) in mPFC slices from *Ncam*<sup>-/-</sup> mice and their wild-type littermates (*Ncam*<sup>+/+</sup> mice). (A) In normal aCSF (untreated), slices from *Ncam*<sup>-/-</sup> mice showed reduced levels of TBS-induced LTP compared with *Ncam*<sup>+/+</sup> mice. (B) In the presence of sarcosine (0.75 mM), LTP levels in slices from *Ncam*<sup>-/-</sup> mice were fully restored to the level of wild-type controls. Arrows indicate the time points at which five trains of TBS were applied via stimulation electrode. Example fEPSPs (insets) represent averages of 30 fEPSPs recorded during a 10-min time interval before TBS (basal recording, black trace) and 50–60 min after TBS (gray trace) in each condition. Slopes of fEPSPs are presented as the percentage of mean fEPSP slope measured during basal recording. (C) A summary bar graph showing mean LTP levels recorded 50–60 min after TBS in slices from *Ncam*<sup>-/-</sup> mice in each treatment. <sup>###</sup>*P* < 0.001, for description of statistical analysis, please see the text. Numbers of slices recorded (n) and mice used (N) are shown in bars as n/N. Data are presented as mean ± SEM.

## 4. DISCUSSION

The data obtained in the present study provide evidence that the glycan polySia supports NMDAR-dependent synaptic plasticity at excitatory synapses by controlling the balance between extrasynaptic and synaptic NMDARs in the mPFC (for a graphical summary, see **Fig. 4.1**). Using patch-clamp recordings, we revealed that acute enzymatic depletion of polySia using endoNF or genetic ablation of its polySia-synthesizing enzyme ST8SIA4 led to substantial increases in evoked GluN2B-NMDAR-mediated currents as well as in tonic, extrasynaptic NMDAR-mediated currents recorded from pyramidal cells in mPFC slices. Field EPSP recordings further showed that these changes in signaling through GluN2B-containing NMDARs resulted in impaired LTP in the mPFC not only in endoNF-treated slices but also in slices from ST8SIA4-deficient mice. Importantly, in polySia-depleted slices, short-chain polySia fragments NANA12 inhibited a fraction of NMDAR-mediated currents, which was similar to that blocked by the highly selective GluN2B antagonist Ro 25-6981, when applied at 0.3  $\mu\text{M}$ , a low micromolar concentration specific for GluN1/GluN2B-NMDARs. Thus, we hypothesized that suppression of GluN1/GluN2B-NMDARs would alleviate impaired synaptic plasticity in this region. In line with this view, application of 0.3  $\mu\text{M}$  Ro 25-6981 and NANA12 fully restored LTP induction in the mPFC after endoNF treatment and in ST8SIA4-deficient mice. In addition, we showed that these LTP deficits could be also rescued by potentiating synaptic NMDARs using sarcosine, a clinically used inhibitor of the glycine transporter type 1 (GlyT1). Together, these data indicate that re-balancing the signaling through synaptic versus extrasynaptic NMDARs rescues synaptic plasticity in polySia/NCAM-deficient mice. Since schizophrenia patients show increased serum levels of polySia-NCAM correlated with impaired declarative memory, negative symptoms, and reduced PFC volume (Piras et al., 2015), our data suggest that NANA12 and highly potent GlyT1 inhibitors might provide promising options for treatment of the cognitive disturbances observed in these patients.

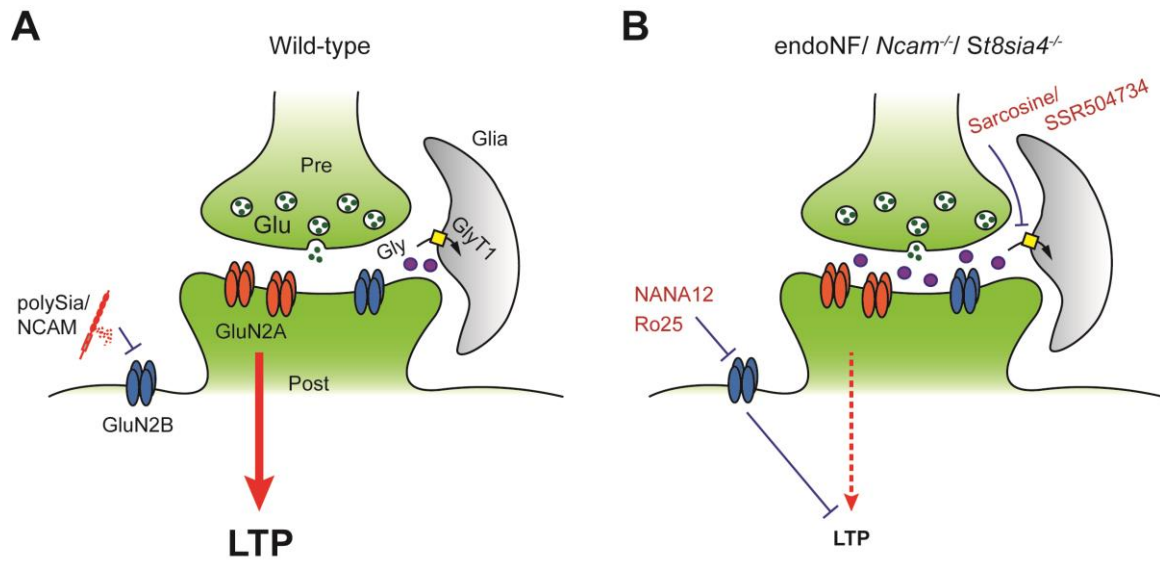


**Fig. 4.1. Proposed mechanism underlying polySia-mediated modulation of NMDAR-dependent LTP at excitatory synapses in the murine mPFC.** (A) In wild-type mice, polySia-NCAM inhibits currents through extrasynaptic GluN2B subunit-containing NMDARs. In our recording conditions, LTP in the wild-type mPFC is mainly supported by synaptic NMDARs containing the GluN2A subunit. Please note that the glial glycine transporter 1 (GlyT1) removes glycine from the synaptic space, thereby maintaining a low glycine concentration in the vicinity of postsynaptic NMDARs under physiological conditions. (B) Enzymatic removal of polySia using endoNF treatment or genetic ablation of polySia in *St8sia4<sup>-/-</sup>* or *Ncam<sup>-/-</sup>* mice lead to increased evoked and tonic currents that might be predominantly mediated through extrasynaptic GluN1/GluN2B-NMDARs, whereas currents through synaptic NMDARs might be reduced. These changes ultimately result in strongly reduced LTP levels in endoNF-treated slices and slices from *St8sia4<sup>-/-</sup>* or *Ncam<sup>-/-</sup>* mice. Abnormal LTP is fully restored by resetting the synaptic to extrasynaptic NMDARs ratio using several pharmacological treatments, including i) GluN2B-NMDAR-specific antagonist Ro 25-6981 (Ro25) at 0.3  $\mu$ M, ii) polySia containing 12 sialic acid residues (NANA12), and iii) glycine transporter 1 inhibitors sarcosine or SSR 504734. Pre, presynapse; Post, postsynapse; Glu, glutamate; Gly, glycine.

#### 4.1. Effects of polySia removal on NMDARs and synaptic plasticity in the mPFC

We recorded synaptically evoked NMDAR-mediated currents at room temperature (22–24°C) instead at physiological temperature (35–37°C). Our decision was based on previous reports (Asztely et al., 1997; Kullmann and Asztely, 1998) showing that the glutamate transporter-

dependent clearance of glutamate from the extrasynaptic space is less efficient at lower temperatures, thereby allowing for a larger diffusion, also known as spillover, of extracellular glutamate at room temperature compared with 35–37°C. In line with this view, Aszetyly and colleagues (1997) showed that activation of extrasynaptic NMDARs by a single-pulse electrical stimulation is stronger at 22–24°C than at 35–37°C. Accordingly, we argue that the elevated GluN2B-mediated component in our synaptic NMDAR-EPSCs reflects the excessive activation of extrasynaptic rather than synaptic GluN2B subunits. Although we did not record evoked and tonic currents at 35–37°C, at this temperature, we would expect reduced amplitudes of evoked GluN2B-mediated currents and tonic NMDAR-mediated currents compared with our recordings at room temperature. Our extracellular recordings revealed that extracellular GluN2B-mediated impairments in LTP induction in ST8SIA4-deficient mice can be observed both at room and physiological temperature. It has been shown that short trains of electrical stimuli or theta-burst stimulation lead to overactivation of extrasynaptic GluN2B-NMDARs (Lozovaya et al., 2004), which most likely occurs not only at room but also at physiological temperature. We did not attempt to compare TBS-induced activation of extrasynaptic NMDARs at physiological temperature, because even a single TBS train may induce plasticity of NMDAR-mediated component and, thus, preclude accurate estimation of Ro 25-6981-sensitive component. Instead, we relied on single-pulse stimulation at room temperature, which allowed us to reliably isolate Ro 25-sensitive component of NMDARs currents.

To study the contribution of heterodimeric GluN1/GluN2B-containing NMDARs to synaptic plasticity in the mPFC, we took advantage of low concentrations of Ro 25-6981, an allosteric, high-affinity, selective antagonist of the GluN2B subunit, which shows a complex mode of action (Karakas et al., 2011). It has been shown that Ro 25-6981 binds at the interface of the heterodimer consisting of the GluN1 and GluN2B subunits (Karakas et al., 2011). Ro 25-6981 is structurally related to ifenprodil, which is also non-competitive antagonist at GluN2B-NMDARs (Williams, 1993). Compared with ifenprodil, however, Ro 25-6981's potency in blocking NMDARs containing GluN2B subunits is ~25-fold higher (Fischer et al., 1997). Recent studies have reported that Ro 25-6981, at concentrations of up to 1  $\mu$ M, specifically blocks GluN1/GluN2B-NMDARs with an  $IC_{50}$  value in the nanomolar range (Volianskis et al., 2013). Based on this characterization, France and coworkers have used 1  $\mu$ M Ro 25-6981 to dissect the contribution of GluN1/GluN2B-NMDARs to long-term depression (LTD) in the CA1 subregion



of the juvenile hippocampus (France et al., 2017). In contrast, Ro 25-6981, at concentrations 3–30  $\mu\text{M}$ , inhibits heterotrimeric GluN1/GluN2A/GluN2B-NMDARs, and Ro 25-6981 concentrations higher than 30  $\mu\text{M}$  partially inhibit GluN1/GluN2A-NMDARs (Fischer et al., 1997; Hatton and Paoletti, 2005; Volianskis et al., 2013; Hansen et al., 2014).

Moreover, the level of inhibition of NMDA-induced currents by Ro 25-6981 does not change at different holding potentials, indicating a voltage-independent mode of action (Fischer et al., 1997). Altogether, these effects of Ro 25-6981 suggest that the pharmacological data obtained using GluN2B-specific antagonists should be interpreted with special caution. One further limitation of pharmacological manipulations using subunit blockers is that these drugs affect NMDARs, which are expressed on both pyramidal cells and interneurons, thus affecting the level of synaptic plasticity (reviewed by (Shipton and Paulsen, 2014)).

Acute removal of polySia by endoNF treatment caused a pronounced increase in tonic NMDAR-mediated currents, which is consistent with the increase of GluN2B-mediated component of evoked NMDAR-mediated currents in endoNF-treated mPFC slices. It is important to note that these tonic NMDAR-mediated currents reflect the tonic activation of extrasynaptic GluN2B-NMDARs by ambient glutamate, and they have been reported to persist after blockade of synaptic activity by TTX (Sah et al., 1989; Herman and Jahr, 2007; Le Meur et al., 2007; Papouin et al., 2012; Povysheva and Johnson, 2012). The basal amplitude of tonic, NMDAR-mediated holding currents recorded in the current study is in line with previous electrophysiological experiments in brain slices containing the hippocampal CA1 subregion (Sah et al., 1989; Le Meur et al., 2007; Papouin et al., 2012) or mPFC (Povysheva and Johnson, 2012). In support of elevated activation of extrasynaptic GluN2B-NMDAs upon endoNF, two-photon  $\text{Ca}^{2+}$  imaging has revealed strongly increased GluN2B-mediated  $\text{Ca}^{2+}$  transients recorded from the aspiny, most likely extrasynaptic, portion of CA1 pyramidal cell dendrites after endoNF treatment of hippocampal slices, and this phenotype could be restored by application of long-chain polySia (Kochlamazashvili et al., 2010). Likewise, field EPSP recordings in hippocampal slices have shown increased GluN2B- and decreased GluN2A-mediated synaptic transmission in the CA1 subregion of adult NCAM-deficient mice (Kochlamazashvili et al., 2010). To assess the contribution of GluN2A subunit to NMDAR-mediated fEPSPs, Kochlamazashvili and co-workers (2010) have used the GluN2A-specific antagonist NVP-AAMO77. At a concentration of 0.25  $\mu\text{M}$ , NVP-AAMO77 has been shown to block ~80% of GluN1/2A-NMDAR-mediated

current and ~20% of GluN1/2B-NMDAR-mediated current (Bartlett et al., 2007). Based on these previous findings in the polySia-deficient hippocampus, we assume that the observed increase via GluN2B-mediated neurotransmission in the polySia-deficient mPFC might be accompanied by a substantial decrease in GluN2A-mediated current.

Although ST8SIA4-deficient mPFC slices showed increased GluN2B-mediated component in synaptically evoked NMDAR-mediated currents, tonic NMDAR-mediated currents in ST8SIA4-deficient slices were not changed, indicating that the constitutive genetic ablation of polySia results in a milder phenotype compared with acute polySia depletion. This phenotypic discrepancy might be explained by compensatory mechanisms arising over the course of brain development, and such mechanisms have been reported in several mouse models of neurodegenerative diseases (reviewed by (Kreiner, 2015)). Nevertheless, both in endoNF-treated slices and in ST8SIA4-deficient mice, the decay of NMDAR-mediated currents was strongly affected by Ro 25-6981, and LTP was similarly impaired, suggesting that even if tonic NMDAR currents are normalized, still signaling in response to evoked glutamate release may activate more extrasynaptic GluN2B-NMDARs. This is an important point for further studies: not to rely exclusively on analysis of tonic current but also to measure the evoked ones.

Taken together, our whole-cell patch-clamp recordings of evoked and tonic NMDAR-mediated currents suggest that acute polySia depletion leads to elevated neurotransmission through GluN2B-containing NMDARs not only in the CA1 subregion but also in the mPFC.

Several lines of evidence suggest that short-chain polySia NANA12 specifically inhibits extrasynaptic heterodimeric GluN1/GluN2B-containing NMDARs in the mPFC. First, we revealed that, in sham-treated mPFC slices, NANA12 largely precluded the inhibitory effect of 0.3  $\mu$ M Ro 25-6981, indicating that NANA12 and GluN1/GluN2B-selective concentrations of Ro 25-6981 block a similar subset of GluN2B-NMDARs. Second, in HEK293 cells, NANA12 blocked GluN1/GluN2B-mediated currents induced by application of 3  $\mu$ M glutamate (Hussam Hayani, unpublished results), a low micromolar glutamate concentration that is similar to the basal concentration of glutamate in the extracellular space (Sherwin, 1999; Ueda et al., 2000). In contrast, NANA12 does not inhibit GluN1/GluN2B-mediated currents induced by application of 100  $\mu$ M glutamate (Hussam Hayani, unpublished results), a relatively high glutamate concentration that is in the range of glutamate concentrations expected after presynaptic

glutamate release in the synaptic cleft. Third, these findings are in agreement with previous studies showing that long-chain polySia (25–50 residues) specifically inhibits GluN2B-NMDAR-mediated currents elicited by low micromolar glutamate concentrations in cultured hippocampal neurons (Hammond et al., 2006). Fourth, single-channel patch-clamp recordings have revealed that polySia selectively inhibits recombinant heterodimeric GluN1/Glu2B and heterotrimeric GluN1/GluN2A/GluN2B-NMDARs that are reconstituted in lipid bilayers, whereas polySia has no effect on GluN1/GluN2A-NMDARs (Kochlamazashvili et al., 2010). Fifth, the majority of extrasynaptic NMDARs in the hippocampal CA1 subregion contain predominantly GluN1/GluN2B-NMDARs (Fellin et al., 2004; Hardingham and Bading, 2010). Sixth, application of the enzymatic glutamate scavenger glutamic-pyruvic transaminase (GPT) rescues abnormal LTP in slices from NCAM-deficient mice (Kochlamazashvili et al., 2010). This glutamate scavenger has been revealed to decrease glutamate concentrations in the extracellular space (Tsvetkov et al., 2004), implying that the impairment of LTP induction is mediated through increased activation of extrasynaptic NMDARs.

Although oligoSia with a degree of polymerization equal to 5, NANA5, inhibited NMDAR-mediated currents, we assume that, in contrast to NANA12, NANA5 did not affect specifically GluN2B-containing NMDARs; consequently, it cannot be excluded that NANA5 has side effects, which need to be addressed in future experiments. This view is supported by the negative effects of NANA5 on LTP induction in polySia-deficient slices as well as in slices from wild-type mice. Hammond and colleagues (2006) have proposed that polySia might bind positively charged amino acids located at the extracellular S1 and S2 domains of the GluN2 subunit, thereby directly interfering with glutamate binding to the NMDAR, although an indirect mechanism cannot be completely excluded. A modelling study has identified that NMDAR shows four to six GluN2-specific amino acid residues, which are located at the periphery of the glutamate-binding pocket (Kinarsky et al., 2005), implying that only antagonists with a sufficiently large size are able to reach and interact with these GluN2-specific residues. This might explain why GluN2B subunit-containing NMDARs are specifically inhibited by NANA12 but not by NANA5 or by monomers of sialic acid, NANA1.

Interestingly, brain-derived neurotrophic factor (BDNF) directly binds to polySia under physiological conditions *in vitro*, and the formation of the BDNF–polySia complex depends on chain length of polySia, requiring at least 12 sialic acid residues (Kanato et al., 2008). The same

study has also shown that, after complex formation, BDNF binds to its receptors, TrkB and p75NTR. Since polySia expression is altered in the prefrontal cortex and hippocampus of schizophrenic patients (Barbeau et al., 1995; Gilabert-Juan et al., 2012) (reviewed by (Vawter, 2000; Brennaman and Maness, 2010)), these changes might impair formation of BDNF–polySia complex, thus indirectly leading to abnormal BDNF concentrations at TrkB receptors (Kanato et al., 2008). Similarly, the interaction of polySia with BDNF provides an alternative explanation for the impaired LTP in the mPFC of transgenic mice overexpressing the soluble extracellular domain of NCAM (NCAM-EC) (Brennaman et al., 2011). Therefore, in future experiments, it would be interesting to analyze BDNF signaling in the mPFC of these mice.

In contrast to short-chain NANA12, tegaserod, a polySia mimetic and 5-HT<sub>4</sub> receptor agonist, strongly inhibited NMDAR-mediated currents in the mPFC in control, sham-treated slices. Thus, it is possible that tegaserod blocks transmission through synaptic GluN2A-containing NMDARs, which would impair synaptic plasticity. Since our recordings were performed in the presence of a 5-HT<sub>4</sub> receptor antagonist, we can exclude the involvement of 5-HT<sub>4</sub> serotonin receptors. Recently, tegaserod has been shown to compete with a peptide mimetic of polySia for binding to the polySia-specific antibody 735 (Bushman et al., 2014). Similar to polySia, tegaserod potently increases neurite outgrowth of Schwann cells, cerebellar granule neurons, dorsal-root-ganglion neurons, and motoneurons *in vitro* (Bushman et al., 2014). These effects are mediated through NCAM because tegaserod has no effect on neurite extension in motoneurons from NCAM-deficient mice (Bushman et al., 2014). In *in vivo* mouse models, tegaserod shows positive effects on functional recovery from peripheral nerve injury (Bushman et al., 2014) and spinal cord injury (Pan et al., 2014). Given these findings in the peripheral nervous system, the observed unspecific inhibition of NMDAR-mediated currents by tegaserod in the cortex is interesting, but it suggests that its polySia-mimicking action is limited and depends on which polySia receptors are involved in peripheral versus central nervous system.

In the present study, we performed recordings of NMDAR-mediated currents and LTP in the prelimbic cortex, which is a part of the mPFC in the mouse brain (Van De Werd et al., 2010). In our previous study, our laboratory has established recordings in the prelimbic area of mice overexpressing the extracellular domain of NCAM (Brennaman et al., 2011). To standardize recording conditions and to ensure comparability between studies, we decided to record from the same area of the mPFC. Behavioral studies have shown differences in the circuitry between the

prelimbic and infralimbic cortex of the mPFC. In brief, projections of the prelimbic cortex to the basal amygdala support expression of fear memories, whereas projections of the infralimbic cortex to the amygdala-intercalated cells contribute to fear extinction (reviewed by (Sotres-Bayon and Quirk, 2010)).

#### **4.2. Contribution of GluN2A and GluN2B subunits of NMDAR to synaptic plasticity**

In untreated mPFC slices from adult 2–4-month-old C57BL/6 mice, we showed that application of 0.3  $\mu$ M Ro 25-6981 had no effect on evoked NMDAR-EPCSs and did not alter mPFC LTP, supporting the notion that the majority of synaptic NMDARs in the adult mPFC are heterotrimeric GluN1/GluN2A/GluN2B-containing NMDARs. The lack of inhibition by 0.3  $\mu$ M Ro 25-6981 and NANA12 in sham-treated mPFC slices is in agreement with recent studies showing that synaptic, but not extrasynaptic, NMDARs promote induction of LTP in the hippocampal CA1 subregion (Rusakov et al., 2004; Kochlamazashvili et al., 2010; Papouin et al., 2012). Similarly, in the CA1 subregion, application of 0.5  $\mu$ M Ro 25-6981 has no effect on LTP induction, whereas 0.5  $\mu$ M Ro 25-6981 blocks the induction of long-term depression in hippocampal slices from 3–4-week-old rats (Liu et al., 2004).

The role of GluN2A and GluN2B subunits in LTP has been extensively debated over the last decade, and their contribution might depend on several factors, including animal age, type of LTP-inducing protocol, and specificity of subunit antagonists (reviewed by (Paoletti et al., 2013; Papouin and Oliet, 2014; Shipton and Paulsen, 2014)). Several studies have shown that activation of GluN2A-containing NMDARs might mediate the induction of LTP, whereas GluN2B-containing NMDARs might support the induction of LTD (Liu et al., 2004; Massey et al., 2004; Zhao and Constantine-Paton, 2007; Papouin et al., 2012). In contrast, several reports have demonstrated that GluN2B might also contribute to LTP (Berberich et al., 2005; Zhao et al., 2005; von Engelhardt et al., 2008); however, the possibility that these GluN2B-NMDARs are synaptic rather than extrasynaptic cannot be completely excluded. Nevertheless, a previous study has shown that Ro 25-6981, at concentrations of 0.3  $\mu$ M and 3  $\mu$ M, inhibited ~20% of evoked NMDAR-mediated currents from layer II/III neurons in the anterior cingulate cortex (AAC), and 0.3  $\mu$ M Ro 25-6981 blocked TBS-induced LTP at layer V–layer II/III synapses in AAC slices (Zhao et al., 2005). This is in contrast to our findings in mPFC. These discrepancies in results

might be explained by several differences in cortical subregion, cortical layer, animal age, and species. In this regard, it is noteworthy that we recorded NMDAR-mediated currents in layer V of the prelimbic cortex from mice older than 8 weeks, while Zhao and coworkers recorded from layer II/III neurons of the AAC from rats at the age of 6–8 weeks.

### 4.3. The impact of GABAergic inhibition

To study the contribution of GABAergic interneurons during LTP-inducing theta-burst stimulation, we analyzed the ratio of GABA<sub>A</sub> receptor-mediated inhibitory postsynaptic currents (IPSCs) to excitatory postsynaptic currents (EPSCs), which were recorded from layer V pyramidal cells in endoNF- and sham-treated mPFC slices. The unaltered ratio between inhibitory and excitatory currents after endoNF treatment suggests that, under our recording conditions, polySia depletion had no effect on the inhibitory GABAergic innervation of pyramidal cells during LTP induction. These results are in agreement with the prominent effects of endoNF on GluN2B-containing NMDARs on excitatory pyramidal cells in the mPFC, which were accompanied by reduced mPFC LTP levels after polySia removal. Consistently, LTP deficits in the hippocampal CA1 region of polySia-deficient slices persist when LTP is recorded in the presence of the GABA<sub>A</sub> receptor antagonist bicuculline and the GABA<sub>B</sub> receptor antagonist CGP 55845 (Kochlamazashvili et al., 2010). Of note, we also performed recordings of LTP in mPFC slices in the presence of GABA<sub>A</sub> receptor antagonist picrotoxin, but picrotoxin caused seizure-like activities and a pronounced distortion of fEPSP, thus preventing the reliable analysis of fEPSP slope. In support of results from our laboratory, a recent report has shown that enzymatic removal of polySia leads to reduced spine density of pyramidal neurons and decreased expression of vesicular glutamate transporter-1, a marker of excitatory synapses, in the mPFC of adult rats (Castillo-Gómez et al., 2016).

Importantly, several immunohistochemical studies have demonstrated that polySia is expressed on a subset of mature GABAergic interneurons in the mPFC (Nacher et al., 2010; Gomez-Climent et al., 2011; Brennaman et al., 2013) (reviewed by (Nacher et al., 2013)), whereas pyramidal cells in the adult mPFC lack polySia expression, although polySia-positive puncta, which co-express inhibitory synaptic markers, surround the soma and principal apical dendrites of pyramidal neurons (Castillo-Gomez et al., 2011; Gomez-Climent et al., 2011). These findings are consistent with our immunohistochemical stainings showing that polySia can be detected in

close proximity of dendritic spines on proximal dendrites of mPFC pyramidal cells. Thus, it is possible that the effects of polySia removal on LTP are mediated through soluble polySia-NCAM that has been released from interneurons to reach extrasynaptic NMDARs at excitatory synapses (reviewed by (Varbanov and Dityatev, 2016)). Alternatively, polySia ablation might have effects on excitatory synapses that are innervated by polySia-expressing interneurons (Castillo-Gómez et al., 2016). Castillo-Gomez and colleagues (2016) further proposed that the enzymatic depletion of polySia might lead to alterations in the structure and connectivity of polySia-expressing interneurons, thereby affecting plasticity at excitatory synapses. It is noteworthy that endoN treatment increases the density of inhibitory glutamic acid decarboxylase (GAD)65/67-expressing, perisomatic puncta on pyramidal neurons in the mPFC of adult rats (Castillo-Gomez et al., 2011); however, the density of GAD65/67-expressing puncta in the peridendritic region of mPFC pyramidal neurons is not altered after endoN treatment (Castillo-Gomez et al., 2016). Altogether, these findings indicate that polySia-NCAM might regulate the perisomatic innervation of pyramidal cells by GABAergic interneurons. In this regard, the cell-specific role of polySia could be uncovered by analysis of synaptic plasticity after conditional inactivation of the polySia-synthesizing enzyme ST8SIA4 in interneurons versus pyramidal cells.

In addition to the LTP deficits in adult ST8SIA4-deficient mice observed in our laboratory, a recent study has shown reduced densities of somatostatin- and parvalbumin-expressing interneurons in the mPFC of both ST8SIA2- and ST8SIA4-deficient mice, and this reduction has been found already at postnatal day P1 of brain development, suggesting disturbed migration of GABAergic interneurons (Krocher et al., 2014). In light of reduced numbers of interneurons in ST8SIA2-deficient mice, it is surprising that these mice show normal LTP levels (Gaga Kochlamazashvili, unpublished data). This might be explained by the finding that density of polySia-positive cells and polySia expression are normal in the mPFC of ST8SIA2-deficient mice, whereas polySia expression is absent from the mPFC of ST8SIA4-deficient mice (Nacher et al., 2010), suggesting that, at excitatory synapses, the presence of polySia expression might partially compensate for developmental impairments in perisomatic GABAergic innervation. Nevertheless, the contribution of GABAergic interneurons to LTP induction in the mPFC remains to be analyzed. From our recordings of TBS-induced IPSCs, it is plausible to assume that TBS does not effectively recruit somatostatin- and parvalbumin-expressing interneurons, and

hence TBS-induced LTP is rather independent of polySia-mediated modulation of GABAergic mechanisms.

#### 4.4. Pharmacological restoration of synaptic plasticity after polySia removal

In the present study, we further showed that both polySia NANA12 and 0.3  $\mu$ M Ro 25-6981 fully rescued LTP levels in endoNF-treated slices as well as in ST8SIA4-deficient mPFC slices, indicating that this restoration was most likely mediated through inhibition of extrasynaptic GluN2B-NMDARs (see also **Fig. 4.1**). These results are in agreement with the restoration of impaired CA1 LTP in NCAM-deficient mice by application of long-chain polySia (Senkov et al., 2006) and Ro 25-6981 at 5  $\mu$ M (Kochlamazashvili et al., 2010), a relatively high Ro 25-6981 concentration that is known to block heterotrimeric GluN1/GluN2A/GluN2B-NMDARs (Volianskis et al., 2013) (reviewed by (Papouin and Oliet, 2014)). Interestingly, juvenile mice that are haploinsufficiently heterozygous for the extracellular matrix protein Reelin show similar impairments in LTP in the mPFC, which are rescued by a single *in vivo* injection of Ro 25-6981 (Iafrazi et al., 2014). This phenotype resembles our current findings, and it suggests that Reelin deficiency also causes abnormally elevated neurotransmission through GluN2B-containing NMDARs in the mPFC early in brain development.

We also demonstrated that sarcosine, a glycine transporter type 1 (GlyT1) inhibitor, can fully restore impaired LTP in the polySia-deficient mPFC. Likewise, our recordings show that sarcosine fully rescued decreased LTP levels in the mPFC of NCAM-deficient mice. These data are in line with previous studies showing that GlyT1 inhibitors potentiate synaptic NMDAR-mediated currents *ex vivo* in mPFC or in the hippocampal CA1 subregion, as well as NMDA-evoked responses in the mPFC *in vivo* (Bergeron et al., 1998; Chen et al., 2003; Depoortere et al., 2005; Fossat et al., 2012). Consistent with their effects on synaptic NMDARs, GlyT1 inhibitors have been reported to enhance NMDAR-dependent LTP in the CA1 subregion (Martina et al., 2004; Zhang et al., 2008; Alberati et al., 2012) and LTP recorded *in vivo* in the hippocampal dentate gyrus (Kinney et al., 2003; Manahan-Vaughan et al., 2008). Moreover, several studies have revealed that GlyT1 rescue behavioral disturbances in rodent models of schizophrenia and Alzheimer's disease (Boulay et al., 2008; Manahan-Vaughan et al., 2008; Harada et al., 2012; Chaki et al., 2015). In clinical studies, GlyT1 inhibitors have been shown to improve negative and cognitive symptoms in schizophrenic patients that are resistant to standard antipsychotic



treatment (reviewed by (Shim et al., 2008; Tsai and Lin, 2010; Javitt, 2012)). In healthy subjects, GlyT1 inhibitors can also reduce the schizophrenia-like psychotic symptoms induced by the NMDAR antagonist ketamine (D'Souza et al., 2012).

The mechanism of action of GlyT1 inhibitors on NMDARs has been extensively studied (reviewed by (Harvey and Yee, 2013)). In brief, GlyT1 inhibitors control the reuptake of glycine by the GlyT1, which is expressed in glial cells and pre- and postsynaptic neurons at excitatory synapses in several brain regions, including mPFC and hippocampus (Zafra et al., 1995b; Zafra et al., 1995a; Cubelos et al., 2005). It is well known that blocking GlyT1 leads to reduced glycine uptake, increasing synaptic glycine concentrations near postsynaptic NMDARs (Bergeron et al., 1998; Chen et al., 2003; Fossat et al., 2012). Interestingly, a recent study has confirmed this mechanism and has further shown that, under basal physiological conditions, glycine is the endogenous co-agonist at extrasynaptic NMDARs in the hippocampus (Papouin et al., 2012). These studies are also supported by the finding that GlyT1 blockade by sarcosine does not alter the amplitude of extrasynaptic NMDAR-mediated currents (Le Meur et al., 2007). Taken together, our data and previous reports suggest that sarcosine restored the observed LTP deficits in endoNF-treated slices, ST8SIA4-deficient mice, and NCAM-deficient mice via potentiation of synaptic NMDARs.

Over the last decade, several pharmaceutical companies have developed novel synthetic inhibitors showing high selectivity and affinity for the GlyT1 transporter in combination with low neurotoxicity effects. Some of these novel compounds include Bitopertin (also known as RO4917838 and RG1678) by Hoffmann-La Roche, PF-03463275 by Pfizer, GSK1018921 by GlaxoSmithKline, and SCH 900435 (also known as Org 25935) by Yale University and Organon (reviewed by (Harvey and Yee, 2013)). Bitopertin, a non-sarcosine-based, non-competitive GlyT1 inhibitor, has been reported to improve negative and positive symptoms of schizophrenia in two recent phase II randomized, double-blind studies (Bugarski-Kirola et al., 2014; Umbricht et al., 2014), however, the phase III clinical trials with bitopertin have yielded negative results (reviewed by (Beck et al., 2014; Singer et al., 2015)). In an editorial, Beck and co-workers (2016) provided several lines of evidence that might explain bitopertin's failure in the phase III trials. First, the phase III trials tested drug effects on negative symptoms in chronic patients with schizophrenia who show both primary and secondary negative symptoms. While primary negative symptoms are known to be specific for schizophrenia, secondary symptoms are

mediated through associated factors such as social isolation. Second, glutamatergic deficits targeted by GlyT1 inhibitors, mainly occur in the early stages of schizophrenia (Poels et al., 2014). Thus, bitopertin might be more efficient in patients showing only primary symptoms rather than in those who already developed chronic schizophrenia with secondary symptoms (Beck et al., 2016). Third, GlyT1 is not the only glycine transporter that is involved in regulating the uptake of glycine at excitatory synapses—this function has been also reported in the case of the small neutral amino acid transport (SNAT, SLC38) system, also known as System A (Javitt et al., 2005). Considering that sarcosine is less specific for GlyT1 than bitopertin, the existence of these additional transporters might explain sarcosine's beneficial effects on negative symptoms in schizophrenia patients (reviewed by (Javitt, 2012)). Taken together, these studies suggest that new GlyT1 inhibitors with a broad action might represent a promising strategy for the treatment of negative and cognitive symptoms in schizophrenia that are not improved by conventional antipsychotic medications.

#### **4.5. Downstream mechanisms of GluN2B overactivation**

In the CA1 subregion of NCAM-deficient mice and endoNF-treated hippocampal slices, the up-regulation of extrasynaptic GluN2B-NMDARs has been demonstrated to result in reduced LTP levels via increased activation of Ras guanine nucleotide-releasing factor 1 (Ras-GRF1) and increased phosphorylation of the p38 mitogen-activated protein kinase (p38 MAPK) (Kochlamazashvili et al., 2010). Consistently, p38 MAPK is involved in synaptic long-term depression (LTD) (Bolshakov et al., 2000; Hsieh et al., 2006), and Ras-GRF1 has been reported to activate p38 MAPK via GluN2B-containing NMDARs, thereby leading to LTD (Li et al., 2006). Thus, it is possible that polySia deficiency might lead to similar overactivation of the Ras-GRF1–p38 MAPK pathway in the mPFC.

Recent studies have shown that the synapto-nuclear protein Jacob is responsible for the encoding and subsequent synapse-to-nucleus transduction of signals originating from synaptic versus extrasynaptic NMDARs (Karpova et al., 2013) (reviewed by (Kaushik et al., 2014)). After activation of synaptic NMDARs, Jacob is phosphorylated at serine-180 by the extracellular signal-regulated kinase 1/2 (ERK1/2), leading to the ERK1/2-dependent, long-distance translocation of Jacob from the synapse to the nucleus. However, after activation of extrasynaptic NMDARs, non-phosphorylated Jacob is translocated from the synapse to the

nucleus, where it induces CREB shut-off and subsequent cell death (Karpova et al., 2013). According to these findings, upregulation of extrasynaptic GluN2B-NMDARs might also cause CREB shut-off and neurodegeneration via the Jacob signaling pathway in polySia-deficient mice. In line with this view, NCAM-deficient mice show reduced levels of phosphorylated CREB in several brain regions, including the hippocampal CA3 subregion, the mPFC, and the basolateral nucleus of the amygdala (Aonurm-Helm et al., 2008). Since both GluN2A-mediated neurotransmission and CREB activity are decreased in the CA1 subregion of NCAM-deficient mice (Kochlamazashvili et al., 2010), it is plausible that, under physiological conditions, elevated CREB signaling drives the expression of GluN2A subunits. Another molecule that is expressed in a CREB-dependent fashion is the brain-derived neurotrophic factor (BDNF). Notably, NCAM-deficient mice and endoNF-treated organotypic hippocampal cultures reveal impaired CA1 LTP levels via decreased phosphorylation of TrkB, the BDNF receptor, and these LTP deficits are restored by application of BDNF (Muller et al., 2000). Moreover, mice constitutively deficient for Jacob show reduced levels of BDNF mRNA and phosphorylated CREB in the CA1 subregion, resulting in decreased CA1 LTP levels and impaired hippocampus-dependent contextual fear conditioning (Spilker et al., 2016). Together, these findings support the view that polySia restrains the activation of extrasynaptic NMDARs, thereby preventing its detrimental consequences, including CREB shut-off and cell death. On the other hand, polySia might, at least indirectly, promote CREB-dependent expression of proteins, such as GluN2A-NMDARs and BDNF (reviewed by (Varbanov and Dityatev, 2016)).

## 5. REFERENCES

- Aisa B, Gil-Bea FJ, Solas M, Garcia-Alloza M, Chen CP, Lai MK, Francis PT, Ramirez MJ (2010) Altered NCAM expression associated with the cholinergic system in Alzheimer's disease. *Journal of Alzheimer's disease* : JAD 20:659-668.
- Akbarian S, Kim JJ, Potkin SG, Hagman JO, Tafazzoli A, Bunney WE, Jr., Jones EG (1995) Gene expression for glutamic acid decarboxylase is reduced without loss of neurons in prefrontal cortex of schizophrenics. *Archives of general psychiatry* 52:258-266.
- Al-Hallaq RA, Conrads TP, Veenstra TD, Wenthold RJ (2007) NMDA di-heteromeric receptor populations and associated proteins in rat hippocampus. *The Journal of neuroscience : the official journal of the Society for Neuroscience* 27:8334-8343.
- Alberati D, Moreau JL, Lengyel J, Hauser N, Mory R, Borroni E, Pinard E, Knoflach F, Schlotterbeck G, Hainzl D, Wettstein JG (2012) Glycine reuptake inhibitor RG1678: a pharmacologic characterization of an investigational agent for the treatment of schizophrenia. *Neuropharmacology* 62:1152-1161.
- Angata K, Long JM, Bukalo O, Lee W, Dityatev A, Wynshaw-Boris A, Schachner M, Fukuda M, Marth JD (2004) Sialyltransferase ST8Sia-II assembles a subset of polysialic acid that directs hippocampal axonal targeting and promotes fear behavior. *The Journal of biological chemistry* 279:32603-32613.
- Angata T, Kerr SC, Greaves DR, Varki NM, Crocker PR, Varki A (2002) Cloning and characterization of human Siglec-11. A recently evolved signaling molecule that can interact with SHP-1 and SHP-2 and is expressed by tissue macrophages, including brain microglia. *The Journal of biological chemistry* 277:24466-24474.
- Angulo MC, Kozlov AS, Charpak S, Audinat E (2004) Glutamate released from glial cells synchronizes neuronal activity in the hippocampus. *The Journal of neuroscience : the official journal of the Society for Neuroscience* 24:6920-6927.
- Aonurm-Helm A, Zharkovsky T, Jurgenson M, Kalda A, Zharkovsky A (2008) Dysregulated CREB signaling pathway in the brain of neural cell adhesion molecule (NCAM)-deficient mice. *Brain research* 1243:104-112.
- Arai M, Yamada K, Toyota T, Obata N, Haga S, Yoshida Y, Nakamura K, Minabe Y, Ujike H, Sora I, Ikeda K, Mori N, Yoshikawa T, Itokawa M (2006) Association between polymorphisms in the promoter region of the sialyltransferase 8B (SIAT8B) gene and schizophrenia. *Biological psychiatry* 59:652-659.
- Asztely F, Erdemli G, Kullmann DM (1997) Extrasynaptic glutamate spillover in the hippocampus: dependence on temperature and the role of active glutamate uptake. *Neuron* 18:281-293.
- Atkinson BN, Bell SC, De Vivo M, Kowalski LR, Lechner SM, Ognyanov VI, Tham CS, Tsai C, Jia J, Ashton D, Klitenick MA (2001) ALX 5407: a potent, selective inhibitor of the hGlyT1 glycine transporter. *Molecular pharmacology* 60:1414-1420.
- Atz ME, Rollins B, Vawter MP (2007) NCAM1 association study of bipolar disorder and schizophrenia: polymorphisms and alternatively spliced isoforms lead to similarities and differences. *Psychiatric genetics* 17:55-67.
- Balu DT, Coyle JT (2015) The NMDA receptor 'glycine modulatory site' in schizophrenia: D-serine, glycine, and beyond. *Current opinion in pharmacology* 20:109-115.
- Barbeau D, Liang JJ, Robitaille Y, Quirion R, Srivastava LK (1995) Decreased expression of the embryonic form of the neural cell adhesion molecule in schizophrenic brains. *Proceedings of the National Academy of Sciences of the United States of America* 92:2785-2789.
- Bartlett TE, Bannister NJ, Collett VJ, Dargan SL, Massey PV, Bortolotto ZA, Fitzjohn SM, Bashir ZI, Collingridge GL, Lodge D (2007) Differential roles of NR2A and NR2B-containing NMDA receptors in LTP and LTD in the CA1 region of two-week old rat hippocampus. *Neuropharmacology* 52:60-70.

- Bartsch U, Kirchhoff F, Schachner M (1990) Highly sialylated N-CAM is expressed in adult mouse optic nerve and retina. *Journal of neurocytology* 19:550-565.
- Beck K, Javitt DC, Howes OD (2016) Targeting glutamate to treat schizophrenia: lessons from recent clinical studies. *Psychopharmacology* 233:2425-2428.
- Beck K, McCutcheon R, Bloomfield MA, Gaughran F, Reis Marques T, MacCabe J, Selvaraj S, Taylor D, Howes OD (2014) The practical management of refractory schizophrenia--the Maudsley Treatment REview and Assessment Team service approach. *Acta psychiatrica Scandinavica* 130:427-438.
- Becker CG, Artola A, Gerardy-Schahn R, Becker T, Welzl H, Schachner M (1996) The polysialic acid modification of the neural cell adhesion molecule is involved in spatial learning and hippocampal long-term potentiation. *Journal of neuroscience research* 45:143-152.
- Berberich S, Punnakkal P, Jensen V, Pawlak V, Seeburg PH, Hvalby O, Kohr G (2005) Lack of NMDA receptor subtype selectivity for hippocampal long-term potentiation. *The Journal of neuroscience : the official journal of the Society for Neuroscience* 25:6907-6910.
- Bergeron R, Meyer TM, Coyle JT, Greene RW (1998) Modulation of N-methyl-D-aspartate receptor function by glycine transport. *Proceedings of the National Academy of Sciences of the United States of America* 95:15730-15734.
- Blanton MG, Lo Turco JJ, Kriegstein AR (1989) Whole cell recording from neurons in slices of reptilian and mammalian cerebral cortex. *Journal of neuroscience methods* 30:203-210.
- Bliss TV, Collingridge GL (2013) Expression of NMDA receptor-dependent LTP in the hippocampus: bridging the divide. *Molecular brain* 6:5.
- Bodrikov V, Leshchyns'ka I, Sytnyk V, Overvoorde J, den Hertog J, Schachner M (2005) RPTPalph $\alpha$  is essential for NCAM-mediated p59fyn activation and neurite elongation. *The Journal of cell biology* 168:127-139.
- Bolshakov VY, Carboni L, Cobb MH, Siegelbaum SA, Belardetti F (2000) Dual MAP kinase pathways mediate opposing forms of long-term plasticity at CA3-CA1 synapses. *Nature neuroscience* 3:1107-1112.
- Bonfanti L, Theodosis DT (1994) Expression of polysialylated neural cell adhesion molecule by proliferating cells in the subependymal layer of the adult rat, in its rostral extension and in the olfactory bulb. *Neuroscience* 62:291-305.
- Boulay D et al. (2008) Characterization of SSR103800, a selective inhibitor of the glycine transporter-1 in models predictive of therapeutic activity in schizophrenia. *Pharmacology, biochemistry, and behavior* 91:47-58.
- Brenneman LH, Maness PF (2010) NCAM in neuropsychiatric and neurodegenerative disorders. *Advances in experimental medicine and biology* 663:299-317.
- Brenneman LH, Moss ML, Maness PF (2014) EphrinA/EphA-induced ectodomain shedding of neural cell adhesion molecule regulates growth cone repulsion through ADAM10 metalloprotease. *Journal of neurochemistry* 128:267-279.
- Brenneman LH, Kochlamazashvili G, Stoenica L, Nonneman RJ, Moy SS, Schachner M, Dityatev A, Maness PF (2011) Transgenic mice overexpressing the extracellular domain of NCAM are impaired in working memory and cortical plasticity. *Neurobiology of disease* 43:372-378.
- Brenneman LH, Zhang X, Guan H, Triplett JW, Brown A, Demyanenko GP, Manis PB, Landmesser L, Maness PF (2013) Polysialylated NCAM and ephrinA/EphA regulate synaptic development of GABAergic interneurons in prefrontal cortex. *Cerebral cortex (New York, NY : 1991)* 23:162-177.
- Bugarski-Kirola D, Wang A, Abi-Saab D, Blattler T (2014) A phase II/III trial of bitopertin monotherapy compared with placebo in patients with an acute exacerbation of schizophrenia - results from the CandleLyte study. *European neuropsychopharmacology : the journal of the European College of Neuropsychopharmacology* 24:1024-1036.
- Bukalo O, Dityatev A (2012) Synaptic cell adhesion molecules. *Advances in experimental medicine and biology* 970:97-128.

- Bukalo O, Fentrop N, Lee AY, Salmen B, Law JW, Wotjak CT, Schweizer M, Dityatev A, Schachner M (2004) Conditional ablation of the neural cell adhesion molecule reduces precision of spatial learning, long-term potentiation, and depression in the CA1 subfield of mouse hippocampus. *The Journal of neuroscience : the official journal of the Society for Neuroscience* 24:1565-1577.
- Bushman J, Mishra B, Ezra M, Gul S, Schulze C, Chaudhury S, Ripoll D, Wallqvist A, Kohn J, Schachner M, Loers G (2014) Tegaserod mimics the neurostimulatory glycan polysialic acid and promotes nervous system repair. *Neuropharmacology* 79:456-466.
- Buttner B, Horstkorte R (2010) Intracellular ligands of NCAM. *Advances in experimental medicine and biology* 663:55-66.
- Castillo-Gomez E, Varea E, Blasco-Ibanez JM, Crespo C, Nacher J (2011) Polysialic acid is required for dopamine D2 receptor-mediated plasticity involving inhibitory circuits of the rat medial prefrontal cortex. *PloS one* 6:e29516.
- Castillo-Gomez E, Varea E, Blasco-Ibanez JM, Crespo C, Nacher J (2016) Effects of Chronic Dopamine D2R Agonist Treatment and Polysialic Acid Depletion on Dendritic Spine Density and Excitatory Neurotransmission in the mPFC of Adult Rats. *Neural Plast* 2016:1615363.
- Castillo-Gómez E, Varea E, Blasco-Ibáñez JM, Crespo C, Nacher J (2016) Effects of Chronic Dopamine D2R Agonist Treatment and Polysialic Acid Depletion on Dendritic Spine Density and Excitatory Neurotransmission in the mPFC of Adult Rats. *Neural Plasticity* 2016:12.
- Chaki S, Shimazaki T, Karasawa J, Aoki T, Kaku A, Iijima M, Kambe D, Yamamoto S, Kawakita Y, Shibata T, Abe K, Okubo T, Sekiguchi Y, Okuyama S (2015) Efficacy of a glycine transporter 1 inhibitor TASP0315003 in animal models of cognitive dysfunction and negative symptoms of schizophrenia. *Psychopharmacology* 232:2849-2861.
- Chattopadhyaya B, Baho E, Huang ZJ, Schachner M, Di Cristo G (2013) Neural cell adhesion molecule-mediated Fyn activation promotes GABAergic synapse maturation in postnatal mouse cortex. *The Journal of neuroscience : the official journal of the Society for Neuroscience* 33:5957-5968.
- Chen L, Muhlhauser M, Yang CR (2003) Glycine transporter-1 blockade potentiates NMDA-mediated responses in rat prefrontal cortical neurons in vitro and in vivo. *Journal of neurophysiology* 89:691-703.
- Chung KY, Leung KM, Lin CC, Tam KC, Hao YL, Taylor JS, Chan SO (2004) Regionally specific expression of L1 and sialylated NCAM in the retinofugal pathway of mouse embryos. *The Journal of comparative neurology* 471:482-498.
- Close BE, Colley KJ (1998) In vivo autopolysialylation and localization of the polysialyltransferases PST and STX. *The Journal of biological chemistry* 273:34586-34593.
- Cole GJ, Akeson R (1989) Identification of a heparin binding domain of the neural cell adhesion molecule N-CAM using synthetic peptides. *Neuron* 2:1157-1165.
- Cremer H, Chazal G, Goridis C, Represa A (1997) NCAM is essential for axonal growth and fasciculation in the hippocampus. *Molecular and cellular neurosciences* 8:323-335.
- Cremer H, Chazal G, Carleton A, Goridis C, Vincent JD, Lledo PM (1998) Long-term but not short-term plasticity at mossy fiber synapses is impaired in neural cell adhesion molecule-deficient mice. *Proceedings of the National Academy of Sciences of the United States of America* 95:13242-13247.
- Cremer H, Lange R, Christoph A, Plomann M, Vopper G, Roes J, Brown R, Baldwin S, Kraemer P, Scheff S, et al. (1994) Inactivation of the N-CAM gene in mice results in size reduction of the olfactory bulb and deficits in spatial learning. *Nature* 367:455-459.
- Crossin KL, Krushel LA (2000) Cellular signaling by neural cell adhesion molecules of the immunoglobulin superfamily. *Developmental dynamics : an official publication of the American Association of Anatomists* 218:260-279.
- Cubelos B, Gimenez C, Zafra F (2005) Localization of the GLYT1 glycine transporter at glutamatergic synapses in the rat brain. *Cerebral cortex (New York, NY : 1991)* 15:448-459.
- Cunningham BA, Hemperly JJ, Murray BA, Prediger EA, Brackenbury R, Edelman GM (1987) Neural cell adhesion molecule: structure, immunoglobulin-like domains, cell surface modulation, and alternative RNA splicing. *Science (New York, NY)* 236:799-806.

- Curreli S, Arany Z, Gerardy-Schahn R, Mann D, Stamatou NM (2007) Polysialylated neuropilin-2 is expressed on the surface of human dendritic cells and modulates dendritic cell-T lymphocyte interactions. *The Journal of biological chemistry* 282:30346-30356.
- D'Souza DC, Singh N, Elander J, Carbutto M, Pittman B, Udo de Haes J, Sjogren M, Peeters P, Ranganathan M, Schipper J (2012) Glycine transporter inhibitor attenuates the psychotomimetic effects of ketamine in healthy males: preliminary evidence. *Neuropsychopharmacology : official publication of the American College of Neuropsychopharmacology* 37:1036-1046.
- Danysz W, Parsons CG (1998) Glycine and N-methyl-D-aspartate receptors: physiological significance and possible therapeutic applications. *Pharmacological reviews* 50:597-664.
- Daston MM, Bastmeyer M, Rutishauser U, O'Leary DD (1996) Spatially restricted increase in polysialic acid enhances corticospinal axon branching related to target recognition and innervation. *The Journal of neuroscience : the official journal of the Society for Neuroscience* 16:5488-5497.
- Delling M, Wischmeyer E, Dityatev A, Sytnyk V, Veh RW, Karschin A, Schachner M (2002) The neural cell adhesion molecule regulates cell-surface delivery of G-protein-activated inwardly rectifying potassium channels via lipid rafts. *The Journal of neuroscience : the official journal of the Society for Neuroscience* 22:7154-7164.
- Depoortere R et al. (2005) Neurochemical, electrophysiological and pharmacological profiles of the selective inhibitor of the glycine transporter-1 SSR504734, a potential new type of antipsychotic. *Neuropsychopharmacology : official publication of the American College of Neuropsychopharmacology* 30:1963-1985.
- Di Cristo G, Chattopadhyaya B, Kuhlman SJ, Fu Y, Belanger MC, Wu CZ, Rutishauser U, Maffei L, Huang ZJ (2007) Activity-dependent PSA expression regulates inhibitory maturation and onset of critical period plasticity. *Nature neuroscience* 10:1569-1577.
- Diestel S, Schaefer D, Cremer H, Schmitz B (2007) NCAM is ubiquitinated, endocytosed and recycled in neurons. *Journal of cell science* 120:4035-4049.
- Dityatev A, Dityateva G, Schachner M (2000) Synaptic strength as a function of post- versus presynaptic expression of the neural cell adhesion molecule NCAM. *Neuron* 26:207-217.
- Dityatev A, Bukalo O, Schachner M (2008) Modulation of synaptic transmission and plasticity by cell adhesion and repulsion molecules. *Neuron glia biology* 4:197-209.
- Dityatev A, Dityateva G, Sytnyk V, Delling M, Toni N, Nikonenko I, Muller D, Schachner M (2004) Polysialylated neural cell adhesion molecule promotes remodeling and formation of hippocampal synapses. *The Journal of neuroscience : the official journal of the Society for Neuroscience* 24:9372-9382.
- Dodt HU, Ziegglansberger W (1990) Visualizing unstained neurons in living brain slices by infrared DIC-videomicroscopy. *Brain research* 537:333-336.
- Doetsch F (2003) A niche for adult neural stem cells. *Current opinion in genetics & development* 13:543-550.
- Doetsch F, Alvarez-Buylla A (1996) Network of tangential pathways for neuronal migration in adult mammalian brain. *Proceedings of the National Academy of Sciences of the United States of America* 93:14895-14900.
- Doetsch F, Garcia-Verdugo JM, Alvarez-Buylla A (1997) Cellular composition and three-dimensional organization of the subventricular germinal zone in the adult mammalian brain. *The Journal of neuroscience : the official journal of the Society for Neuroscience* 17:5046-5061.
- Doherty P, Williams G, Williams EJ (2000) CAMs and axonal growth: a critical evaluation of the role of calcium and the MAPK cascade. *Molecular and cellular neurosciences* 16:283-295.
- Doyle E, Nolan PM, Bell R, Regan CM (1992) Hippocampal NCAM180 transiently increases sialylation during the acquisition and consolidation of a passive avoidance response in the adult rat. *Journal of neuroscience research* 31:513-523.
- Eckhardt M, Muhlenhoff M, Bethe A, Koopman J, Frosch M, Gerardy-Schahn R (1995) Molecular characterization of eukaryotic polysialyltransferase-1. *Nature* 373:715-718.
- Eckhardt M, Bukalo O, Chazal G, Wang L, Goridis C, Schachner M, Gerardy-Schahn R, Cremer H, Dityatev A (2000) Mice deficient in the polysialyltransferase ST8SiaIV/PST-1 allow

- discrimination of the roles of neural cell adhesion molecule protein and polysialic acid in neural development and synaptic plasticity. *The Journal of neuroscience : the official journal of the Society for Neuroscience* 20:5234-5244.
- Eggers K, Werneburg S, Schertzinger A, Abeln M, Schiff M, Scharenberg MA, Burkhardt H, Muhlenhoff M, Hildebrandt H (2011) Polysialic acid controls NCAM signals at cell-cell contacts to regulate focal adhesion independent from FGF receptor activity. *Journal of cell science* 124:3279-3291.
- Fedorkova L, Rutishauser U, Prosser R, Shen H, Glass JD (2002) Removal of polysialic acid from the SCN potentiates nonphotic circadian phase resetting. *Physiology & behavior* 77:361-369.
- Feldblum S, Erlander MG, Tobin AJ (1993) Different distributions of GAD65 and GAD67 mRNAs suggest that the two glutamate decarboxylases play distinctive functional roles. *Journal of neuroscience research* 34:689-706.
- Fellin T, Pascual O, Gobbo S, Pozzan T, Haydon PG, Carmignoto G (2004) Neuronal synchrony mediated by astrocytic glutamate through activation of extrasynaptic NMDA receptors. *Neuron* 43:729-743.
- Feng G, Mellor RH, Bernstein M, Keller-Peck C, Nguyen QT, Wallace M, Nerbonne JM, Lichtman JW, Sanes JR (2000) Imaging neuronal subsets in transgenic mice expressing multiple spectral variants of GFP. *Neuron* 28:41-51.
- Fields RD, Itoh K (1996) Neural cell adhesion molecules in activity-dependent development and synaptic plasticity. *Trends in neurosciences* 19:473-480.
- Fischer G, Mutel V, Trube G, Malherbe P, Kew JN, Mohacsi E, Heitz MP, Kemp JA (1997) Ro 25-6981, a highly potent and selective blocker of N-methyl-D-aspartate receptors containing the NR2B subunit. Characterization in vitro. *The Journal of pharmacology and experimental therapeutics* 283:1285-1292.
- Foley AG, Ronn LC, Murphy KJ, Regan CM (2003) Distribution of polysialylated neural cell adhesion molecule in rat septal nuclei and septohippocampal pathway: transient increase of polysialylated interneurons in the subtriangular septal zone during memory consolidation. *Journal of neuroscience research* 74:807-817.
- Fossat P, Turpin FR, Sacchi S, Dulong J, Shi T, Rivet JM, Sweedler JV, Pollegioni L, Millan MJ, Oliet SH, Mothet JP (2012) Glial D-serine gates NMDA receptors at excitatory synapses in prefrontal cortex. *Cerebral cortex (New York, NY : 1991)* 22:595-606.
- Fox GB, Kennedy N, Regan CM (1995a) Polysialylated neural cell adhesion molecule expression by neurons and astroglial processes in the rat dentate gyrus declines dramatically with increasing age. *International journal of developmental neuroscience : the official journal of the International Society for Developmental Neuroscience* 13:663-672.
- Fox GB, O'Connell AW, Murphy KJ, Regan CM (1995b) Memory consolidation induces a transient and time-dependent increase in the frequency of neural cell adhesion molecule polysialylated cells in the adult rat hippocampus. *Journal of neurochemistry* 65:2796-2799.
- France G, Fernandez-Fernandez D, Burnell ES, Irvine MW, Monaghan DT, Jane DE, Bortolotto ZA, Collingridge GL, Volianskis A (2017) Multiple roles of GluN2B-containing NMDA receptors in synaptic plasticity in juvenile hippocampus. *Neuropharmacology* 112:76-83.
- Frankle WG, Lerma J, Laruelle M (2003) The synaptic hypothesis of schizophrenia. *Neuron* 39:205-216.
- Franklin KBJ, Paxinos G (2007) *The mouse brain in stereotaxic coordinates*, 3rd Edition. Amsterdam: Elsevier.
- Freedman R (2003) Schizophrenia. *The New England journal of medicine* 349:1738-1749.
- Friedlander DR, Milev P, Karthikeyan L, Margolis RK, Margolis RU, Grumet M (1994) The neuronal chondroitin sulfate proteoglycan neurocan binds to the neural cell adhesion molecules Ng-CAM/L1/NILE and N-CAM, and inhibits neuronal adhesion and neurite outgrowth. *The Journal of cell biology* 125:669-680.
- Frosch M, Gorgen I, Boulnois GJ, Timmis KN, Bitter-Suermann D (1985) NZB mouse system for production of monoclonal antibodies to weak bacterial antigens: isolation of an IgG antibody to the polysaccharide capsules of *Escherichia coli* K1 and group B meningococci. *Proceedings of the National Academy of Sciences of the United States of America* 82:1194-1198.



- Furukawa H, Singh SK, Mancusso R, Gouaux E (2005) Subunit arrangement and function in NMDA receptors. *Nature* 438:185-192.
- Fux CM, Krug M, Dityatev A, Schuster T, Schachner M (2003) NCAM180 and glutamate receptor subtypes in potentiated spine synapses: an immunogold electron microscopic study. *Molecular and cellular neurosciences* 24:939-950.
- Galuska SP, Oltmann-Norden I, Geyer H, Weinhold B, Kuchelmeister K, Hildebrandt H, Gerardy-Schahn R, Geyer R, Muhlenhoff M (2006) Polysialic acid profiles of mice expressing variant allelic combinations of the polysialyltransferases ST8SiaII and ST8SiaIV. *The Journal of biological chemistry* 281:31605-31615.
- Galuska SP, Rollenhagen M, Kaup M, Eggers K, Oltmann-Norden I, Schiff M, Hartmann M, Weinhold B, Hildebrandt H, Geyer R, Muhlenhoff M, Geyer H (2010) Synaptic cell adhesion molecule SynCAM 1 is a target for polysialylation in postnatal mouse brain. *Proceedings of the National Academy of Sciences of the United States of America* 107:10250-10255.
- Geddes AE, Huang XF, Newell KA (2011) Reciprocal signalling between NR2 subunits of the NMDA receptor and neuregulin1 and their role in schizophrenia. *Progress in neuro-psychopharmacology & biological psychiatry* 35:896-904.
- Gilabert-Juan J, Nacher J, Sanjuan J, Molto MD (2013) Sex-specific association of the ST8SIAII gene with schizophrenia in a Spanish population. *Psychiatry research* 210:1293-1295.
- Gilabert-Juan J, Castillo-Gomez E, Perez-Rando M, Molto MD, Nacher J (2011) Chronic stress induces changes in the structure of interneurons and in the expression of molecules related to neuronal structural plasticity and inhibitory neurotransmission in the amygdala of adult mice. *Experimental neurology* 232:33-40.
- Gilabert-Juan J, Varea E, Guirado R, Blasco-Ibanez JM, Crespo C, Nacher J (2012) Alterations in the expression of PSA-NCAM and synaptic proteins in the dorsolateral prefrontal cortex of psychiatric disorder patients. *Neuroscience letters* 530:97-102.
- Glass JD, Lee W, Shen H, Watanabe M (1994) Expression of immunoreactive polysialylated neural cell adhesion molecule in the suprachiasmatic nucleus. *Neuroendocrinology* 60:87-95.
- Glass JD, Shen H, Fedorkova L, Chen L, Tomasiewicz H, Watanabe M (2000) Polysialylated neural cell adhesion molecule modulates photic signaling in the mouse suprachiasmatic nucleus. *Neuroscience letters* 280:207-210.
- Gold JM (2004) Cognitive deficits as treatment targets in schizophrenia. *Schizophrenia research* 72:21-28.
- Gomez-Climent MA, Guirado R, Castillo-Gomez E, Varea E, Gutierrez-Mecinas M, Gilabert-Juan J, Garcia-Mompo C, Vidueira S, Sanchez-Mataredona D, Hernandez S, Blasco-Ibanez JM, Crespo C, Rutishauser U, Schachner M, Nacher J (2011) The polysialylated form of the neural cell adhesion molecule (PSA-NCAM) is expressed in a subpopulation of mature cortical interneurons characterized by reduced structural features and connectivity. *Cerebral cortex (New York, NY : 1991)* 21:1028-1041.
- Guirado R, Perez-Rando M, Sanchez-Mataredona D, Castillo-Gomez E, Liberia T, Rovira-Esteban L, Varea E, Crespo C, Blasco-Ibanez JM, Nacher J (2014) The dendritic spines of interneurons are dynamic structures influenced by PSA-NCAM expression. *Cerebral cortex (New York, NY : 1991)* 24:3014-3024.
- Hammond MS, Sims C, Parameshwaran K, Suppiramaniam V, Schachner M, Dityatev A (2006) Neural cell adhesion molecule-associated polysialic acid inhibits NR2B-containing N-methyl-D-aspartate receptors and prevents glutamate-induced cell death. *The Journal of biological chemistry* 281:34859-34869.
- Hansen KB, Ogden KK, Yuan H, Traynelis SF (2014) Distinct functional and pharmacological properties of Triheteromeric GluN1/GluN2A/GluN2B NMDA receptors. *Neuron* 81:1084-1096.
- Harada K, Nakato K, Yarimizu J, Yamazaki M, Morita M, Takahashi S, Aota M, Saita K, Doihara H, Sato Y, Yamaji T, Ni K, Matsuoka N (2012) A novel glycine transporter-1 (GlyT1) inhibitor, ASP2535 (4-[3-isopropyl-5-(6-phenyl-3-pyridyl)-4H-1,2,4-triazol-4-yl]-2,1,3-benzoxadiazol e), improves cognition in animal models of cognitive impairment in schizophrenia and Alzheimer's disease. *European journal of pharmacology* 685:59-69.

- Hardingham GE, Bading H (2010) Synaptic versus extrasynaptic NMDA receptor signalling: implications for neurodegenerative disorders. *Nature reviews Neuroscience* 11:682-696.
- Harduin-Lepers A, Mollicone R, Delannoy P, Oriol R (2005) The animal sialyltransferases and sialyltransferase-related genes: a phylogenetic approach. *Glycobiology* 15:805-817.
- Harvey RJ, Yee BK (2013) Glycine transporters as novel therapeutic targets in schizophrenia, alcohol dependence and pain. *Nature reviews Drug discovery* 12:866-885.
- Hatton CJ, Paoletti P (2005) Modulation of triheteromeric NMDA receptors by N-terminal domain ligands. *Neuron* 46:261-274.
- Hekmat A, Bitter-Suermann D, Schachner M (1990) Immunocytological localization of the highly polysialylated form of the neural cell adhesion molecule during development of the murine cerebellar cortex. *The Journal of comparative neurology* 291:457-467.
- Henneberger C, Papouin T, Oliet SH, Rusakov DA (2010) Long-term potentiation depends on release of D-serine from astrocytes. *Nature* 463:232-236.
- Herdon HJ, Godfrey FM, Brown AM, Coulton S, Evans JR, Cairns WJ (2001) Pharmacological assessment of the role of the glycine transporter GlyT-1 in mediating high-affinity glycine uptake by rat cerebral cortex and cerebellum synaptosomes. *Neuropharmacology* 41:88-96.
- Herman MA, Jahr CE (2007) Extracellular glutamate concentration in hippocampal slice. *The Journal of neuroscience : the official journal of the Society for Neuroscience* 27:9736-9741.
- Hildebrandt H, Dityatev A (2015) Polysialic Acid in Brain Development and Synaptic Plasticity. *Topics in current chemistry* 366:55-96.
- Hildebrandt H, Muhlenhoff M, Weinhold B, Gerardy-Schahn R (2007) Dissecting polysialic acid and NCAM functions in brain development. *Journal of neurochemistry* 103 Suppl 1:56-64.
- Hinkle CL, Diestel S, Lieberman J, Maness PF (2006) Metalloprotease-induced ectodomain shedding of neural cell adhesion molecule (NCAM). *Journal of neurobiology* 66:1378-1395.
- Hirano S, Suzuki ST, Redies C (2003) The cadherin superfamily in neural development: diversity, function and interaction with other molecules. *Frontiers in bioscience : a journal and virtual library* 8:d306-355.
- Honer WG, Falkai P, Young C, Wang T, Xie J, Bonner J, Hu L, Boulianne GL, Luo Z, Trimble WS (1997) Cingulate cortex synaptic terminal proteins and neural cell adhesion molecule in schizophrenia. *Neuroscience* 78:99-110.
- Horstkorte R, Schachner M, Magyar JP, Vorherr T, Schmitz B (1993) The fourth immunoglobulin-like domain of NCAM contains a carbohydrate recognition domain for oligomannosidic glycans implicated in association with L1 and neurite outgrowth. *The Journal of cell biology* 121:1409-1421.
- Howes OD, Kapur S (2009) The dopamine hypothesis of schizophrenia: version III--the final common pathway. *Schizophrenia bulletin* 35:549-562.
- Hsieh H, Boehm J, Sato C, Iwatsubo T, Tomita T, Sisodia S, Malinow R (2006) AMPAR removal underlies Abeta-induced synaptic depression and dendritic spine loss. *Neuron* 52:831-843.
- Huang CC, Wei IH, Huang CL, Chen KT, Tsai MH, Tsai P, Tun R, Huang KH, Chang YC, Lane HY, Tsai GE (2013) Inhibition of glycine transporter-I as a novel mechanism for the treatment of depression. *Biological psychiatry* 74:734-741.
- Huang K, El-Husseini A (2005) Modulation of neuronal protein trafficking and function by palmitoylation. *Current opinion in neurobiology* 15:527-535.
- Huang YY, Simpson E, Kellendonk C, Kandel ER (2004) Genetic evidence for the bidirectional modulation of synaptic plasticity in the prefrontal cortex by D1 receptors. *Proceedings of the National Academy of Sciences of the United States of America* 101:3236-3241.
- Iafrazi J, Orejarena MJ, Lassalle O, Bouamrane L, Gonzalez-Campo C, Chavis P (2014) Reelin, an extracellular matrix protein linked to early onset psychiatric diseases, drives postnatal development of the prefrontal cortex via GluN2B-NMDARs and the mTOR pathway. *Molecular psychiatry* 19:417-426.
- Ibanez CF (2010) Beyond the cell surface: new mechanisms of receptor function. *Biochemical and biophysical research communications* 396:24-27.

- Inanobe A, Yoshimoto Y, Horio Y, Morishige KI, Hibino H, Matsumoto S, Tokunaga Y, Maeda T, Hata Y, Takai Y, Kurachi Y (1999) Characterization of G-protein-gated K<sup>+</sup> channels composed of Kir3.2 subunits in dopaminergic neurons of the substantia nigra. *The Journal of neuroscience : the official journal of the Society for Neuroscience* 19:1006-1017.
- Isomura R, Kitajima K, Sato C (2011) Structural and functional impairments of polysialic acid by a mutated polysialyltransferase found in schizophrenia. *The Journal of biological chemistry* 286:21535-21545.
- Javitt DC (2012) Glycine transport inhibitors in the treatment of schizophrenia. *Handbook of experimental pharmacology*:367-399.
- Javitt DC, Zukin SR (1991) Recent advances in the phencyclidine model of schizophrenia. *The American journal of psychiatry* 148:1301-1308.
- Javitt DC, Duncan L, Balla A, Sershen H (2005) Inhibition of system A-mediated glycine transport in cortical synaptosomes by therapeutic concentrations of clozapine: implications for mechanisms of action. *Molecular psychiatry* 10:275-287.
- Jelacic TM, Kennedy ME, Wickman K, Clapham DE (2000) Functional and biochemical evidence for G-protein-gated inwardly rectifying K<sup>+</sup> (GIRK) channels composed of GIRK2 and GIRK3. *The Journal of biological chemistry* 275:36211-36216.
- Jensen PH, Soroka V, Thomsen NK, Ralets I, Berezin V, Bock E, Poulsen FM (1999) Structure and interactions of NCAM modules 1 and 2, basic elements in neural cell adhesion. *Nature structural biology* 6:486-493.
- Jin K, Peel AL, Mao XO, Xie L, Cottrell BA, Henshall DC, Greenberg DA (2004) Increased hippocampal neurogenesis in Alzheimer's disease. *Proceedings of the National Academy of Sciences of the United States of America* 101:343-347.
- Johnson CP, Fujimoto I, Rutishauser U, Leckband DE (2005) Direct evidence that neural cell adhesion molecule (NCAM) polysialylation increases intermembrane repulsion and abrogates adhesion. *The Journal of biological chemistry* 280:137-145.
- Johnson JW, Ascher P (1987) Glycine potentiates the NMDA response in cultured mouse brain neurons. *Nature* 325:529-531.
- Jorgensen OS, Bock E (1974) Brain specific synaptosomal membrane proteins demonstrated by crossed immunoelectrophoresis. *Journal of neurochemistry* 23:879-880.
- Jurgenson M, Aonurm-Helm A, Zharkovsky A (2010) Behavioral profile of mice with impaired cognition in the elevated plus-maze due to a deficiency in neural cell adhesion molecule. *Pharmacology, biochemistry, and behavior* 96:461-468.
- Jurgenson M, Aonurm-Helm A, Zharkovsky A (2012) Partial reduction in neural cell adhesion molecule (NCAM) in heterozygous mice induces depression-related behaviour without cognitive impairment. *Brain research* 1447:106-118.
- Kalus I, Bormann U, Mzoughi M, Schachner M, Kleene R (2006) Proteolytic cleavage of the neural cell adhesion molecule by ADAM17/TACE is involved in neurite outgrowth. *Journal of neurochemistry* 98:78-88.
- Kanato Y, Kitajima K, Sato C (2008) Direct binding of polysialic acid to a brain-derived neurotrophic factor depends on the degree of polymerization. *Glycobiology* 18:1044-1053.
- Kantrowitz JT, Javitt DC (2010) N-methyl-d-aspartate (NMDA) receptor dysfunction or dysregulation: the final common pathway on the road to schizophrenia? *Brain research bulletin* 83:108-121.
- Karakas E, Simorowski N, Furukawa H (2011) Subunit arrangement and phenylethanolamine binding in GluN1/GluN2B NMDA receptors. *Nature* 475:249-253.
- Karpova A, Mikhaylova M, Bera S, Bar J, Reddy PP, Behnisch T, Rankovic V, Spilker C, Bethge P, Sahin J, Kaushik R, Zuschratter W, Kahne T, Naumann M, Gundelfinger ED, Kreutz MR (2013) Encoding and transducing the synaptic or extrasynaptic origin of NMDA receptor signals to the nucleus. *Cell* 152:1119-1133.
- Kaufman DL, Houser CR, Tobin AJ (1991) Two forms of the gamma-aminobutyric acid synthetic enzyme glutamate decarboxylase have distinct intraneuronal distributions and cofactor interactions. *Journal of neurochemistry* 56:720-723.

- Kaur M, Sharma S, Kaur G (2008) Age-related impairments in neuronal plasticity markers and astrocytic GFAP and their reversal by late-onset short term dietary restriction. *Biogerontology* 9:441-454.
- Kaushik R, Grochowska KM, Butnaru I, Kreutz MR (2014) Protein trafficking from synapse to nucleus in control of activity-dependent gene expression. *Neuroscience* 280:340-350.
- Kinarsky L, Feng B, Skifter DA, Morley RM, Sherman S, Jane DE, Monaghan DT (2005) Identification of subunit- and antagonist-specific amino acid residues in the N-Methyl-D-aspartate receptor glutamate-binding pocket. *The Journal of pharmacology and experimental therapeutics* 313:1066-1074.
- Kinney GG, Sur C, Burno M, Mallorga PJ, Williams JB, Figueroa DJ, Wittmann M, Lemaire W, Conn PJ (2003) The glycine transporter type 1 inhibitor N-[3-(4'-fluorophenyl)-3-(4'-phenylphenoxy)propyl]sarcosine potentiates NMDA receptor-mediated responses in vivo and produces an antipsychotic profile in rodent behavior. *The Journal of neuroscience : the official journal of the Society for Neuroscience* 23:7586-7591.
- Kiselyov VV, Berezin V, Maar TE, Soroka V, Edvardsen K, Schousboe A, Bock E (1997) The first immunoglobulin-like neural cell adhesion molecule (NCAM) domain is involved in double-reciprocal interaction with the second immunoglobulin-like NCAM domain and in heparin binding. *The Journal of biological chemistry* 272:10125-10134.
- Kiselyov VV, Skladchikova G, Hinsby AM, Jensen PH, Kulahin N, Soroka V, Pedersen N, Tsetlin V, Poulsen FM, Berezin V, Bock E (2003) Structural basis for a direct interaction between FGFR1 and NCAM and evidence for a regulatory role of ATP. *Structure (London, England : 1993)* 11:691-701.
- Kiss JZ, Wang C, Olive S, Rougon G, Lang J, Baetens D, Harry D, Pralong WF (1994) Activity-dependent mobilization of the adhesion molecule polysialic NCAM to the cell surface of neurons and endocrine cells. *The EMBO journal* 13:5284-5292.
- Kleckner NW, Dingledine R (1988) Requirement for glycine in activation of NMDA-receptors expressed in *Xenopus oocytes*. *Science (New York, NY)* 241:835-837.
- Kleene R, Schachner M (2004) Glycans and neural cell interactions. *Nature reviews Neuroscience* 5:195-208.
- Kleene R, Mzoughi M, Joshi G, Kalus I, Bormann U, Schulze C, Xiao MF, Dityatev A, Schachner M (2010a) NCAM-induced neurite outgrowth depends on binding of calmodulin to NCAM and on nuclear import of NCAM and fak fragments. *The Journal of neuroscience : the official journal of the Society for Neuroscience* 30:10784-10798.
- Kleene R, Cassens C, Bähring R, Theis T, Xiao MF, Dityatev A, Schafer-Nielsen C, Döring F, Wischmeyer E, Schachner M (2010b) Functional consequences of the interactions among the neural cell adhesion molecule NCAM, the receptor tyrosine kinase TrkB, and the inwardly rectifying K<sup>+</sup> channel KIR3.3. *The Journal of biological chemistry* 285:28968-28979.
- Kochlamazashvili G, Bukalo O, Senkov O, Salmen B, Gerardy-Schahn R, Engel AK, Schachner M, Dityatev A (2012) Restoration of synaptic plasticity and learning in young and aged NCAM-deficient mice by enhancing neurotransmission mediated by GluN2A-containing NMDA receptors. *The Journal of neuroscience : the official journal of the Society for Neuroscience* 32:2263-2275.
- Kochlamazashvili G, Senkov O, Grebenyuk S, Robinson C, Xiao MF, Stummeyer K, Gerardy-Schahn R, Engel AK, Feig L, Semyanov A, Suppiramaniam V, Schachner M, Dityatev A (2010) Neural cell adhesion molecule-associated polysialic acid regulates synaptic plasticity and learning by restraining the signaling through GluN2B-containing NMDA receptors. *The Journal of neuroscience : the official journal of the Society for Neuroscience* 30:4171-4183.
- Kreiner G (2015) Compensatory mechanisms in genetic models of neurodegeneration: are the mice better than humans? *Frontiers in cellular neuroscience* 9:56.
- Krocher T, Rockle I, Diederichs U, Weinhold B, Burkhardt H, Yanagawa Y, Gerardy-Schahn R, Hildebrandt H (2014) A crucial role for polysialic acid in developmental interneuron migration and the establishment of interneuron densities in the mouse prefrontal cortex. *Development (Cambridge, England)* 141:3022-3032.

- Kröcher T, Malinovskaja K, Jurgenson M, Aonurm-Helm A, Zharkovskaya T, Kalda A, Rockle I, Schiff M, Weinhold B, Gerardy-Schahn R, Hildebrandt H, Zharkovsky A (2015) Schizophrenia-like phenotype of polysialyltransferase ST8SIA2-deficient mice. *Brain structure & function* 220:71-83.
- Kruger RP, Aurandt J, Guan KL (2005) Semaphorins command cells to move. *Nature reviews Molecular cell biology* 6:789-800.
- Krystal JH, Karper LP, Seibyl JP, Freeman GK, Delaney R, Bremner JD, Heninger GR, Bowers MB, Jr., Charney DS (1994) Subanesthetic effects of the noncompetitive NMDA antagonist, ketamine, in humans. Psychotomimetic, perceptual, cognitive, and neuroendocrine responses. *Archives of general psychiatry* 51:199-214.
- Kulahin N, Rudenko O, Kiselyov V, Poulsen FM, Berezin V, Bock E (2005) Modulation of the homophilic interaction between the first and second Ig modules of neural cell adhesion molecule by heparin. *Journal of neurochemistry* 95:46-55.
- Kullmann DM, Asztely F (1998) Extrasynaptic glutamate spillover in the hippocampus: evidence and implications. *Trends in neurosciences* 21:8-14.
- Kustermann S, Hildebrandt H, Bolz S, Dengler K, Kohler K (2010) Genesis of rods in the zebrafish retina occurs in a microenvironment provided by polysialic acid-expressing Muller glia. *The Journal of comparative neurology* 518:636-646.
- Lane HY, Chang YC, Liu YC, Chiu CC, Tsai GE (2005) Sarcosine or D-serine add-on treatment for acute exacerbation of schizophrenia: a randomized, double-blind, placebo-controlled study. *Archives of general psychiatry* 62:1196-1204.
- Lau CG, Zukin RS (2007) NMDA receptor trafficking in synaptic plasticity and neuropsychiatric disorders. *Nature reviews Neuroscience* 8:413-426.
- Le Meur K, Galante M, Angulo MC, Audinat E (2007) Tonic activation of NMDA receptors by ambient glutamate of non-synaptic origin in the rat hippocampus. *The Journal of physiology* 580:373-383.
- LeDoux JE (2000) Emotion circuits in the brain. *Annual review of neuroscience* 23:155-184.
- Leger M, Quideville A, Bouet V, Haelewyn B, Boulouard M, Schumann-Bard P, Freret T (2013) Object recognition test in mice. *Nature protocols* 8:2531-2537.
- Lewis DA, Lieberman JA (2000) Catching up on schizophrenia: natural history and neurobiology. *Neuron* 28:325-334.
- Lewis DA, Moghaddam B (2006) Cognitive dysfunction in schizophrenia: convergence of gamma-aminobutyric acid and glutamate alterations. *Archives of neurology* 63:1372-1376.
- Li H, Babiarz J, Woodbury J, Kane-Goldsmith N, Grumet M (2004) Spatiotemporal heterogeneity of CNS radial glial cells and their transition to restricted precursors. *Developmental biology* 271:225-238.
- Li S, Tian X, Hartley DM, Feig LA (2006) Distinct roles for Ras-guanine nucleotide-releasing factor 1 (Ras-GRF1) and Ras-GRF2 in the induction of long-term potentiation and long-term depression. *The Journal of neuroscience : the official journal of the Society for Neuroscience* 26:1721-1729.
- Liedtke S, Geyer H, Wuhler M, Geyer R, Frank G, Gerardy-Schahn R, Zahringer U, Schachner M (2001) Characterization of N-glycans from mouse brain neural cell adhesion molecule. *Glycobiology* 11:373-384.
- Lievens PM, Kuznetsova T, Kochlamazashvili G, Cesca F, Gorinski N, Galil DA, Cherkas V, Ronkina N, Lafera J, Gaestel M, Ponimaskin E, Dityatev A (2016) ZDHHC3 tyrosine phosphorylation regulates NCAM palmitoylation. *Molecular and cellular biology*.
- Lindhout T, Iqbal U, Willis LM, Reid AN, Li J, Liu X, Moreno M, Wakarchuk WW (2011) Site-specific enzymatic polysialylation of therapeutic proteins using bacterial enzymes. *Proceedings of the National Academy of Sciences of the United States of America* 108:7397-7402.
- Little EB, Edelman GM, Cunningham BA (1998) Palmitoylation of the cytoplasmic domain of the neural cell adhesion molecule N-CAM serves as an anchor to cellular membranes. *Cell adhesion and communication* 6:415-430.
- Liu L, Wong TP, Pozza MF, Lingenhoehl K, Wang Y, Sheng M, Auberson YP, Wang YT (2004) Role of NMDA receptor subtypes in governing the direction of hippocampal synaptic plasticity. *Science (New York, NY)* 304:1021-1024.

- Liu M, Geddis MS, Wen Y, Setlik W, Gershon MD (2005) Expression and function of 5-HT<sub>4</sub> receptors in the mouse enteric nervous system. *American journal of physiology Gastrointestinal and liver physiology* 289:G1148-1163.
- Livingston BD, Paulson JC (1993) Polymerase chain reaction cloning of a developmentally regulated member of the sialyltransferase gene family. *The Journal of biological chemistry* 268:11504-11507.
- Lopez-Corcuera B, Martinez-Maza R, Nunez E, Roux M, Supplisson S, Aragon C (1998) Differential properties of two stably expressed brain-specific glycine transporters. *Journal of neurochemistry* 71:2211-2219.
- Lopez-Fernandez MA, Montaron MF, Varea E, Rougon G, Venero C, Abrous DN, Sandi C (2007) Upregulation of polysialylated neural cell adhesion molecule in the dorsal hippocampus after contextual fear conditioning is involved in long-term memory formation. *The Journal of neuroscience : the official journal of the Society for Neuroscience* 27:4552-4561.
- Lozovaya NA, Grebenyuk SE, Tsintsadze T, Feng B, Monaghan DT, Krishtal OA (2004) Extrasynaptic NR2B and NR2D subunits of NMDA receptors shape 'superslow' afterburst EPSC in rat hippocampus. *The Journal of physiology* 558:451-463.
- Luscher C, Jan LY, Stoffel M, Malenka RC, Nicoll RA (1997) G protein-coupled inwardly rectifying K<sup>+</sup> channels (GIRKs) mediate postsynaptic but not presynaptic transmitter actions in hippocampal neurons. *Neuron* 19:687-695.
- Lüthi A, Laurent JP, Figueroa A, Müller D, Schachner M (1994) Hippocampal long-term potentiation and neural cell adhesion molecules L1 and NCAM. *Nature* 372:777-779.
- Malenka RC, Bear MF (2004) LTP and LTD: an embarrassment of riches. *Neuron* 44:5-21.
- Manahan-Vaughan D, Wildforster V, Thomsen C (2008) Rescue of hippocampal LTP and learning deficits in a rat model of psychosis by inhibition of glycine transporter-1 (GlyT1). *The European journal of neuroscience* 28:1342-1350.
- Maness PF, Schachner M (2007) Neural recognition molecules of the immunoglobulin superfamily: signaling transducers of axon guidance and neuronal migration. *Nature neuroscience* 10:19-26.
- Markram K, Gerardy-Schahn R, Sandi C (2007a) Selective learning and memory impairments in mice deficient for polysialylated NCAM in adulthood. *Neuroscience* 144:788-796.
- Markram K, Lopez Fernandez MA, Abrous DN, Sandi C (2007b) Amygdala upregulation of NCAM polysialylation induced by auditory fear conditioning is not required for memory formation, but plays a role in fear extinction. *Neurobiology of learning and memory* 87:573-582.
- Martina M, Gorfinkel Y, Halman S, Lowe JA, Periyalwar P, Schmidt CJ, Bergeron R (2004) Glycine transporter type 1 blockade changes NMDA receptor-mediated responses and LTP in hippocampal CA1 pyramidal cells by altering extracellular glycine levels. *The Journal of physiology* 557:489-500.
- Massey PV, Johnson BE, Moulton PR, Auberson YP, Brown MW, Molnar E, Collingridge GL, Bashir ZI (2004) Differential roles of NR2A and NR2B-containing NMDA receptors in cortical long-term potentiation and long-term depression. *The Journal of neuroscience : the official journal of the Society for Neuroscience* 24:7821-7828.
- McAuley EZ, Scimone A, Tiwari Y, Agahi G, Mowry BJ, Holliday EG, Donald JA, Weickert CS, Mitchell PB, Schofield PR, Fullerton JM (2012) Identification of sialyltransferase 8B as a generalized susceptibility gene for psychotic and mood disorders on chromosome 15q25-26. *PloS one* 7:e38172.
- McGale EH, Pye IF, Stonier C, Hutchinson EC, Aber GM (1977) Studies of the inter-relationship between cerebrospinal fluid and plasma amino acid concentrations in normal individuals. *Journal of neurochemistry* 29:291-297.
- Mendiratta SS, Sekulic N, Lavie A, Colley KJ (2005) Specific amino acids in the first fibronectin type III repeat of the neural cell adhesion molecule play a role in its recognition and polysialylation by the polysialyltransferase ST8Sia IV/PST. *The Journal of biological chemistry* 280:32340-32348.

- Mikkonen M, Soininen H, Tapiola T, Alafuzoff I, Miettinen R (1999) Hippocampal plasticity in Alzheimer's disease: changes in highly polysialylated NCAM immunoreactivity in the hippocampal formation. *The European journal of neuroscience* 11:1754-1764.
- Milev P, Maurel P, Haring M, Margolis RK, Margolis RU (1996) TAG-1/axonin-1 is a high-affinity ligand of neurocan, phosphacan/protein-tyrosine phosphatase-zeta/beta, and N-CAM. *The Journal of biological chemistry* 271:15716-15723.
- Milev P, Friedlander DR, Sakurai T, Karthikeyan L, Flad M, Margolis RK, Grumet M, Margolis RU (1994) Interactions of the chondroitin sulfate proteoglycan phosphacan, the extracellular domain of a receptor-type protein tyrosine phosphatase, with neurons, glia, and neural cell adhesion molecules. *The Journal of cell biology* 127:1703-1715.
- Miller PD, Chung WW, Lagenaur CF, DeKosky ST (1993) Regional distribution of neural cell adhesion molecule (N-CAM) and L1 in human and rodent hippocampus. *The Journal of comparative neurology* 327:341-349.
- Minana R, Duran JM, Tomas M, Renau-Piqueras J, Guerri C (2001) Neural cell adhesion molecule is endocytosed via a clathrin-dependent pathway. *The European journal of neuroscience* 13:749-756.
- Minelli A, Brecha NC, Karschin C, DeBiasi S, Conti F (1995) GAT-1, a high-affinity GABA plasma membrane transporter, is localized to neurons and astroglia in the cerebral cortex. *The Journal of neuroscience : the official journal of the Society for Neuroscience* 15:7734-7746.
- Mishra B, von der Ohe M, Schulze C, Bian S, Makhina T, Loers G, Kleene R, Schachner M (2010) Functional role of the interaction between polysialic acid and extracellular histone H1. *The Journal of neuroscience : the official journal of the Society for Neuroscience* 30:12400-12413.
- Misztal M, Skangiel-Kramska J, Niewiadomska G, Danysz W (1996) Subchronic intraventricular infusion of quinolinic acid produces working memory impairment--a model of progressive excitotoxicity. *Neuropharmacology* 35:449-458.
- Moghaddam B, Javitt D (2012) From revolution to evolution: the glutamate hypothesis of schizophrenia and its implication for treatment. *Neuropsychopharmacology : official publication of the American College of Neuropsychopharmacology* 37:4-15.
- Monlezun S, Ouali S, Poulain DA, Theodosis DT (2005) Polysialic acid is required for active phases of morphological plasticity of neurosecretory axons and their glia. *Molecular and cellular neurosciences* 29:516-524.
- Monyer H, Burnashev N, Laurie DJ, Sakmann B, Seeburg PH (1994) Developmental and regional expression in the rat brain and functional properties of four NMDA receptors. *Neuron* 12:529-540.
- Morishita W, Lu W, Smith GB, Nicoll RA, Bear MF, Malenka RC (2007) Activation of NR2B-containing NMDA receptors is not required for NMDA receptor-dependent long-term depression. *Neuropharmacology* 52:71-76.
- Morris RG (2013) NMDA receptors and memory encoding. *Neuropharmacology* 74:32-40.
- Mothet JP, Parent AT, Wolosker H, Brady RO, Jr., Linden DJ, Ferris CD, Rogawski MA, Snyder SH (2000) D-serine is an endogenous ligand for the glycine site of the N-methyl-D-aspartate receptor. *Proceedings of the National Academy of Sciences of the United States of America* 97:4926-4931.
- Muhlenhoff M, Eckhardt M, Bethe A, Frosch M, Gerardy-Schahn R (1996) Autocatalytic polysialylation of polysialyltransferase-1. *The EMBO journal* 15:6943-6950.
- Muller-Lissner SA, Fumagalli I, Bardhan KD, Pace F, Pecher E, Nault B, Ruegg P (2001) Tegaserod, a 5-HT(4) receptor partial agonist, relieves symptoms in irritable bowel syndrome patients with abdominal pain, bloating and constipation. *Alimentary pharmacology & therapeutics* 15:1655-1666.
- Muller D, Djebbara-Hannas Z, Jourdain P, Vutskits L, Durbec P, Rougon G, Kiss JZ (2000) Brain-derived neurotrophic factor restores long-term potentiation in polysialic acid-neural cell adhesion molecule-deficient hippocampus. *Proceedings of the National Academy of Sciences of the United States of America* 97:4315-4320.
- Muller D, Wang C, Skibo G, Toni N, Cremer H, Calaora V, Rougon G, Kiss JZ (1996) PSA-NCAM is required for activity-induced synaptic plasticity. *Neuron* 17:413-422.

- Murphy KJ, O'Connell AW, Regan CM (1996) Repetitive and transient increases in hippocampal neural cell adhesion molecule polysialylation state following multitrial spatial training. *Journal of neurochemistry* 67:1268-1274.
- Murray HC, Low VF, Swanson ME, Dieriks BV, Turner C, Faull RL, Curtis MA (2016) Distribution of PSA-NCAM in normal, Alzheimer's and Parkinson's disease human brain. *Neuroscience* 330:359-375.
- Myme CI, Sugino K, Turrigiano GG, Nelson SB (2003) The NMDA-to-AMPA ratio at synapses onto layer 2/3 pyramidal neurons is conserved across prefrontal and visual cortices. *Journal of neurophysiology* 90:771-779.
- Nacher J, Blasco-Ibanez JM, McEwen BS (2002a) Non-granule PSA-NCAM immunoreactive neurons in the rat hippocampus. *Brain research* 930:1-11.
- Nacher J, Lanuza E, McEwen BS (2002b) Distribution of PSA-NCAM expression in the amygdala of the adult rat. *Neuroscience* 113:479-484.
- Nacher J, Guirado R, Castillo-Gomez E (2013) Structural plasticity of interneurons in the adult brain: role of PSA-NCAM and implications for psychiatric disorders. *Neurochemical research* 38:1122-1133.
- Nacher J, Alonso-Llosa G, Rosell D, McEwen B (2002c) PSA-NCAM expression in the piriform cortex of the adult rat. Modulation by NMDA receptor antagonist administration. *Brain research* 927:111-121.
- Nacher J, Guirado R, Varea E, Alonso-Llosa G, Rockle I, Hildebrandt H (2010) Divergent impact of the polysialyltransferases ST8SiaII and ST8SiaIV on polysialic acid expression in immature neurons and interneurons of the adult cerebral cortex. *Neuroscience* 167:825-837.
- Nelson RW, Bates PA, Rutishauser U (1995) Protein determinants for specific polysialylation of the neural cell adhesion molecule. *The Journal of biological chemistry* 270:17171-17179.
- Ni Dhuill CM, Fox GB, Pittock SJ, O'Connell AW, Murphy KJ, Regan CM (1999) Polysialylated neural cell adhesion molecule expression in the dentate gyrus of the human hippocampal formation from infancy to old age. *Journal of neuroscience research* 55:99-106.
- Nielsen J, Kulahin N, Walmod PS (2010) Extracellular protein interactions mediated by the neural cell adhesion molecule, NCAM: heterophilic interactions between NCAM and cell adhesion molecules, extracellular matrix proteins, and viruses. *Advances in experimental medicine and biology* 663:23-53.
- Nielsen J, Gotfryd K, Li S, Kulahin N, Soroka V, Rasmussen KK, Bock E, Berezin V (2009) Role of glial cell line-derived neurotrophic factor (GDNF)-neural cell adhesion molecule (NCAM) interactions in induction of neurite outgrowth and identification of a binding site for NCAM in the heel region of GDNF. *The Journal of neuroscience : the official journal of the Society for Neuroscience* 29:11360-11376.
- Niethammer P, Dellling M, Sytnyk V, Dityatev A, Fukami K, Schachner M (2002) Cosignaling of NCAM via lipid rafts and the FGF receptor is required for neuriteogenesis. *The Journal of cell biology* 157:521-532.
- Nishiyama A, Komitova M, Suzuki R, Zhu X (2009) Polydendrocytes (NG2 cells): multifunctional cells with lineage plasticity. *Nature reviews Neuroscience* 10:9-22.
- Oltmann-Norden I, Galuska SP, Hildebrandt H, Geyer R, Gerardy-Schahn R, Geyer H, Muhlenhoff M (2008) Impact of the polysialyltransferases ST8SiaII and ST8SiaIV on polysialic acid synthesis during postnatal mouse brain development. *The Journal of biological chemistry* 283:1463-1471.
- Ong E, Nakayama J, Angata K, Reyes L, Katsuyama T, Arai Y, Fukuda M (1998) Developmental regulation of polysialic acid synthesis in mouse directed by two polysialyltransferases, PST and STX. *Glycobiology* 8:415-424.
- Ono S, Hane M, Kitajima K, Sato C (2012) Novel regulation of fibroblast growth factor 2 (FGF2)-mediated cell growth by polysialic acid. *The Journal of biological chemistry* 287:3710-3722.
- Pan HC, Shen YQ, Loers G, Jakovcevski I, Schachner M (2014) Tegaserod, a small compound mimetic of polysialic acid, promotes functional recovery after spinal cord injury in mice. *Neuroscience* 277:356-366.



- Paoletti P, Bellone C, Zhou Q (2013) NMDA receptor subunit diversity: impact on receptor properties, synaptic plasticity and disease. *Nature reviews Neuroscience* 14:383-400.
- Papouin T, Oliet SH (2014) Organization, control and function of extrasynaptic NMDA receptors. *Philosophical transactions of the Royal Society of London Series B, Biological sciences* 369:20130601.
- Papouin T, Ladepeche L, Ruel J, Sacchi S, Labasque M, Hanini M, Groc L, Pollegioni L, Mothet JP, Oliet SH (2012) Synaptic and extrasynaptic NMDA receptors are gated by different endogenous coagonists. *Cell* 150:633-646.
- Paratcha G, Ledda F, Ibanez CF (2003) The neural cell adhesion molecule NCAM is an alternative signaling receptor for GDNF family ligands. *Cell* 113:867-879.
- Pencea V, Luskin MB (2003) Prenatal development of the rodent rostral migratory stream. *The Journal of comparative neurology* 463:402-418.
- Perry EK, Johnson M, Ekonomou A, Perry RH, Ballard C, Attems J (2012) Neurogenic abnormalities in Alzheimer's disease differ between stages of neurogenesis and are partly related to cholinergic pathology. *Neurobiology of disease* 47:155-162.
- Persohn E, Pollerberg GE, Schachner M (1989) Immunoelectron-microscopic localization of the 180 kD component of the neural cell adhesion molecule N-CAM in postsynaptic membranes. *The Journal of comparative neurology* 288:92-100.
- Pillai-Nair N, Panicker AK, Rodriguiz RM, Gilmore KL, Demyanenko GP, Huang JZ, Wetsel WC, Maness PF (2005) Neural cell adhesion molecule-secreting transgenic mice display abnormalities in GABAergic interneurons and alterations in behavior. *The Journal of neuroscience : the official journal of the Society for Neuroscience* 25:4659-4671.
- Piras F, Schiff M, Chiapponi C, Bossu P, Muhlenhoff M, Caltagirone C, Gerardy-Schahn R, Hildebrandt H, Spalletta G (2015) Brain structure, cognition and negative symptoms in schizophrenia are associated with serum levels of polysialic acid-modified NCAM. *Translational psychiatry* 5:e658.
- Poels EM, Kegeles LS, Kantrowitz JT, Slifstein M, Javitt DC, Lieberman JA, Abi-Dargham A, Girgis RR (2014) Imaging glutamate in schizophrenia: review of findings and implications for drug discovery. *Molecular psychiatry* 19:20-29.
- Pollerberg GE, Burrige K, Krebs KE, Goodman SR, Schachner M (1987) The 180-kD component of the neural cell adhesion molecule N-CAM is involved in cell-cell contacts and cytoskeleton-membrane interactions. *Cell and tissue research* 250:227-236.
- Polo-Parada L, Bose CM, Landmesser LT (2001) Alterations in transmission, vesicle dynamics, and transmitter release machinery at NCAM-deficient neuromuscular junctions. *Neuron* 32:815-828.
- Poltorak M, Khoja I, Hemperly JJ, Williams JR, el-Mallakh R, Freed WJ (1995) Disturbances in cell recognition molecules (N-CAM and L1 antigen) in the CSF of patients with schizophrenia. *Experimental neurology* 131:266-272.
- Ponimaskin E, Dityateva G, Ruonala MO, Fukata M, Fukata Y, Kobe F, Wouters FS, Delling M, Bredt DS, Schachner M, Dityatev A (2008) Fibroblast growth factor-regulated palmitoylation of the neural cell adhesion molecule determines neuronal morphogenesis. *The Journal of neuroscience : the official journal of the Society for Neuroscience* 28:8897-8907.
- Potschka H, Pekcec A, Weinhold B, Gerardy-Schahn R (2008) Deficiency of neural cell adhesion molecule or its polysialylation modulates pharmacological effects of the AMPA receptor antagonist NBQX. *Neuroscience* 152:1093-1098.
- Povysheva NV, Johnson JW (2012) Tonic NMDA receptor-mediated current in prefrontal cortical pyramidal cells and fast-spiking interneurons. *Journal of neurophysiology* 107:2232-2243.
- Probstmeier R, Bilz A, Schneider-Schaulies J (1994) Expression of the neural cell adhesion molecule and polysialic acid during early mouse embryogenesis. *Journal of neuroscience research* 37:324-335.
- Prosser RA, Rutishauser U, Ungers G, Fedorkova L, Glass JD (2003) Intrinsic role of polysialylated neural cell adhesion molecule in photic phase resetting of the Mammalian circadian clock. *The Journal of neuroscience : the official journal of the Society for Neuroscience* 23:652-658.

- Purcell AE, Rocco MM, Lenhart JA, Hyder K, Zimmerman AW, Pevsner J (2001) Assessment of neural cell adhesion molecule (NCAM) in autistic serum and postmortem brain. *Journal of autism and developmental disorders* 31:183-194.
- Purves D, Augustine GJ, Fitzpatrick D (2008) *Neuroscience*, 4th Edition Edition: Sinauer Associates.
- Radyushkin K, Anokhin K, Meyer BI, Jiang Q, Alvarez-Bolado G, Gruss P (2005) Genetic ablation of the mammillary bodies in the Foxb1 mutant mouse leads to selective deficit of spatial working memory. *The European journal of neuroscience* 21:219-229.
- Ranheim TS, Edelman GM, Cunningham BA (1996) Homophilic adhesion mediated by the neural cell adhesion molecule involves multiple immunoglobulin domains. *Proceedings of the National Academy of Sciences of the United States of America* 93:4071-4075.
- Rauner C, Kohr G (2011) Triheteromeric NR1/NR2A/NR2B receptors constitute the major N-methyl-D-aspartate receptor population in adult hippocampal synapses. *The Journal of biological chemistry* 286:7558-7566.
- Retzler C, Gohring W, Rauch U (1996) Analysis of neurocan structures interacting with the neural cell adhesion molecule N-CAM. *The Journal of biological chemistry* 271:27304-27310.
- Rockle I, Hildebrandt H (2016) Deficits of olfactory interneurons in polysialyltransferase- and NCAM-deficient mice. *Developmental neurobiology* 76:421-433.
- Rodriguez JJ, Dallerac GM, Tabuchi M, Davies HA, Colyer FM, Stewart MG, Doyere V (2008) N-methyl-D-aspartate receptor independent changes in expression of polysialic acid-neural cell adhesion molecule despite blockade of homosynaptic long-term potentiation and heterosynaptic long-term depression in the awake freely behaving rat dentate gyrus. *Neuron glia biology* 4:169-178.
- Rolf B, Bastmeyer M, Schachner M, Bartsch U (2002) Pathfinding errors of corticospinal axons in neural cell adhesion molecule-deficient mice. *The Journal of neuroscience : the official journal of the Society for Neuroscience* 22:8357-8362.
- Ronn LC, Berezin V, Bock E (2000) The neural cell adhesion molecule in synaptic plasticity and ageing. *International journal of developmental neuroscience : the official journal of the International Society for Developmental Neuroscience* 18:193-199.
- Rougon G, Dubois C, Buckley N, Magnani JL, Zollinger W (1986) A monoclonal antibody against meningococcus group B polysaccharides distinguishes embryonic from adult N-CAM. *The Journal of cell biology* 103:2429-2437.
- Rousselot P, Nottebohm F (1995) Expression of polysialylated N-CAM in the central nervous system of adult canaries and its possible relation to function. *The Journal of comparative neurology* 356:629-640.
- Rusakov DA, Scimemi A, Walker MC, Kullmann DM (2004) Comment on "Role of NMDA receptor subtypes in governing the direction of hippocampal synaptic plasticity". *Science (New York, NY)* 305:1912; author reply.
- Rutishauser U (2008) Polysialic acid in the plasticity of the developing and adult vertebrate nervous system. *Nature reviews Neuroscience* 9:26-35.
- Rutishauser U, Landmesser L (1996) Polysialic acid in the vertebrate nervous system: a promoter of plasticity in cell-cell interactions. *Trends in neurosciences* 19:422-427.
- Rutishauser U, Watanabe M, Silver J, Troy FA, Vimr ER (1985) Specific alteration of NCAM-mediated cell adhesion by an endoneuraminidase. *The Journal of cell biology* 101:1842-1849.
- Sadoul R, Hirn M, Deagostini-Bazin H, Rougon G, Goridis C (1983) Adult and embryonic mouse neural cell adhesion molecules have different binding properties. *Nature* 304:347-349.
- Saffell JL, Williams EJ, Mason IJ, Walsh FS, Doherty P (1997) Expression of a dominant negative FGF receptor inhibits axonal growth and FGF receptor phosphorylation stimulated by CAMs. *Neuron* 18:231-242.
- Sah P, Hestrin S, Nicoll RA (1989) Tonic activation of NMDA receptors by ambient glutamate enhances excitability of neurons. *Science (New York, NY)* 246:815-818.

- Sajo M, Sugiyama H, Yamamoto H, Tanii T, Matsuki N, Ikegaya Y, Koyama R (2016) Neuraminidase-Dependent Degradation of Polysialic Acid Is Required for the Lamination of Newly Generated Neurons. *PLoS one* 11:e0146398.
- Sandi C, Merino JJ, Cordero MI, Krut ND, Murphy KJ, Regan CM (2003) Modulation of hippocampal NCAM polysialylation and spatial memory consolidation by fear conditioning. *Biological psychiatry* 54:599-607.
- Santuccione A, Sytnyk V, Leshchyn'ska I, Schachner M (2005) Prion protein recruits its neuronal receptor NCAM to lipid rafts to activate p59fyn and to enhance neurite outgrowth. *The Journal of cell biology* 169:341-354.
- Sato C, Hane M, Kitajima K (2016) Relationship between ST8SIA2, polysialic acid and its binding molecules, and psychiatric disorders. *Biochimica et biophysica acta* 1860:1739-1752.
- Sato C, Kitajima K, Inoue S, Seki T, Troy FA, 2nd, Inoue Y (1995) Characterization of the antigenic specificity of four different anti-(alpha 2-->8-linked polysialic acid) antibodies using lipid-conjugated oligo/polysialic acids. *The Journal of biological chemistry* 270:18923-18928.
- Schachner M (1997) Neural recognition molecules and synaptic plasticity. *Current opinion in cell biology* 9:627-634.
- Schiff M, Weinhold B, Grothe C, Hildebrandt H (2009) NCAM and polysialyltransferase profiles match dopaminergic marker gene expression but polysialic acid is dispensable for development of the midbrain dopamine system. *Journal of neurochemistry* 110:1661-1673.
- Schnaar RL, Gerardy-Schahn R, Hildebrandt H (2014) Sialic acids in the brain: gangliosides and polysialic acid in nervous system development, stability, disease, and regeneration. *Physiological reviews* 94:461-518.
- Schuster T, Krug M, Hassan H, Schachner M (1998) Increase in proportion of hippocampal spine synapses expressing neural cell adhesion molecule NCAM180 following long-term potentiation. *Journal of neurobiology* 37:359-372.
- Seidenfaden R, Krauter A, Hildebrandt H (2006) The neural cell adhesion molecule NCAM regulates neuritogenesis by multiple mechanisms of interaction. *Neurochemistry international* 49:1-11.
- Seidenfaden R, Krauter A, Schertzinger F, Gerardy-Schahn R, Hildebrandt H (2003) Polysialic acid directs tumor cell growth by controlling heterophilic neural cell adhesion molecule interactions. *Molecular and cellular biology* 23:5908-5918.
- Seki T, Arai Y (1991) Expression of highly polysialylated NCAM in the neocortex and piriform cortex of the developing and the adult rat. *Anatomy and embryology* 184:395-401.
- Seki T, Arai Y (1993) Distribution and possible roles of the highly polysialylated neural cell adhesion molecule (NCAM-H) in the developing and adult central nervous system. *Neuroscience research* 17:265-290.
- Senkov O, Tikhobrazova O, Dityatev A (2012) PSA-NCAM: synaptic functions mediated by its interactions with proteoglycans and glutamate receptors. *The international journal of biochemistry & cell biology* 44:591-595.
- Senkov O, Sun M, Weinhold B, Gerardy-Schahn R, Schachner M, Dityatev A (2006) Polysialylated neural cell adhesion molecule is involved in induction of long-term potentiation and memory acquisition and consolidation in a fear-conditioning paradigm. *The Journal of neuroscience : the official journal of the Society for Neuroscience* 26:10888-109898.
- Seyrantepe V, Poupetova H, Froissart R, Zobot MT, Maire I, Pshezhetsky AV (2003) Molecular pathology of NEU1 gene in sialidosis. *Human mutation* 22:343-352.
- Shahraz A, Kopatz J, Mathy R, Kappler J, Winter D, Kapoor S, Schutza V, Scheper T, Gieselmann V, Neumann H (2015) Anti-inflammatory activity of low molecular weight polysialic acid on human macrophages. *Scientific reports* 5:16800.
- Shaw AD, Tiwari Y, Kaplan W, Heath A, Mitchell PB, Schofield PR, Fullerton JM (2014) Characterisation of genetic variation in ST8SIA2 and its interaction region in NCAM1 in patients with bipolar disorder. *PLoS one* 9:e92556.

- Shen H, Glass JD, Seki T, Watanabe M (1999) Ultrastructural analysis of polysialylated neural cell adhesion molecule in the suprachiasmatic nuclei of the adult mouse. *The Anatomical record* 256:448-457.
- Shen H, Watanabe M, Tomaszewicz H, Glass JD (2001) Genetic deletions of NCAM and PSA impair circadian function in the mouse. *Physiology & behavior* 73:185-193.
- Shen H, Watanabe M, Tomaszewicz H, Rutishauser U, Magnuson T, Glass JD (1997) Role of neural cell adhesion molecule and polysialic acid in mouse circadian clock function. *The Journal of neuroscience : the official journal of the Society for Neuroscience* 17:5221-5229.
- Shen HY, van Vliet EA, Bright KA, Hanthorn M, Lytle NK, Gorter J, Aronica E, Boison D (2015) Glycine transporter 1 is a target for the treatment of epilepsy. *Neuropharmacology* 99:554-565.
- Sherwin AL (1999) Neuroactive amino acids in focally epileptic human brain: a review. *Neurochemical research* 24:1387-1395.
- Shim SS, Hammonds MD, Kee BS (2008) Potentiation of the NMDA receptor in the treatment of schizophrenia: focused on the glycine site. *European archives of psychiatry and clinical neuroscience* 258:16-27.
- Shiozaki K, Koseki K, Yamaguchi K, Shiozaki M, Narimatsu H, Miyagi T (2009) Developmental change of sialidase neu4 expression in murine brain and its involvement in the regulation of neuronal cell differentiation. *The Journal of biological chemistry* 284:21157-21164.
- Shipton OA, Paulsen O (2014) GluN2A and GluN2B subunit-containing NMDA receptors in hippocampal plasticity. *Philosophical transactions of the Royal Society of London Series B, Biological sciences* 369:20130163.
- Singer P, Feldon J, Yee BK (2009) The glycine transporter 1 inhibitor SSR504734 enhances working memory performance in a continuous delayed alternation task in C57BL/6 mice. *Psychopharmacology* 202:371-384.
- Singer P, Dubrova S, Yee BK (2015) Inhibition of glycine transporter 1: The yellow brick road to new schizophrenia therapy? *Current pharmaceutical design* 21:3771-3787.
- Sjostrand D, Carlsson J, Paratcha G, Persson B, Ibanez CF (2007) Disruption of the GDNF binding site in NCAM dissociates ligand binding and homophilic cell adhesion. *The Journal of biological chemistry* 282:12734-12740.
- Smith KE, Borden LA, Hartig PR, Branchek T, Weinshank RL (1992) Cloning and expression of a glycine transporter reveal colocalization with NMDA receptors. *Neuron* 8:927-935.
- Socala K, Nieoczym D, Rundfeldt C, Wlaz P (2010) Effects of sarcosine, a glycine transporter type 1 inhibitor, in two mouse seizure models. *Pharmacological reports : PR* 62:392-397.
- Soroka V, Kolkova K, Kastrup JS, Diederichs K, Breed J, Kiselyov VV, Poulsen FM, Larsen IK, Welte W, Berezin V, Bock E, Kasper C (2003) Structure and interactions of NCAM Ig1-2-3 suggest a novel zipper mechanism for homophilic adhesion. *Structure (London, England : 1993)* 11:1291-1301.
- Sotres-Bayon F, Quirk GJ (2010) Prefrontal control of fear: more than just extinction. *Current opinion in neurobiology* 20:231-235.
- Spilker C et al. (2016) A Jacob/Nsmf Gene Knockout Results in Hippocampal Dysplasia and Impaired BDNF Signaling in Dendritogenesis. *PLoS genetics* 12:e1005907.
- Steinpreis RE (1996) The behavioral and neurochemical effects of phencyclidine in humans and animals: some implications for modeling psychosis. *Behavioural brain research* 74:45-55.
- Stoenica L, Senkov O, Gerardy-Schahn R, Weinhold B, Schachner M, Dityatev A (2006) In vivo synaptic plasticity in the dentate gyrus of mice deficient in the neural cell adhesion molecule NCAM or its polysialic acid. *The European journal of neuroscience* 23:2255-2264.
- Stork O, Welzl H, Cremer H, Schachner M (1997) Increased intermale aggression and neuroendocrine response in mice deficient for the neural cell adhesion molecule (NCAM). *The European journal of neuroscience* 9:1117-1125.
- Stork O, Welzl H, Wotjak CT, Hoyer D, Dellling M, Cremer H, Schachner M (1999) Anxiety and increased 5-HT1A receptor response in NCAM null mutant mice. *Journal of neurobiology* 40:343-355.

- Stork O, Welzl H, Wolfer D, Schuster T, Mantei N, Stork S, Hoyer D, Lipp H, Obata K, Schachner M (2000) Recovery of emotional behaviour in neural cell adhesion molecule (NCAM) null mutant mice through transgenic expression of NCAM180. *The European journal of neuroscience* 12:3291-3306.
- Storms SD, Anvekar VM, Adams LD, Murray BA (1996a) Heterophilic NCAM-mediated cell adhesion to proteoglycans from chick embryonic brain membranes. *Experimental cell research* 223:385-394.
- Storms SD, Kim AC, Tran BH, Cole GJ, Murray BA (1996b) NCAM-mediated adhesion of transfected cells to agrin. *Cell adhesion and communication* 3:497-509.
- Strekalova H, Buhmann C, Kleene R, Eggers C, Saffell J, Hemperly J, Weiller C, Muller-Thomsen T, Schachner M (2006) Elevated levels of neural recognition molecule L1 in the cerebrospinal fluid of patients with Alzheimer disease and other dementia syndromes. *Neurobiology of aging* 27:1-9.
- Stummeyer K, Dickmanns A, Muhlenhoff M, Gerardy-Schahn R, Ficner R (2005) Crystal structure of the polysialic acid-degrading endosialidase of bacteriophage K1F. *Nature structural & molecular biology* 12:90-96.
- Sullivan PF, Keefe RS, Lange LA, Lange EM, Stroup TS, Lieberman J, Maness PF (2007) NCAM1 and neurocognition in schizophrenia. *Biological psychiatry* 61:902-910.
- Supplisson S, Bergman C (1997) Control of NMDA receptor activation by a glycine transporter co-expressed in *Xenopus* oocytes. *The Journal of neuroscience : the official journal of the Society for Neuroscience* 17:4580-4590.
- Sytnyk V, Leshchyn'ska I, Nikonenko AG, Schachner M (2006) NCAM promotes assembly and activity-dependent remodeling of the postsynaptic signaling complex. *The Journal of cell biology* 174:1071-1085.
- Takahashi K, Mitoma J, Hosono M, Shiozaki K, Sato C, Yamaguchi K, Kitajima K, Higashi H, Nitta K, Shima H, Miyagi T (2012) Sialidase NEU4 hydrolyzes polysialic acids of neural cell adhesion molecules and negatively regulates neurite formation by hippocampal neurons. *The Journal of biological chemistry* 287:14816-14826.
- Tao R, Li C, Zheng Y, Qin W, Zhang J, Li X, Xu Y, Shi YY, Feng G, He L (2007) Positive association between SIAT8B and schizophrenia in the Chinese Han population. *Schizophrenia research* 90:108-114.
- Taube JS, Schwartzkroin PA (1988) Mechanisms of long-term potentiation: EPSP/spike dissociation, intradendritic recordings, and glutamate sensitivity. *The Journal of neuroscience : the official journal of the Society for Neuroscience* 8:1632-1644.
- Ter Horst JP, Loscher JS, Pickering M, Regan CM, Murphy KJ (2008) Learning-associated regulation of polysialylated neural cell adhesion molecule expression in the rat prefrontal cortex is region-, cell type- and paradigm-specific. *The European journal of neuroscience* 28:419-427.
- Theodosis DT, Bonhomme R, Vitiello S, Rougon G, Poulain DA (1999) Cell surface expression of polysialic acid on NCAM is a prerequisite for activity-dependent morphological neuronal and glial plasticity. *The Journal of neuroscience : the official journal of the Society for Neuroscience* 19:10228-10236.
- Todaro L, Puricelli L, Gioseffi H, Guadalupe Pallotta M, Lastiri J, Bal de Kier Joffe E, Varela M, Sacerdote de Lustig E (2004) Neural cell adhesion molecule in human serum. Increased levels in dementia of the Alzheimer type. *Neurobiology of disease* 15:387-393.
- Tomasiewicz H, Ono K, Yee D, Thompson C, Goridis C, Rutishauser U, Magnuson T (1993) Genetic deletion of a neural cell adhesion molecule variant (N-CAM-180) produces distinct defects in the central nervous system. *Neuron* 11:1163-1174.
- Traynelis SF, Wollmuth LP, McBain CJ, Menniti FS, Vance KM, Ogden KK, Hansen KB, Yuan H, Myers SJ, Dingledine R (2010) Glutamate receptor ion channels: structure, regulation, and function. *Pharmacological reviews* 62:405-496.
- Trotter J, Karram K, Nishiyama A (2010) NG2 cells: Properties, progeny and origin. *Brain research reviews* 63:72-82.
- Tsai GE, Lin PY (2010) Strategies to enhance N-methyl-D-aspartate receptor-mediated neurotransmission in schizophrenia, a critical review and meta-analysis. *Current pharmaceutical design* 16:522-537.

- Tsvetkov E, Shin RM, Bolshakov VY (2004) Glutamate uptake determines pathway specificity of long-term potentiation in the neural circuitry of fear conditioning. *Neuron* 41:139-151.
- Ueda Y, Doi T, Tokumaru J, Mitsuyama Y, Willmore LJ (2000) Kindling phenomena induced by the repeated short-term high potassium stimuli in the ventral hippocampus of rats: on-line monitoring of extracellular glutamate overflow. *Experimental brain research* 135:199-203.
- Umbricht D, Alberati D, Martin-Facklam M, Borroni E, Youssef EA, Ostland M, Wallace TL, Knoflach F, Dorflinger E, Wettstein JG, Bausch A, Garibaldi G, Santarelli L (2014) Effect of bitopertin, a glycine reuptake inhibitor, on negative symptoms of schizophrenia: a randomized, double-blind, proof-of-concept study. *JAMA psychiatry* 71:637-646.
- Vaithianathan T, Matthias K, Bahr B, Schachner M, Suppiramaniam V, Dityatev A, Steinhauser C (2004) Neural cell adhesion molecule-associated polysialic acid potentiates alpha-amino-3-hydroxy-5-methylisoxazole-4-propionic acid receptor currents. *The Journal of biological chemistry* 279:47975-47984.
- Van De Werd HJ, Rajkowska G, Evers P, Uylings HB (2010) Cytoarchitectonic and chemoarchitectonic characterization of the prefrontal cortical areas in the mouse. *Brain structure & function* 214:339-353.
- van Kammen DP, Poltorak M, Kelley ME, Yao JK, Gurklis JA, Peters JL, Hemperly JJ, Wright RD, Freed WJ (1998) Further studies of elevated cerebrospinal fluid neuronal cell adhesion molecule in schizophrenia. *Biological psychiatry* 43:680-686.
- Varbanov H, Dityatev A (2016) Regulation of extrasynaptic signaling by polysialylated NCAM: Impact for synaptic plasticity and cognitive functions. *Molecular and cellular neurosciences*.
- Varea E, Nacher J, Blasco-Ibanez JM, Gomez-Climent MA, Castillo-Gomez E, Crespo C, Martinez-Guijarro FJ (2005) PSA-NCAM expression in the rat medial prefrontal cortex. *Neuroscience* 136:435-443.
- Varea E, Castillo-Gomez E, Gomez-Climent MA, Blasco-Ibanez JM, Crespo C, Martinez-Guijarro FJ, Nacher J (2007) PSA-NCAM expression in the human prefrontal cortex. *Journal of chemical neuroanatomy* 33:202-209.
- Varea E, Guirado R, Gilabert-Juan J, Marti U, Castillo-Gomez E, Blasco-Ibanez JM, Crespo C, Nacher J (2012) Expression of PSA-NCAM and synaptic proteins in the amygdala of psychiatric disorder patients. *Journal of psychiatric research* 46:189-197.
- Vawter MP (2000) Dysregulation of the neural cell adhesion molecule and neuropsychiatric disorders. *European journal of pharmacology* 405:385-395.
- Vawter MP, Hemperly JJ, Freed WJ, Garver DL (1998a) CSF N-CAM in neuroleptic-naive first-episode patients with schizophrenia. *Schizophrenia research* 34:123-131.
- Vawter MP, Howard AL, Hyde TM, Kleinman JE, Freed WJ (1999) Alterations of hippocampal secreted N-CAM in bipolar disorder and synaptophysin in schizophrenia. *Molecular psychiatry* 4:467-475.
- Vawter MP, Cannon-Spoor HE, Hemperly JJ, Hyde TM, VanderPutten DM, Kleinman JE, Freed WJ (1998b) Abnormal expression of cell recognition molecules in schizophrenia. *Experimental neurology* 149:424-432.
- Vawter MP, Usen N, Thatcher L, Ladenheim B, Zhang P, VanderPutten DM, Conant K, Herman MM, van Kammen DP, Sedvall G, Garver DL, Freed WJ (2001) Characterization of human cleaved N-CAM and association with schizophrenia. *Experimental neurology* 172:29-46.
- Vazza G, Bertolin C, Scudellaro E, Vettori A, Boaretto F, Rampinelli S, De Sanctis G, Perini G, Peruzzi P, Mostacciolo ML (2007) Genome-wide scan supports the existence of a susceptibility locus for schizophrenia and bipolar disorder on chromosome 15q26. *Molecular psychiatry* 12:87-93.
- Venero C, Herrero AI, Touyarot K, Cambon K, Lopez-Fernandez MA, Berezin V, Bock E, Sandi C (2006) Hippocampal up-regulation of NCAM expression and polysialylation plays a key role on spatial memory. *The European journal of neuroscience* 23:1585-1595.
- Volianskis A, Bannister N, Collett VJ, Irvine MW, Monaghan DT, Fitzjohn SM, Jensen MS, Jane DE, Collingridge GL (2013) Different NMDA receptor subtypes mediate induction of long-term potentiation and two forms of short-term potentiation at CA1 synapses in rat hippocampus in vitro. *The Journal of physiology* 591:955-972.

- Volk D, Austin M, Pierri J, Sampson A, Lewis D (2001) GABA transporter-1 mRNA in the prefrontal cortex in schizophrenia: decreased expression in a subset of neurons. *The American journal of psychiatry* 158:256-265.
- Volk DW, Edelson JR, Lewis DA (2016) Altered expression of developmental regulators of parvalbumin and somatostatin neurons in the prefrontal cortex in schizophrenia. *Schizophrenia research* 177:3-9.
- von Engelhardt J, Doganci B, Jensen V, Hvalby O, Gongrich C, Taylor A, Barkus C, Sanderson DJ, Rawlins JN, Seeburg PH, Bannerman DM, Monyer H (2008) Contribution of hippocampal and extra-hippocampal NR2B-containing NMDA receptors to performance on spatial learning tasks. *Neuron* 60:846-860.
- Vorobiev I, Matskevich V, Kovnir S, Orlova N, Knorre V, Jain S, Genkin D, Gabibov A, Miroshnikov A (2013) Chemical polysialylation: design of conjugated human oxyntomodulin with a prolonged anorexic effect in vivo. *Biochimie* 95:264-270.
- Vutskits L, Djebbara-Hannas Z, Zhang H, Paccard JP, Durbec P, Rougon G, Muller D, Kiss JZ (2001) PSA-NCAM modulates BDNF-dependent survival and differentiation of cortical neurons. *The European journal of neuroscience* 13:1391-1402.
- Walsh FS, Doherty P (1997) Neural cell adhesion molecules of the immunoglobulin superfamily: role in axon growth and guidance. *Annual review of cell and developmental biology* 13:425-456.
- Wang Y, Neumann H (2010) Alleviation of neurotoxicity by microglial human Siglec-11. *The Journal of neuroscience : the official journal of the Society for Neuroscience* 30:3482-3488.
- Warburton EC, Brown MW (2015) Neural circuitry for rat recognition memory. *Behavioural brain research* 285:131-139.
- Wechsler A, Teichberg VI (1998) Brain spectrin binding to the NMDA receptor is regulated by phosphorylation, calcium and calmodulin. *The EMBO journal* 17:3931-3939.
- Weinhold B, Seidenfaden R, Rockle I, Muhlenhoff M, Schertzinger F, Conzelmann S, Marth JD, Gerardy-Schahn R, Hildebrandt H (2005) Genetic ablation of polysialic acid causes severe neurodevelopmental defects rescued by deletion of the neural cell adhesion molecule. *The Journal of biological chemistry* 280:42971-42977.
- Weitlauf C, Honse Y, Auberson YP, Mishina M, Lovinger DM, Winder DG (2005) Activation of NR2A-containing NMDA receptors is not obligatory for NMDA receptor-dependent long-term potentiation. *The Journal of neuroscience : the official journal of the Society for Neuroscience* 25:8386-8390.
- Werneburg S, Muhlenhoff M, Stangel M, Hildebrandt H (2015) Polysialic acid on SynCAM 1 in NG2 cells and on neuropilin-2 in microglia is confined to intracellular pools that are rapidly depleted upon stimulation. *Glia* 63:1240-1255.
- Westphal N, Kleene R, Lutz D, Theis T, Schachner M (2016) Polysialic acid enters the cell nucleus attached to a fragment of the neural cell adhesion molecule NCAM to regulate the circadian rhythm in mouse brain. *Molecular and cellular neurosciences* 74:114-127.
- Williams K (1993) Ifenprodil discriminates subtypes of the N-methyl-D-aspartate receptor: selectivity and mechanisms at recombinant heteromeric receptors. *Molecular pharmacology* 44:851-859.
- Wischmeyer E, Doring F, Wischmeyer E, Spauschus A, Thomzig A, Veh R, Karschin A (1997) Subunit interactions in the assembly of neuronal Kir3.0 inwardly rectifying K<sup>+</sup> channels. *Molecular and cellular neurosciences* 9:194-206.
- Wolf G, Keilhoff G, Fischer S, Hass P (1990) Subcutaneously applied magnesium protects reliably against quinolinate-induced N-methyl-D-aspartate (NMDA)-mediated neurodegeneration and convulsions in rats: are there therapeutical implications. *Neuroscience letters* 117:207-211.
- Wu PL, Tang HS, Lane HY, Tsai CA, Tsai GE (2011) Sarcosine therapy for obsessive compulsive disorder: a prospective, open-label study. *Journal of clinical psychopharmacology* 31:369-374.
- Xiao MF, Xu JC, Tereshchenko Y, Novak D, Schachner M, Kleene R (2009) Neural cell adhesion molecule modulates dopaminergic signaling and behavior by regulating dopamine D2 receptor internalization. *The Journal of neuroscience : the official journal of the Society for Neuroscience* 29:14752-14763.

- Yabe U, Sato C, Matsuda T, Kitajima K (2003) Polysialic acid in human milk. CD36 is a new member of mammalian polysialic acid-containing glycoprotein. *The Journal of biological chemistry* 278:13875-13880.
- Yang P, Yin X, Rutishauser U (1992) Intercellular space is affected by the polysialic acid content of NCAM. *The Journal of cell biology* 116:1487-1496.
- Yew DT, Li WP, Webb SE, Lai HW, Zhang L (1999) Neurotransmitters, peptides, and neural cell adhesion molecules in the cortices of normal elderly humans and Alzheimer patients: a comparison. *Experimental gerontology* 34:117-133.
- Zafra F, Gomeza J, Olivares L, Aragon C, Gimenez C (1995a) Regional distribution and developmental variation of the glycine transporters GLYT1 and GLYT2 in the rat CNS. *The European journal of neuroscience* 7:1342-1352.
- Zafra F, Aragon C, Olivares L, Danbolt NC, Gimenez C, Storm-Mathisen J (1995b) Glycine transporters are differentially expressed among CNS cells. *The Journal of neuroscience : the official journal of the Society for Neuroscience* 15:3952-3969.
- Zerwas M, Trouche S, Richetin K, Escude T, Halley H, Gerardy-Schahn R, Verret L, Rampon C (2015) Environmental enrichment rescues memory in mice deficient for the polysialyltransferase ST8SiaIV. *Brain structure & function*.
- Zhang H, Vutskits L, Calaora V, Durbec P, Kiss JZ (2004) A role for the polysialic acid-neural cell adhesion molecule in PDGF-induced chemotaxis of oligodendrocyte precursor cells. *Journal of cell science* 117:93-103.
- Zhang HX, Hyrc K, Thio LL (2009a) The glycine transport inhibitor sarcosine is an NMDA receptor co-agonist that differs from glycine. *The Journal of physiology* 587:3207-3220.
- Zhang HX, Lyons-Warren A, Thio LL (2009b) The glycine transport inhibitor sarcosine is an inhibitory glycine receptor agonist. *Neuropharmacology* 57:551-555.
- Zhang LH, Gong N, Fei D, Xu L, Xu TL (2008) Glycine uptake regulates hippocampal network activity via glycine receptor-mediated tonic inhibition. *Neuropsychopharmacology : official publication of the American College of Neuropsychopharmacology* 33:701-711.
- Zhao JP, Constantine-Paton M (2007) NR2A<sup>-/-</sup> mice lack long-term potentiation but retain NMDA receptor and L-type Ca<sup>2+</sup> channel-dependent long-term depression in the juvenile superior colliculus. *The Journal of neuroscience : the official journal of the Society for Neuroscience* 27:13649-13654.
- Zhao MG, Toyoda H, Lee YS, Wu LJ, Ko SW, Zhang XH, Jia Y, Shum F, Xu H, Li BM, Kaang BK, Zhuo M (2005) Roles of NMDA NR2B subtype receptor in prefrontal long-term potentiation and contextual fear memory. *Neuron* 47:859-872.
- Zhuo M (2009) Plasticity of NMDA receptor NR2B subunit in memory and chronic pain. *Molecular brain* 2:4.



## AKNOWLEDGEMENTS

I was very lucky to join the research lab of Prof. Dr. Alexander Dityatev in November 2012 as one of his first lab members in Magdeburg and to perform the work for my thesis in a harmonic and creative atmosphere. I would like to thank Prof. Alexander Dityatev for giving me the opportunity to join his group, for his guidance, fruitful discussions, and for his continuous scientific and moral support during these years, as well as for providing excellent facilities, including a completely new dual patch-clamp setup, an automatic electrode puller, and an excellent vibratome. I am also very thankful to Prof. Dityatev for giving me the opportunity to study the molecular mechanisms underlying long-term potentiation in the prefrontal cortex, thanks again for the fascinating ideas, unlimited patience, and for his openness to new ideas and suggestions. I also appreciate very much that Prof. Dityatev gave me the opportunity to be part of several highly promising projects, and even a first-author review. I also want to thank Prof. Dityatev for allowing me to write the first draft of manuscripts and for giving me excellent tips and sources in scientific writing, which were always a great inspiration. Many thanks also for all his efforts and suggestions during times of writing or experiments.

I would like to thank also Dr. Gaga Kochlamazashvili for initiating this project and providing all his expertise and experience on recordings in the prefrontal cortex, which he successfully established with Prof. Dityatev before I joined the lab. I am very thankful to Dr. Kochlamazashvili for our fruitful and valuable discussions on my LTP recordings, critical reading of the manuscript, and his helpful support for technical issues.

Prof. Rita Gerardy-Schahn and Prof. Herbert Hildebrandt I would like to thank for kindly providing all the NANA12 and endoNF, and polySia antibodies used in this project, as well as the initial batches of PST-KO and NCAM-KO mice for our studies. Many thanks to Prof. Gerardy-Schahn and Prof. Hildebrandt for our valuable scientific discussions, critical suggestions to our manuscript, and their continuous support.

I would like to cordially thank Dr. Juan Nacher, Prof. Vadim Bolshakov, and Prof. Sabine Spijker, and Dr. Inseon Song for their valuable efforts as reviewers of the present doctoral thesis.

I would like to thank Dr. Inseon Song for our valuable discussions, great support and help, and the countless tips on electrophysiological recordings, which largely enhanced my practical knowledge in patch-clamp technique. I am very thankful to Jenny Schneeberg and Katrin Böhm for their excellent technical assistance, and great help with ordering animals, breeding, genotyping, and immunohistochemistry. I also want to thank Dr. Oleg Senkov for sharing his expertise on *in vivo* electrophysiology and behavior, for the excellent supervision of the implantations and object-recognition tests for our publication, and for his valuable advice on scientific presentations. Many thanks to Dr. Stoyan Stoyanov, Shaobo Jia, Mohamed El Tabbal, Hussam Hayani, and Weilun Sun for the fruitful and successful collaboration on *in vivo* experiments in the polySia project, and for their valuable support and discussions. I want to thank

also Dr. Rahul Kaushik for fruitful advice, support, and discussions with immunohistochemical analysis and virus production during our collaboration. Here, I also wanted to thank Dr. Song and Dr. Kaushik for being great office mates.

I am also thankful to Sandra Dittman and Karen Müller-Zabel, who provided excellent support with administrative issues, especially before and after scientific conferences. I want to thank also Maura Ferrer-Ferrer and Gabriela Matuszko, who were also very supportive colleagues. Many thanks to all the members of our laboratory for making my PhD thesis such a positive, friendly, and productive experience, and, of course, for your friendship.

And last but not least, I want to thank my parents and my fiance Amelie for their unlimited support, motivation, patience, and inspiration that they taught me during the last years.

## SELBSTSTÄNDIGKEITSERKLÄRUNG – STATEMENT OF INTEREST

Hristo Varbanov  
Eggersdorfer Str. 13,  
39122 Magdeburg

### Erklärung

Hiermit erkläre ich, dass ich die von mir eingereichte Dissertation zum dem Thema

***“The role of the neural cell adhesion molecule-associated polysialic acid in synaptic plasticity in the medial prefrontal cortex of the mouse (Mus musculus)”***

selbständig verfasst, nicht schon als Dissertation verwendet habe und die benutzten Hilfsmittel und Quellen vollständig angegeben wurden.

Weiterhin erkläre ich, dass ich weder diese noch eine andere Arbeit zur Erlangung des akademischen Grades doctor rerum naturalium (Dr. rer. nat.) an anderen Einrichtungen eingereicht habe.

Magdeburg, den 27.03.2017

.....  
Hristo Varbanov

## CURRICULUM VITAE

### **PERSONAL DETAILS:**

Name: Hristo Varbanov  
Working address: German Center for Neurodegenerative Diseases (DZNE)  
Prof. Dr. Alexander Dityatev (Group Leader)  
Molecular Neuroplasticity Research Group  
Leipziger Straße 44 / Haus 64/ R408, R419  
39120 Magdeburg, Germany

Home address: Eggersdorfer Str. 13, 39122 Magdeburg  
E-mail: [hristo.varbanov.hv@gmail.com](mailto:hristo.varbanov.hv@gmail.com)  
Tel. (mobile): 01575 96421621  
Date of birth: 17.07.1983  
Place of birth: Pleven, Bulgaria  
Nationality: Bulgarian, German

### **EDUCATION:**

Since Nov 2012: German Center for Neurodegenerative Diseases (DZNE), Magdeburg;  
PhD thesis at the laboratory of Prof. Dr. Alexander Dityatev,  
Title: *“The role of the neural cell adhesion molecule-associated polysialic acid in synaptic plasticity in the medial prefrontal cortex of the mouse (Mus musculus)”*

Mar 2012–Sep 2012: University of Cologne, Germany;  
Master’s thesis at the laboratory of Prof. Dr. Peter Kloppenburg , Title:  
*“Effects of insulin on the electrophysiological properties of melanin-concentrating hormone (MCH)-expressing neurons of the mouse lateral hypothalamus”*

Apr 2010–Oct 2012: University of Cologne;  
Master of Science (MSc) Program in Experimental and Clinical Neuroscience, Grade point average: 1.5

Oct 2009–Feb 2010: University of Cologne;  
Bachelor’s thesis at the laboratory of Prof. Dr. Wolfgang Walkowiak,  
Title: *“Cytoarchitecture of the septal nuclei in the brain of the Chinese fire-bellied toad Bombina orientalis: An electrophysiological and neuroanatomical study”*

Oct 2007–Mar 2010: University of Cologne;  
Bachelor of Science (BSc) Program in Neuroscience,  
Grade point average: 1.1

2002–2006: University of Ulm, Dentistry Studies

1996–2002: Geo Milev High School for Mathematics and Natural Sciences, Pleven, Bulgaria, Grade point average: 1.0

**SCHOLARSHIPS:**

2010–2011: NRW-Stipend of the Maria Pesch Foundation and NRW Scholarship Program

2012–2015: Three-year research grant from the Fondazione Santa Lucia, Via Ardeatina 306, 00179 Roma, Italy

April 2016: Travel support for attending the conference “Frontiers in sialic acid research conference”, Bad Lauterberg, Germany, April 23–25, 2016

## LIST OF PUBLICATIONS

Published: Varbanov H, Dityatev A. Regulation of extrasynaptic signaling by polysialylated NCAM: Impact for synaptic plasticity and cognitive functions. Mol Cell Neurosci. 2016 Nov 16. pii: S1044-7431(16)30239-1. doi: 10.1016/j.mcn.2016.11.005. [Epub ahead of print] Review. PMID: 27865768

Hausen AC, Ruud J, Jiang H, Hess S, Varbanov H, Kloppenburg P, Brüning JC. Insulin-Dependent Activation of MCH Neurons Impairs Locomotor Activity and Insulin Sensitivity in Obesity. Cell Rep. 2016 Dec 6;17(10):2512-2521. doi: 10.1016/j.celrep.2016.11.030. PMID: 27926856

Bahari-Javan S, Varbanov H, Halder R, Benito E, Kaurani L, Burkhardt S, Anderson-Schmidt H, Anghelescu I, Budde M, Stilling RM, Costa J, Medina J, Dietrich DE, Figge C, Folkerts H, Gade K, Heilbronner U, Koller M, Konrad C, Nussbeck SY, Scherk H, Spitzer C, Stierl S, Stöckel J, Thiel A, von Hagen M, Zimmermann J, Zitzelsberger A, Schulz S, Schmitt A, Delalle I, Falkai P, Schulze TG, Dityatev A, Sananbenesi F, Fischer A. HDAC1 links early life stress to schizophrenia-like phenotypes. Proc Natl Acad Sci U S A. 2017 Jun 6;114(23):E4686-E4694. doi: 10.1073/pnas.1613842114. Epub 2017 May 22.

Submitted: Hristo Varbanov, Gaga Kochlamazashvili, Shaobo Jial, Mohamed El Tabbal, Hussam Hayani, Stoyan Stoyanov, Weilun Sun, Jörg Ehrit, Sebastiano Curreli, Patricia Maness, Herbert Hildebrandt, Rita Gerardy-Schahn, Oleg Senkov, Alexander Dityatev.  
RESETTING THE BALANCE BETWEEN SYNAPTIC AND EXTRASYNAPTIC NMDA RECEPTORS IN THE PREFRONTAL CORTEX OF MICE DEFICIENT IN NCAM-ASSOCIATED POLYSIALIC ACID. (submitted)